University of Calgary

PRISM Repository **https://prism.ucalgary.ca**

The Vault Open Theses and Dissertations

2017

Relative Permeability Hysteresis Effects on Water Alternating CO2 Flooding

Binesh, Raz

Binesh, R. (2017). Relative Permeability Hysteresis Effects on Water Alternating CO2 Flooding (Master's thesis, University of Calgary, Calgary, Canada). Retrieved from https://prism.ucalgary.ca. doi:10.11575/PRISM/27609

http://hdl.handle.net/11023/4264

Downloaded from PRISM Repository, University of Calgary

UNIVERSITY OF CALGARY

Relative Permeability Hysteresis Effects on Water Alternating CO_2 Flooding

by

Raz Binesh

A THESIS

SUBMITTED TO THE FACULTY OF GRADUATE STUDIES

IN PARTIAL FULFILMENT OF THE REQUIREMENTS FOR THE

DEGREE OF MASTER OF SCIENCE

GRADUATE PROGRAM IN CHEMICAL AND PETROLEUM ENGINEERING

CALGARY, ALBERTA

November, 2017

© Raz Binesh 2017

Abstract

This research justifies the improvement of the oil recovery by using the water alternating CO_2 flooding method for the right candidates, also indicates the importance of considering relative permeability hysteresis effects in WAG numerical simulations.

Good reservoir candidates for water alternating CO_2 injection have been prepared in this study considering different wettability characteristics (oil-wet and water-wet) and different oil viscosities. In addition, some simulations have been performed on the models with severe permeability distribution in their layers.

First, it was shown that CO_2-WAG (water alternating gas) results in much higher oil production in all the simulations compared to water flooding or CO_2 flooding.

Then CO_2-WAG simulations were conducted with and without considering the relative permeability hysteresis effects. It was concluded that the models with the hysteresis effects have higher oil production for different scenarios of oil viscosity and reservoir wettability.

Moreover, including hysteresis effects has bigger impacts on the oil production in the cases of low viscosity oil and a severe permeability reservoir.

Finally, water flooding and CO_2 flooding worked differently with respect to the rock and fluid properties such as reservoir permeability distribution and oil viscosity.

Acknowledgements

I express my gratitude to everyone who supported me throughout my petroleum Master's studies.

First, I would like to express my sincere gratitude to my supervisor Prof. John Chen, co-supervisors Dr. Long Nghiem and Dr. Shawket Ghedan for their continuous support of my M.Sc. study and related research, for their patience, motivation, and immense knowledge. Their guidance helped me in all the time of research and writing of this thesis. I could not have imagined having better advisors and mentors for my petroleum study.

Besides my supervisors, I would like to thank the rest of my thesis committee, Prof. Nader Mahinpey and Prof. Behrouz Far. I do appreciate their time and support and helpful comments.

My sincere thanks also go to Prof. Alex De Visscher for always being available to give me the best advices in order to meet all the requirements of my Master's studies.

I am hugely indebted and thoroughly grateful to all the wonderful people in CMG Ltd., specially Dr. Chaodong Yang, Dr. Mohamed Hassam, Dr. Amir Shahbazi and Dr. Reza Heidari for their great suggestions and encouragement during my petroleum studies. Their doors have been always opened for me to ask my questions and they have been the best help for me to understand and learn CMG software.

I must also acknowledge Jamie McInnis, Fengyue Lin, Marie Ferris and Genna Fulber for ever being so kind; they have been always very supportive and positive, especially Jamie who has been always available when I needed somebody to talk to and ask for some guidance.

I would also like to thank my friends, especially Bo Yang, Ehsan Ranjbar, Hamid Behmanesh, Raheleh Salehi Mojarad, Farzaneh Rahmdel and Mohamad Mojarab for helping me technically

and spiritually throughout my studies and my life in general. Ehsan Ranjbar has been helping me from the first day I started my petroleum studies by helping me scheduling the prerequisite courses, whenever I had a petroleum question, he was the first person to call and he has been always the best help.

Finally but not the least, I must express my very profound gratitude to my parents, brothers, sister in law, grandmother and especially my husband Baher Binesh for providing me with unfailing support and continuous encouragement throughout my years of study and through the process of researching and writing this thesis. Baher taught me the thermodynamic and transport phenomena concepts and helped me a lot while I was taking those courses. He has been always the greatest help when I was stressed out. This accomplishment would not have been possible without him. Thank you.

To all the wonderful people who

supported me in my master studies and

my lovely grandmother Setareh.

Table of Contents

Abstract ii

Acknowledgements iii

Dedication v

Table of Contents vi

List of Tables viii

List of Figures and Illustrations ix

List of Symbols, Abbreviations xii

Chapter 1: Introduction 1

1.1 Research Objectives 1

Chapter 2: Literature Review 3

2.1 Water Alternating Gas Oil Recovery Mechanism (WAG) 3

2.1.1 Types of the WAG Process Design 3

2.2 Effective Factors in WAG Process Design 4

2.2.1 Heterogeneity of the Reservoir 6

2.2.2 Fluid Properties and Rock-Fluid Interaction 6

2.2.3 Injection Pattern 7

2.2.4 WAG Ratio and WAG Cycle Time 7

2.2.5 Injector and Producer Bottom-Hole Pressure 8

2.2.6 Three-Phase Relative Permeability 8

2.3 Hysteresis of the Relative Permeability 10

2.3.1 Importance of Hysteresis Effects in WAG 10

2.3.2 Studies of Hysteresis Effects of Relative Permeability 10

2.3.2.1 Two-Phase Hysteresis Models 12

2.3.3.2 Three-Phase Hysteresis Models 13

2.3.2.3 Evaluating Impact of Using Different Hysteresis Models 16

Chapter 3: Properties of the Reservoir Models and Fluids 29

3.1 Properties of the Reservoir Models 29

3.1.1 Reservoir Base Models Gridding 29

3.1.2 Reservoir Base Models' Porosity 30

3.1.3 Reservoir Base Models' Permeability 31

3.2 Properties of the Fluids 33

3.3 Rock-Fluids' Properties 37
3.4 Method of Comparison 40
3.5 Relative Permeability Models 41
3.6 Hysteresis Models 42
3.6.1 Carlson Hysteresis Model 43
Chapter 4: Results and Discussion **44**
4.1 CO_2-WAG Recovery and Effects of Hysteresis on CO_2-WAG Models 44
4.1.1 WAG Performance in Comparison with Water Flooding and CO_2 Flooding 45
4.1.2 Effect of Hysteresis on CO_2-WAG Models 62
4.2 Fine Gridding Effect on CO_2-WAG Simulation 72
4.3 Effect of Hysteresis and Oil Viscosity on CO_2-WAG Models 75
4.4 Effect of Hysteresis and High Permeability Contrast on WAG Models 80
Chapter 5: Conclusions **84**
References **89**
Appendix A: Copyright Permission **92**

List of Tables

Table 2.1 Synthetic reservoir test case simulation results adapted from Spiteri and Juanes, 2006. 25

Table 2.2 PUNQ-S3 test case simulation results for heterogeneous reservoir adapted from Spiteri and Juanes, 2006. 25

Table 2.3 Comparing different relative permeability models for WAG experiments adapted from Shahrokhi et al., 2014. 26

Table 2.4 WAG-1 simulation results- water-wet core starting with water injection adapted from Shahrokhi et al., 2014. 27

Table 2.5 WAG-2 - mixed-wet core starting with water injection adapted from Shahrokhi et al., 2014..... 27

Table 2.6 WAG-3 - mixed-wet core starting with gas injection adapted from Shahrokhi et al., 2014..... 28

Table 3.1 Reservoir fluid properties. 34

Table 3.2 Fluid composition. 34

Table 3.3 Data used in CCE experiment..... 35

Table 3.4 Data used in Diff Lib experiment. 35

Table 3.5 Lower viscosity fluid composition. 36

Table 4.1 Oil Recovery Factor..... 61

Table 4.2 Oil Recovery Factor..... 71

Table 4.3 Oil Recovery Factor..... 79

Table 4.4 Oil Recovery Factor..... 83

Table 5.1 Oil Recovery Factor for Water-Wet Model..... 84

Table 5.2 Oil Recovery Factor for Oil-Wet Model..... 85

List of Figures and Illustrations

Figure 2.1 Oak's relative permeability data for selected experiments' saturation paths by Spiteri and Juanes, 2006. 19

Figure 2.2 Water relative permeabilities correlation between experimental and modeled for each displacement path by Spiteri and Juanes, 2006. 19

Figure 2.3 Oil relative permeabilities correlation between experimental and Stone I interpolation by Spiteri and Juanes, 2006. 20

Figure 2.4 Oil relative permeabilities correlation between experimental and Baker interpolation model by Spiteri and Juanes, 2006. 21

Figure 2.5 Experimental data paths and Stone II model of predicted oil isoperms by and by Spiteri and Juanes, 2006. 21

Figure 2.6 Different three-phase displacements paths 3 and 4 gas relative permeability comparison, with the two-phase gas relative permeability from an oil/gas gas-flood experiment by Spiteri and Juanes, 2006. 22

Figure 2.7 Killough's two-phase hysteresis model of a three-phase water-flood, path 4's scatter plot, by Spiteri and Juanes, 2006. 23

Figure 2.8 Carlson's two-phase hysteresis model of a three-phase water-flood, path 4 model's scatter plot, by Spiteri and Juanes, 2006. 23

Figure 2.9 Gas relative permeability predicted by the WAG three-phase hysteresis of a three-phase water-flood, path 4 model's scatter plot, by Spiteri and Juanes, 2006. 24

Figure 3.1 Base models 3D grid top. 29

Figure 3.2 Porosity of layers 1 and 2 on the left and layers 3 and 4 on the right. 31

Figure 3.3 Porosity of layers 5 and 6 on the left and layers 7 and 8 on the right. 31

Figure 3.4 Permeability of layer 1 on the left and layer 2 on the right. 32

Figure 3.5 Permeability of layer 3 on the left and layer 4 on the right. 32

Figure 3.6 Permeability of layer 5 on the left and layer 6 on the right. 32

Figure 3.7 Permeability of layer 7 on the left and layer 8 on the right. 33

Figure 3.8 Relative permeability curves, water/oil, water-wet system. 37

Figure 3.9 Relative permeability curves, liquid/gas, water-wet system. 37

Figure 3.10 Capillary pressure curves, water-wet system. 38

Figure 3.11 Relative permeability curves, water/oil, oil-wet system. 38

Figure 3.12 Relative permeability curves, liquid/gas, oil-wet system. 39

Figure 3.13 Capillary pressure curves, oil-wet system. 39

Figure 4.1 Cumulative CO_2 Injection, Oil-Wet and Water-Wet Models. 46

Figure 4.2 Cumulative Water Injection, Oil-Wet and Water-Wet Models. 47
Figure 4.3 Oil Production Rate, Oil-Wet and Water-Wet Models. 48
Figure 4.4 Cumulative Oil Production Oil-Wet and Water-Wet Models. 49
Figure 4.5 Gas Oil Ratio, Oil-Wet and Water-Wet Models. 50
Figure 4.6 Water Cut, Oil-Wet and Water-Wet Models. 51
Figure 4.7 Reservoir Pressure, Oil-Wet Model. 53
Figure 4.8 Reservoir Pressure, Water-Wet Model. 54
Figure 4.9 Reservoir Pressure, Oil-Wet Model. 55
Figure 4.10 Reservoir Pressure, Water-Wet Model. 55
Figure 4.11 Oil Production Rate, Oil-Wet Model. 56
Figure 4.12 Oil Production Rate, Oil-Wet Model. 57
Figure 4.13 Cumulative Oil Production, Oil-Wet Model. 58
Figure 4.14 Cumulative Oil Production, Water-Wet Model. 58
Figure 4.15 Water Injection Rate, Oil-Wet Model. 59
Figure 4.16 Water Injection Rate, Water-Wet Model. 59
Figure 4.17 Water Cut, Oil-Wet Model. 60
Figure 4.18 Oil Production Rate, Oil-Wet Model. 62
Figure 4.19 Oil Production Rate, Water-Wet Model. 63
Figure 4.20 Cumulative Oil Production, Oil-Wet Model. 64
Figure 4.21 Cumulative Oil Production, Water-Wet Model. 64
Figure 4.22 Cumulative Gas Injection, Oil-Wet and Water-Wet Models. 65
Figure 4.23 Gas Oil Ratio, Oil-Wet and Water-Wet Models. 66
Figure 4.24 Gas Oil Ratio, Oil-Wet and Water-Wet Models. 67
Figure 4.25 Cumulative Water Injection Oil-Wet and Water-Wet Models. 67
Figure 4.26 Water Cut Oil-Wet and Water-Wet Models. 68
Figure 4.27 Reservoir Pressure, Oil-Wet and Water-Wet Models. 68
Figure 4.28 CO_2 Molality Layer 3, Oil-Wet. 70
Figure 4.29 CO_2 Molality Layer 3, Water-Wet. 71
Figure 4.30 Cumulative Oil Production. 72
Figure 4.31 Oil Production Rate. 73
Figure 4.32 Cumulative CO_2 Injection. 74

Figure 4.33 Cumulative Water Injection. 74
Figure 4.34 Oil Production Rate, Oil-Wet Model..... 75
Figure 4.35 Cumulative Oil Production, Oil-Wet Model. 76
Figure 4.36 CO_2 Molality in Layer 3, Oil-Wet Model. 77
Figure 4.37 Gas Oil Ratio, Oil-Wet Model..... 78
Figure 4.38 Average Reservoir Pressure, Oil-Wet. 79
Figure 4.39 Permeability of layers 3 and 7 on the left and layer 4 and 8 on the right..... 80
Figure 4.40 Oil-Wet Model Gas Oil Ratio..... 81
Figure 4.41 Cumulative Oil Production for Oil-Wet Model..... 82
Figure 4.42 Average Reservoir Pressure in Oil-Wet Model..... 83
Figure 5.1 Oil Recovery Factor for Oil-Wet Model with Higher Oil Viscosity..... 86
Figure 5.2 Oil Recovery Factor for Oil-Wet Model with Lower Oil Viscosity. 86
Figure 5.3 Oil Recovery Factor for Oil-Wet Model with High Permeability Contrast. 87
Figure 5.4 Oil Recovery Factor for Water-Wet Model with Higher Oil Viscosity. 87
Figure 5.5 Oil Recovery Factor for Water-Wet Model with Lower Oil Viscosity..... 88
Figure 5.6 Oil Recovery Factor for Water-Wet Model with High Permeability Contrast. 88

List of Symbols, Abbreviations

Symbol	Definition
API	American petroleum institute gravity
Bbl	Barrel
BHP	Bottom hole pressure
CO_2	Carbon dioxide
EOR	Enhanced oil recovery
FVF	Formation volume factor
GOR	Gas oil ratio
HWAG	Hybrid water alternating gas flooding
IWAG	Immiscible water alternating gas flooding
MMcf	One million cubic feet
MMP	Minimum miscibility pressure
MWAG	Miscible water alternating gas flooding
SSWAG	Selectively simultaneous water alternating gas flooding
SWAG	Simultaneous water alternating gas flooding
WAG	Water alternating gas flooding
WCUT	Water cut

Chapter 1: Introduction

1.1 Research Objectives

In oil reservoirs after the primary operation and secondary recovery methods, tertiary recovery methods or EOR (enhanced oil recovery) techniques will be needed to recover the remaining oil left behind. EOR methods recover the remaining oil by modifying a mobility ratio and sweep efficiency.

EOR can be done by injecting one or more fluids to a formation, for example, water and/or CO_2. The injected fluids will displace the oil toward producing wells. Water alternating gas or WAG injection improves the oil recovery by combining effects of water flooding and gas flooding. Therefore, a water saturation direction keeps changing from increasing to decreasing and vice versa. This induces hysteresis effects in relative permeability.

Therefore, three-phase relative permeability should be studied specifically for WAG processes considering cyclic hysteresis effects. There have been some studies concluding that considering hysteresis effects in numerical simulation leads to more realistic results (Killough, 1976; Carlson, 1981; Lenhard and Parker, 1987; Lenhard and Oostrom, 1998; Jerauld, 1997; Larsen Skauge 1998; Blunt, 2000; Kjosavik et al., 2002; Spiteri et al., 2008, Shahrokhi et al., 2014). Unfortunately, these studies were mostly focused on water-wet reservoirs and there have not been many studies on field scale reservoirs considering different wettability characteristics.

In this research simulations were conducted on reservoirs with different wettability characteristics and also different oil viscosities via the GEM simulator and the effects of hysteresis on relative permeability have been studied. Moreover, the hysteresis effects of the relative permeability were

investigated for models with high permeability contrasts in layers. A hysteresis model used in the simulations is the Larsen-Skauge model (Larsen and Skauge, 1998).

Chapter 2 includes a literature review explaining WAG processes and relative permeability models considered in commercial simulations and a summary of studies performed on the relative permeability hysteresis effects.

In Chapter 3, the reservoir and fluid properties of the simulation models are described. Moreover, the methodology used in this research is expressed in Chapter 3.

Finally, Chapter 4 contains the results conducted in this study and Chapter 5 includes conclusions from the results.

Chapter 2: Literature Review

2.1 Water Alternating Gas Oil Recovery Mechanism (WAG)

Oil production operations of oil reservoirs are mostly carried out in three stages of primary, secondary and tertiary. Primary production is the initial production caused by natural energy sources in a reservoir, which includes gravity drainage, fluid and rock expansion, solution gas drive, gas cap drive and natural water drive. After primary operation declines, secondary recovery methods will be applied to maintain the depleted reservoir pressure by injecting water or gas. The injected water or gas displaces oil toward producing wells. In tertiary recovery operations one or more fluids will be injected into the oil reservoir to recover the remaining oil left behind the primary and secondary processes. Tertiary methods are called EOR which stands for enhanced oil recovery. In 1998, Green and Willhite classified EOR methods in five categories: thermal, miscible, chemical, mobility control and microbial processes.

Water alternating gas or WAG injection is an EOR technique for improving oil recovery by combining effects of water flooding and gas flooding. Basically, WAG injects slugs of gas and water sequentially in several cycles.

2.1.1 Types of the WAG Process Design

Depending on the injection methods and the reservoir pressure WAG processes are often classified in five groups. Miscible WAG (MWAG), immiscible WAG (IWAG), hybrid WAG (HWAG), simultaneous WAG (SWAG) and selectively simultaneous WAG (SSWAG) are common WAG processes (Christensen et al., 1998; Al- Mamari et al., 2007; Skauge and Dale, 2007).

A miscible WAG process occurs when the reservoir pressure is above the MMP (minimum miscibility pressure) and the injected gas is miscible with oil in either the first contact or multiple

contacts. The MWAG method mobilizes the trapped oil by decreasing the oil viscosity. However, in an immiscible WAG process, reservoir pressure is below the MMP and the injected gas is not miscible with the reservoir oil (Green and Willhite, 1998).

Hybrid WAG is referred to injecting a large slug of gas followed by injecting a small number of slugs of water and gas. In this method, a big amount of the gas injected to a reservoir is costly.

In simultaneous WAG, water and gas are injected into a reservoir at the same time through a single injection well. This method is not economical because the injected gas in this method cannot be reinjected to the reservoir. When water and gas are injected at the same time but through a dual completion injector without mixing them on the surface, the WAG process is called selectively simultaneous WAG. In the SSWAG method usually water is injected at the upper portion and gas is injected in the lower part of a formation.

2.2 Effective Factors in WAG Process Design

WAG injection is an EOR technique to improve oil recovery by modifying a mobility ratio and sweep efficiency.

The displacement efficiency *E* is considered as the product of microscopic and macroscopic displacement efficiencies:

$$\boldsymbol{E = E_{Macro} * E_{Micro}}$$

where *E* is the volume of oil recovery by EOR divided by the amount of the initial oil in place at the start of *EOR* (Green and Willhite, 1998).

Microscopic sweep efficiency represents the displacement of the oil at the pore level. Basically, E_{Micro} refers to the effect of the displacing fluid in mobilizing the oil at the pore scale. The volumetric or macroscopic displacement efficiency is displacing fluids in a volumetric scale which

refers to the vertical and horizontal sweep efficiencies of the displacing fluid in sweeping out the volume of a reservoir (Green and Willhite, 1998):

$$\boldsymbol{E_{Macro} = E_v * E_h}$$

Gas microscopic efficiency of the oil is normally better than the water microscopic displacement at the pore scale, because there is lower IFT (interfacial tension) in a gas-oil system compared to an oil-water system. However, gas low viscosity and high mobility result in gas fingering and early gas breakthrough, and, therefore, water has better macroscopic sweep efficiency. Hence, it is essential to control the gas-oil mobility ratio in a WAG injection process (Green and Willhite, 1998).

A mobility ratio is defined by Thomas (Green and Willhite, 1998) as the mobility of the displacing fluid (λ_D) divided by the mobility of the displaced fluid (λ_d):

$$\boldsymbol{M = \lambda_D / \lambda_d}$$

Mobility is defined as relative permeability divided by viscosity.

$$\boldsymbol{\lambda_D = \frac{k_D}{\mu_D}} \text{ and } \boldsymbol{\lambda_d = \frac{k_d}{\mu_d}}$$

Considering a gas-oil system we have:

$$\boldsymbol{\lambda_g = \frac{k_{rg}}{\mu_g}} \text{ and } \boldsymbol{\lambda_o = \frac{k_{ro}}{\mu_o}}$$

where k_{rg} and k_{ro} are the relative permeabilities of gas and oil and μ_g and μ_o are the viscosities ofr gas and oil, respectively. Therefore, gas has a high mobility due to its low viscosity.

A mobility ratio less than one (M<1) is considered favourable, and the mobility ratio greater than 1 (M>1) is unfavorable, which happens when the injected gas has a higher mobility than the reservoir oil (Green and Willhite, 1998).

Gravity segregation is another factor affecting the oil recovery by WAG which influences the vertical sweep efficiency. Injected water migrates towards the lower layers of a formation because of the gravity segregation effect, and the injected gas rises to the top of the reservoir (Green and Willhite, 1998).

As a result of the above discussions, injecting too much water will result in the poor microscopic efficiency and injecting large amounts of gas will reduce the macroscopic sweep efficiency. In order to optimize the WAG efficiency, we need to adjust the right amount of the injected gas and water into the reservoir.

2.2.1 Heterogeneity of the Reservoir

Heterogeneity refers to the different degree of interaction between the pores of a formation. The non-uniformity of pore sizes causes complex fluid flow in reservoir pores. Basically, a heterogeneous reservoir is a formation with different porosity and permeability in the reservoir pores and layers. Heterogeneity of the reservoir affects various parameters such as relative permeability, a mobility ratio and capillary pressure (Bradley, 1987; Green and Willhite, 1998). Therefore, reservoir heterogeneity has a big effect on the sweep displacement during a WAG process.

2.2.2 Fluid Properties and Rock-Fluid Interaction

The properties of a reservoir fluid are determined in the laboratory. Rock-fluid interactions depend on the fluid properties and the wettability of the reservoir. Rock wettability impacts the rock main attributes of multi-phase properties such as capillary pressure and relative permeability curves and as a result fluid movement and distribution in reservoir pores. Most of reservoirs rocks are not

completely water-wet or oil-wet; they have mixed-wettability (Bradley, 1987; Green and Willhite, 1998).

2.2.3 Injection Pattern

The injection gas in a WAG process can be hydrocarbon or non-hydrocarbon, for example, CO_2. The type of the gas injecting in a reservoir depends on the location and availability of the gas and also the economic concerns. Generally, CO_2-WAG injection is known as a miscible WAG process but depending on the reservoir temperature and pressure and oil viscosity, CO_2-WAG injection can be miscible, immiscible or partially miscible (Bradley, 1987; Green and Willhite, 1998).

The sweep efficiency of oil is strongly influenced by the distance between an injector and producers (Christensen et al., 1998). Therefore, the well spacing plays a big role in a WAG process. The most popular patterns used in WAG injection are five-spot and nine-spot patterns.

In this study, injected gas is CO_2 and the well spacing pattern is 5-spot, including one injector and four producers.

2.2.4 WAG Ratio and WAG Cycle Time

A WAG ratio is the ratio of the water slugs to the gas slugs injecting alternately within a reservoir. A WAG ratio is very important in obtaining optimal oil recovery (Christensen et al., 2001; Skauge and Dale, 2007; Wu et al., 2004). According to some literature, a WAG ratio can be dependent on the reservoir wettability and fluid properties (Skauge and Dale, 2007; Wu et al., 2004).

A small WAG ratio may cause pressure to decline rapidly and an early gas breakthrough, while a big WAG ratio may trap some oil by water blocking (Skauge and Dale, 2007; Wu et al., 2004).

A WAG cycle in another important factor, which can be optimized by doing a sensitivity analysis using simulator software (Skauge and Dale, 2007; Wu et al., 2004).

2.2.5 Injector and Producer Bottom-Hole Pressure

Well facilities have some limitations such as the injector bottom-hole pressure should not exceed a certain limit. The producer bottom hole-pressure plays an important role in oil production; if this pressure is very lower than the bubble point pressure, more gas will be produced and if it is above the solvent or gas minimum miscibility it will make the process a miscible WAG injection.

In this study, the producer bottom-hole pressure is considered higher than the bubble point pressure and less than the MMP pressure so that around the producers CO_2 is not miscible with oil.

2.2.6 Three-Phase Relative Permeability

The relative permeability concept was defined to modify Darcy's law for multi-phase flow in porous media. Relative permeability values strongly control the flow mechanics, and are defined as functions of water saturation (in a water/oil system) or liquid saturation (in a gas/liquid system).

In the system of two phases, one phase saturation is either increasing or decreasing so it is not hard to estimate the relative permeabilities. However, in the case of three phases, there are infinite scenarios of displacement paths to consider. Unfortunately, there is not a very accurate method to estimate the relative permeability in a three-phase system.

Three-phase relative permeabilities are essential in determining the phase mobility, and, therefore, they have a strong impact on the oil recovery.

There are two approaches to determine the three-phase permeability. One method is the direct measurement of the three-phase relative permeability by core flooding experiments, and the other approach is an estimation of the three-phase relative permeability using the relative permeability data from two-phase systems.

In this research, the second approach was considered. Well known correlations of the three-phase relative permeability by using two-phase data are by Stone and Baker (Stone, 1970; Baker, 1988). In 1970, Stone presented a probability method which provided interpolated data for three-phase flow from corrected two-phase data. The interpolations are continuous functions of the phase saturations. Then, in 1973, he modified his model by involving the gas and water relative permeabilities in the calculation of the oil three-phase relative permeability. Both Stone models were normalized by Aziz and Settari in 1979. The Stone models have a good agreement with the experimental data and are the common models used in simulation software.

The first and second Stone models were proposed for a water-wet system, in which gas and water relative permeabilities are dependent only on gas and water saturations, respectively, although they have been used for any reservoir wettability. A saturation weighted interpolation between two phase relative permeability data was presented by Baker in 1988. In Baker's model, the oil relative permeability is based on a simple saturation weighted interpolation between the oil/gas and water/oil two-phase data. Baker also proposed a linear interpolation. This model assumes a straight line between the corresponding equal permeabilities on the oil/gas and oil/water curves in the ternary diagram and determines the three-phase oil relative permeability.

2.3 Hysteresis of the Relative Permeability

2.3.1 Importance of Hysteresis Effects in WAG

Hysteresis effects result from the reversal of the saturation changes from increasing to decreasing or vice versa, for example, changing from imbibition to drainage or drainage to imbibition. The hysteresis effect in relative permeability can be considered between two consecutive injections when they are carried out in the same direction, for example, alternating injection of water and gas in the same direction. Therefore, good knowledge of three-phase relative permeability accounting for cyclic hysteresis effects is needed for the numerical simulation of a WAG process.

Hysteresis effects were studied widely for both two phases and three phases. In the next section some of these studies are summarized.

2.3.2 Studies of Hysteresis Effects of Relative Permeability

In the multiphase flow in porous media the concept of relative permeability is very important. Relative permeability of a given phase accounts for the reduction in its flow due to the mutual interaction of different flowing phases. Relative permeability is a function of saturations, similar to other rock and fluid properties (e.g., wettability, a flow rate, interfacial tension and saturation history).

As mentioned earlier, the most commonly used interpolation models of relative permeability in reservoir simulators are Stone I (Stone, 1970), Stone II (Stone, 1973), and saturation-weighted interpolation (Baker, 1988). However, it has been investigated that the ability of those interpolation models to reproduce direct experimental measurements of three-phase relative permeabilities is very much limited (Baker, 1988; Delshad and Pope, 1989; Oak et al., 1990; Oak, 1990; Hicks and Grader, 1996; Oliveira and Demond, 2003). These simple interpolation models are not able to

reproduce hysteresis effects, which are dependent on the saturation path history. Some relative permeability models have been developed to consider the hysteresis effects (Killough, 1976; Carlson, 1981; Lenhard and Parker, 1987; Lenhard and Oostrom, 1998; Jerauld, 1997; Larsen Skauge 1998; Blunt, 2000; Kjosavik et al., 2002; Spiteri et al., 2008). Unfortunately, only few of them are implemented in commercial reservoir simulators.

Different authors have investigated the impact of using different interpolation models in numerical simulations, and got the conclusion that recovery predictions could be very different depending on a relative permeability model and a hysteresis model used (Sato and Aziz, 1987; Guzman et al., 1994; Spiteri and Juanes, 2006).

Spiteri and Juanes performed a quantitative analysis of three-phase relative permeability models that account for hysteresis effects (Spiteri and Juanes, 2006). They followed two objectives: 1. validation of the hysteresis of relative permeability models to reproduce the experimental data and 2. evaluating the impact of using different models for immiscible WAG injection. Their work was limited to water-wet systems.

The wettability characteristics of a porous medium have a definitive impact on oil recovery (Jadhunandan and Morrow, 1995). Therefore, much of the research done on relative permeability hysteresis and trapping was studied and explained by means of pore-scale modeling (Dixit et al., 1999; Øren and Bakke, 2003; Al-Futaisi and Patzek, 2003; Valvatne and Blunt, 2004; Piri and Blunt, 2005; Spiteri et al., 2008). Spiteri et al. developed a new model of trapping and hysteresis for two-phase flow validating by their model (Spiteri 2005) against pore-network simulations. It covers the entire range of wettability conditions.

Below the common hysteresis models for two-phase and three-phase hysteresis are presented.

2.3.2.1 Two-Phase Hysteresis Models

A non-wetting phase saturation left trapped after a flow reversal determines the significance of hysteresis. The non-wetting phase is mostly considered as the gas phase for both water-wet and oil-wet three-phase systems. In 1968, Land proposed a trapping model for gas saturation left after imbibition. The trapped gas saturation by Land is computed as follows:

$$S_{gt} = S_{gc} + \frac{S_{g,hy} - S_{gc}}{1 + C(S_{g,hy} - S_{gc})}$$

where *C* is called the Land trapping parameter which is dependent on the type of rock and fluids and is defined as:

$$C = \frac{1}{S_{gt,max} - S_{gc}} - \frac{1}{S_{g,max} - S_{gc}}$$

Trapped gas saturation	S_{gt}
Critical gas saturation	S_{gc}
Gas saturation after flow reversal	$S_{g,hy}$
Maximum trapped gas saturation	$S_{gt,max}$
Maximum gas saturation	$S_{g,max}$

Most relative permeability hysteresis models that incorporate hysteresis are based on the Land trapping model (Killough, 1976; Carlson 1981; Lenhard and Parker, 1987; Lenhard and Oostrom, 1998; Jerauld, 1997; Blunt, 2000).

The hysteresis models by Killough (1976) and Carlson (1981) are famous models for two-phase systems and they are implemented in commercial simulators. They both presented a model for a scanning imbibition curve and assumed that to be representative of any subsequent drainage process.

Killough proposed the following gas relative permeability scanning curve:

$$k_{rg}^{i}(S_g) = \frac{k_{rg_{(o)}}^{i}(S_{g,norm})k_{rg_{(o)}}^{d}(S_{g,hy})}{k_{rg_{(o)}}^{d}(S_{g,max})}$$

Consider $$S_{g,norm} = S_{gt,max} + \frac{(S_g - S_{gt})(S_{g,max} - S_{gt,max})}{(S_{g,hy} - S_{gt})}$$

Relative permeability value on the bounding imbibition $k_{rg_{(o)}}^{i}$
Relative permeability value on the bounding drainage $k_{rg_{(o)}}^{d}$

In the Carlson model, the scanning curve is considered parallel to the imbibition curve. Basically, the imbibition curve will be shifted horizontally until it intersects the saturation point where the flow reversal occurs.

A new model of trapping and relative permeability hysteresis for all wettability characteristic was proposed in 2008 (Spiteri et al., 2008). In their study, they evaluated the Land model for the trapping phase and relative permeability hysteresis by means of pore-network simulation of primary drainage and water flooding. They used a phase flow pore-network simulator developed by Valvatne and Blunt (2004). The use of pore-network simulations allows them to quantify the effect of wettability and initial oil saturation on the trapping of oil during water flooding. This study validated the Land model for water-wet systems but in oil-wet media the Land model underestimates the relative permeabilities. Therefore, they modified the Land trapping model for oil-wet media using two parameters correspond to the initial slope and the curvature of the curve of the trapped oil saturation versus the initial oil saturation. The modified model was validated using their pore-network simulator.

2.3.3.2 Three-Phase Hysteresis Models

There have been many studies on three-phase relative permeability hysteresis, and it has been observed that the assumption of reversibility of the drainage and imbibition scanning curves in two-phase models is inappropriate. It was shown that the gas relative permeability is higher when

only oil is displacing rather than when a water–oil mixture is displacing after water flooding, and also water permeability is reduced after gas injection (Lenhard and Parker, 1987; Lenhard and Oostrom, 1998; Larsen and Skauge, 1998; Egermann et al., 2000; Spiteri and Juanes, 2006).

The most successful model which is implemented in commercial simulators is by Larsen and Skauge in 1998. This model was implemented for a water-wet system, where the non-wetting phase is gas and the wetting phase is considered water (Larsen and Skauge, 1998).

In the Larsen and Skauge model, the hysteresis model of the gas phase follows the theory of Land and Carlson. The water phase model interpolates between two-phase and three-phase relative permeability curves, where the three-phase water relative permeability is interpreted as the relative permeability after gas flooding.

Considering a typical drainage process for the gas phase (i.e., increasing gas saturation) reaching a maximum gas saturation, followed by an imbibition process (i.e., decreasing gas saturation) leading to a trapped gas saturation, the Land trapped gas saturation is given by (Land, 1968):

$$\boldsymbol{S_{gt} = S_{gc} + \frac{S_{g,hy} - S_{gc}}{1 + C(S_{g,hy} - S_{gc})}}$$

Also the free gas saturation $\boldsymbol{S_{gf}}$ is calculated from Land's equation as:

$$\boldsymbol{S_{gf} = S_{gc} + \frac{1}{2}\left\{(S_g - S_{gt}) + \sqrt{(S_g - S_{gt})^2 + \frac{4}{C}(S_g - S_{gt})}\right\}}$$

The gas relative permeability on the drainage to imbibition scanning curve is given by (Larsen and Skauge, 1998):

$$\boldsymbol{k_{rg}(S_g) = k_{rg}^{d}(S_{gf})}$$

If once again, the gas saturation decreases, then a secondary drainage curve will be followed. The secondary drainage curves are calculated using the following equation (Larsen and Skauge, 1998):

$$k_{rg}^{d}\left(S_g; S_g^{start}; S_w^{start}\right) = k_{rg}^{i}\left(S_g^{start}\right) + \left(k_{rg}^{input}(S_g) - k_{rg}^{input}\left(S_g^{start}\right)\right)\left(\frac{S_{wc}}{S_w^{start}}\right)^{\alpha}$$

Relative permeability calculated for the secondary drainage	k_{rg}^{d}
Relative permeability at the start of the secondary drainage process (which is k_{rg} at the end of the imbibition curve)	$k_{rg}^{i}\left(S_g^{start}\right)$
Input relative permeability at S_g	k_{rg}^{d}
Input relative permeability at the gas saturation (at the start of the secondary drainage curve)	$k_{rg}^{d}\left(S_g^{start}\right)$
Connate water saturation	S_{wc}
Water saturation at the start of the secondary drainage curve	S_w^{start}
Reduction exponent	α

α accounts for a reduction in the gas phase relative permeability in the presence of mobile water. The above equation implies that the gas phase relative permeability is a function of the history of both the gas and water phase saturations (Larsen and Skauge, 1998).

Further imbibition curves will be calculated by transforming the saturation using Land's free gas saturation equation with the trapped gas saturation (S_{gt}) defined as the maximum trapped gas over all the WAG cycles. The transformed saturation will be then looked up on the secondary drainage curve (Larsen and Skauge, 1998).

The water mobility following gas flooding is significantly reduced relative to its mobility in the original oil-water system. Therefore, in addition to the usual two-phase relative permeability curve of oil-water flow another curve for a three-phase flow scenario that represents the water relative permeability following gas flooding is required as well (Larsen and Skauge, 1998).

For an imbibition process which is increasing in water saturation, the relative permeability is interpolated between the two- ($\boldsymbol{W_1}$) and three-phase ($\boldsymbol{W_2}$) curves as follows (Larsen and Skauge, 1998):

$$\boldsymbol{k_{rw}^{i} = k_{rw}^{W_1}\left(1 - \frac{S_g^I}{S_{g,max}}\right) k_{rw}^{W_2}\left(\frac{S_g^I}{S_{g,max}}\right)}$$

Calculated imbibition relative permeability	$\boldsymbol{k_{rw}^{i}}$
Relative permeability read from the two-phase curve	$\boldsymbol{k_{rw}^{W_1}}$
Three-phase relative permeability	$\boldsymbol{k_{rw}^{W_2}}$
Maximum attainable gas saturation, $1 - \mathrm{S_{wcon}} - \mathrm{S_{oirg}}$	$\boldsymbol{S_{g,max}}$
Gas saturation at the start of the increasing water saturation (imbibition) process	$\boldsymbol{S_g^I}$
Connate water saturation	$\boldsymbol{S_{wcon}}$
Irreducible oil in the gas-liquid table	$\boldsymbol{S_{oirg}}$

A subsequent drainage relative permeability will be handled by interpolation between the imbibition curve and either the three-phase curve or the two-phase curve, depending on the gas saturation (Larsen and Skauge, 1998).

2.3.2.3 Evaluating Impact of Using Different Hysteresis Models

The impact of using different interpolation models in field-scale simulations have been reported by a number of researchers. It was observed that recovery predictions could be significantly different depending on a three-phase relative permeability model.

Sato and Aziz investigated the sensitivity of predictions to three-phase relative permeability for steam displacement and their analysis showed that relatively high water and gas relative permeabilities from two-phase data lead to higher oil relative permeability in Stone I and Stone II models, and the reverse is valid when gas and water relative permeabilities are relatively low. Also, the differences in predicted oil relative permeability by the Stone models are the greatest where oil saturations is low (Sato and Aziz, 1987).

Sato and Aziz's research was done using three sets of relative permeability data. Data Sets 1, 2 and 3 were characterized, respectively, by moderate, low and high values of water and gas relative permeabilities. The oil relative permeability predicted for Data Set 1 by two Stone models was about the same. But oil relative permeability values by Stone models were quite different in Data Sets 2 and 3. However, oil production predictions with Stone I and Stone II for Data Set 3 are not very different. Stone models showed significant differences in the simulation results for Data Set 2. They also investigated saturation profiles near production and injection wells. It was observed that low water and gas relative permeability values in Data Set 2 tend to drive saturations into the range where two Stone models give different results, and high water and gas relative permeabilities values in Data Set 3 tend to keep saturations in the range where the two Stone models give similar results (Sato and Aziz, 1987).

Therefore, the differences in predicted oil relative permeability by Stone I and Stone II models are most likely to influence steam-flood simulation results.

In 1990, Oak also reported the errors of interpolating three-phase relative permeability hysteresis from two-phase data. He investigated that interpolated values may differ significantly from experimental values.

Oak studied two-phase and three-phase relative permeabilities of water-wet Berea sandstone. The experimental results did not support Stone models predictions of three-phase oil relative permeability. He got the conclusion that the effect of saturation history on the water (wetting phase) permeability is not significant and two-phase and three-phase relative permeabilities are approximately the same at the same water saturations. Also, two-phase and three-phase gas (non-wetting phase) permeabilities were approximately the same at the same saturation and saturation history of the gas phase. However, oil (the intermediate phase) relative permeability depends on

the oil saturation of all three phases - oil, gas and water and the Stone models do not account the displacement of trapped oil by gas which is an important factor impacting three-phase oil permeability. He also concluded that a critical oil phase saturation exists to initiate three-phase flow from water-oil two-phase flow, which can be different from that in the two-phase flow (Oak, 1990).

In addition, Guzman in 1994 reported that there was a significant difference on the predictions associated with the three-phase relative permeability models for field-scale simulations of gas and WAG injections.

In 2005, Spiteri and Juanes evaluated the accuracy of relative permeability models by comparing their predictions with Oak experimental data in his research in 1990. In order to check the accuracy of the relative permeability models they have done three experiments. The following figures from their paper show the saturation path in the experiments and the correlation between modeled and experimental data for water relative permeabilities for each displacement path, respectively (Spiteri and Juanes, 2006).

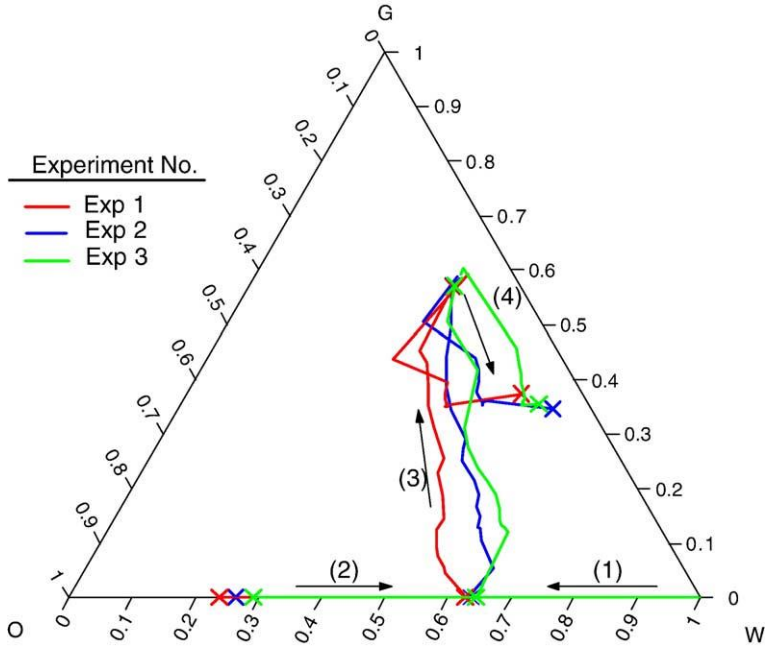

Figure 2.1 Oak's relative permeability data for selected experiments' saturation paths by Spiteri and Juanes, 2006.

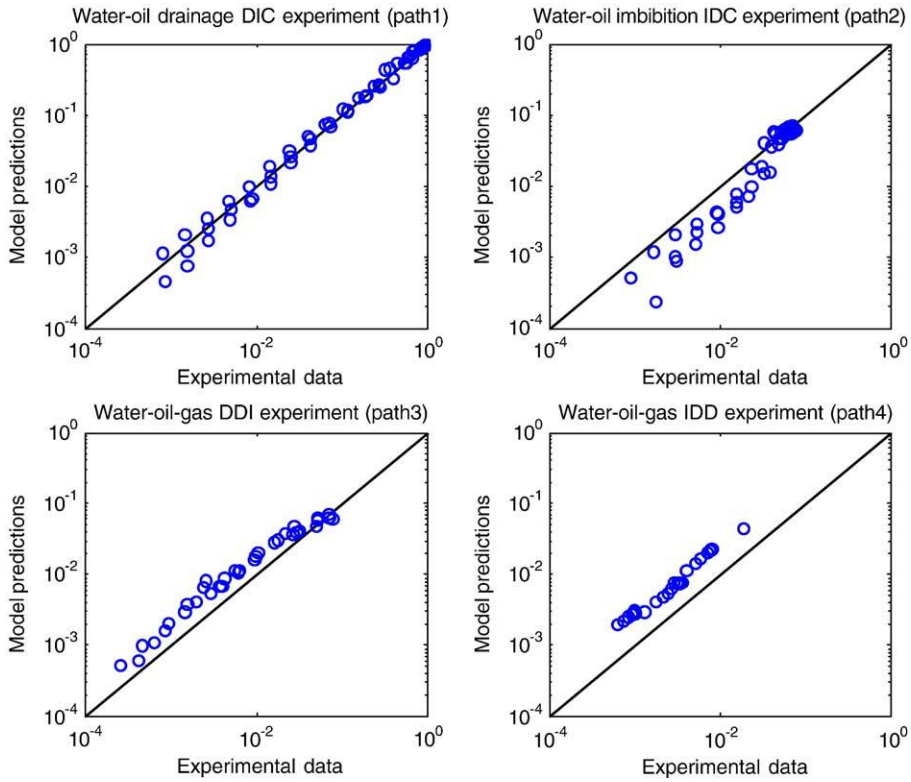

Figure 2.2 Water relative permeabilities correlation between experimental and modeled for each displacement path by Spiteri and Juanes, 2006.

According to the constructed scatter plots by Spiteri and Juanes, the predicted relative permeabilities for the first displacement path 1 are accurate for all three experiments. The predicted relative permeabilities in the path 2 slightly underestimated the water relative permeability at low saturations. In the gas injection process path 3, the relative permeability values are overestimated. Finally, path 4 showed less accuracy where there is water flooding after gas flooding and it overestimated the water relative permeability values. Therefore, they concluded that the water relative permeability is only a function of water saturation and it is not dependent on the saturation history. Hence, they concluded that the relative permeabilities obtained from the primary drainage oil–water experiment are sufficiently accurate for modeling water relative permeability.

The following figures show the Stone I, Stone II and Baker models are not accurate for interpolating oil relative permeability from two-phase data. The Stone 1 model performance was the best in comparison to the Stone II and Baker models for water flooding and gas flooding in any saturation range (Spiteri and Juanes, 2006).

Since the Stone II model predictions for path 3 and 4 were significantly underestimated, a scatter plot would not be helpful and they presented their results with the saturation path figures.

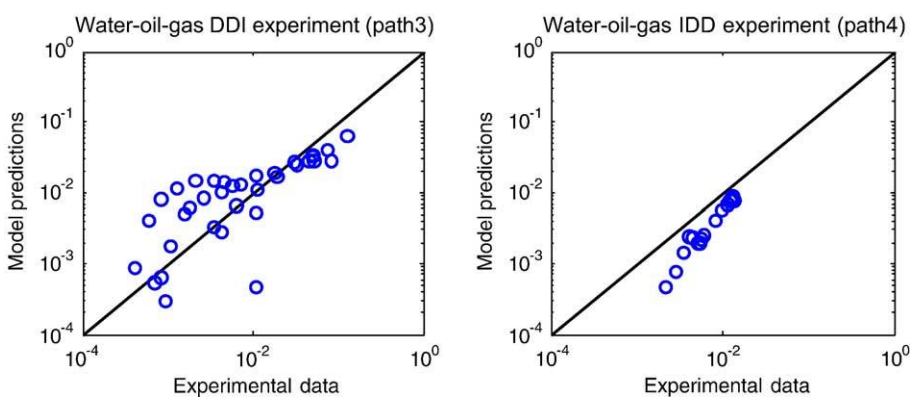

Figure 2.3 Oil relative permeabilities correlation between experimental and Stone I interpolation by Spiteri and Juanes, 2006.

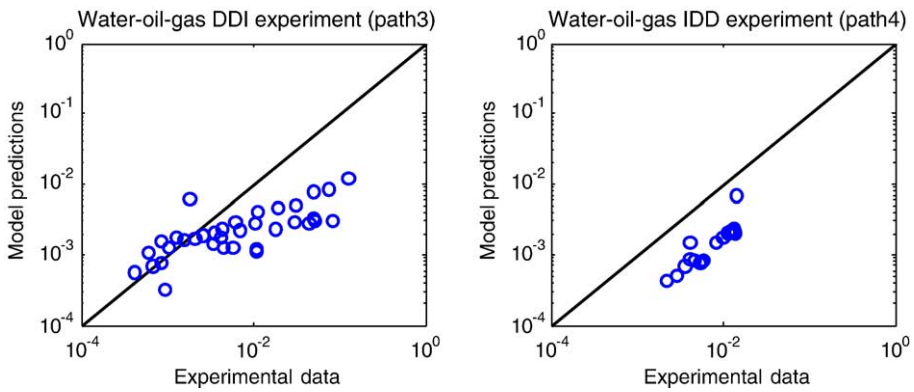

Figure 2.4 Oil relative permeabilities correlation between experimental and Baker interpolation model by Spiteri and Juanes, 2006.

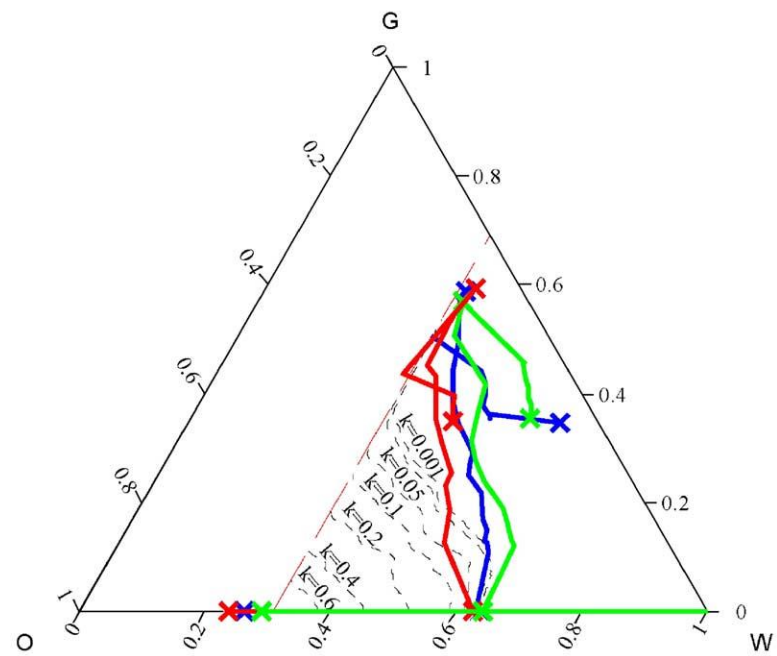

Figure 2.5 Experimental data paths and Stone II model of predicted oil isoperms by and by Spiteri and Juanes, 2006.

This study also indicated that the predicted relative permeabilities are slightly higher than experimental ones in the gas injection process especially in the low gas saturation region. In addition, in the water injection process following the gas injection, the predicted relative permeabilities are overestimated in comparison with the three-phase experimental ones, because the impact of gas trapping was not considered in the modeling.

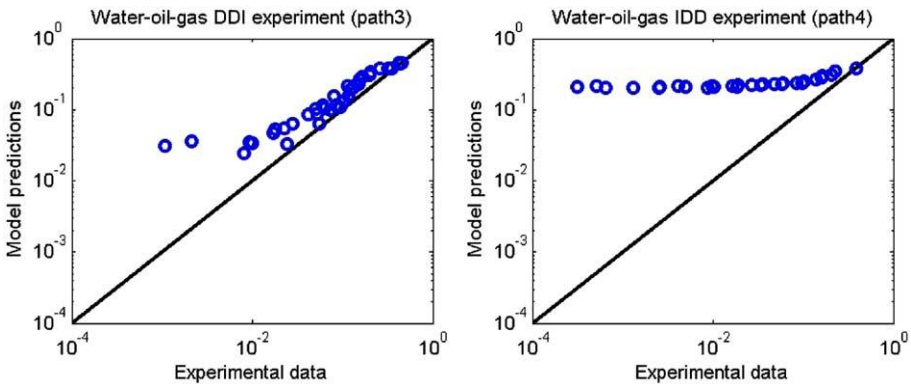

Figure 2.6 Different three-phase displacements paths 3 and 4 gas relative permeability comparison, with the two-phase gas relative permeability from an oil/gas gas-flood experiment by Spiteri and Juanes, 2006.

Since hysteresis models are mostly based on the Land trapping model, Spiteri and Juans investigated the Land trapping coefficient and their experimental data indicated that the Land coefficient depends on the advancing contact angle remarkably.

Spiteri and Juanes then evaluated the current hysteretic relative permeability models in commercial reservoir simulators by Killough in 1976, Carlson in 1981 for two phases and Larsen and Skauge in 1998 for three phases. The following scatter plots of their investigation show that all these models overestimate the gas relative permeability during cyclic water and gas injection processes.

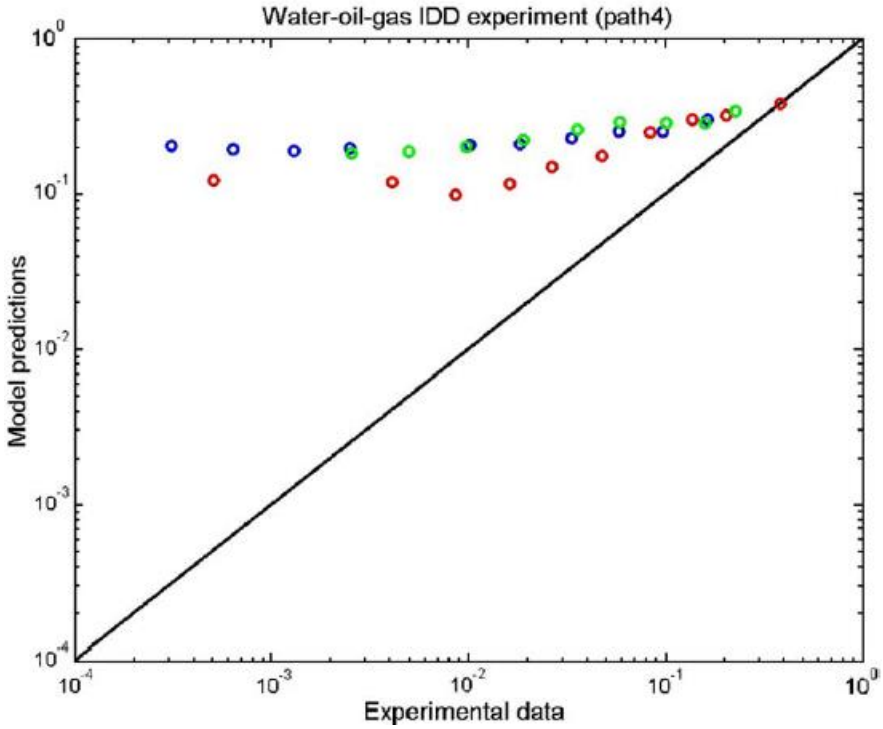

Figure 2.7 Killough's two-phase hysteresis model of a three-phase water-flood, path 4's scatter plot, by Spiteri and Juanes, 2006.

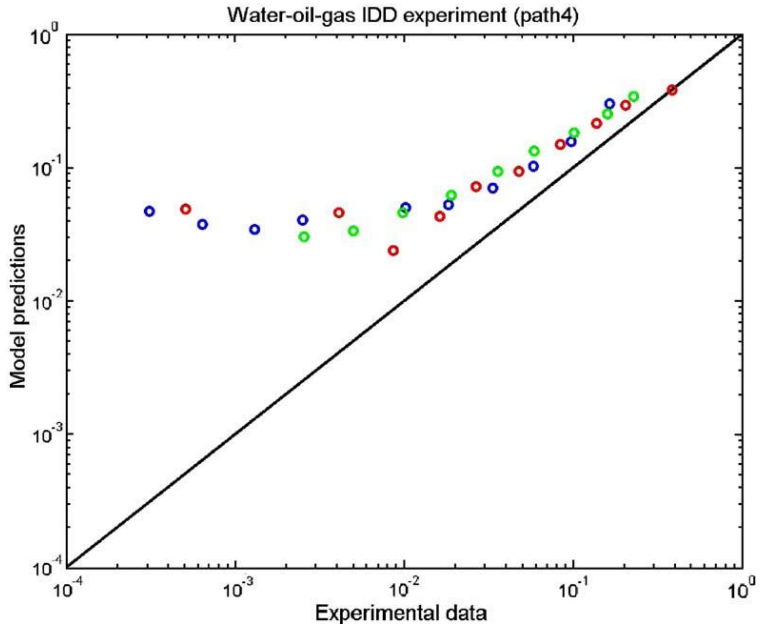

Figure 2.8 Carlson's two-phase hysteresis model of a three-phase water-flood, path 4 model's scatter plot, by Spiteri and Juanes, 2006.

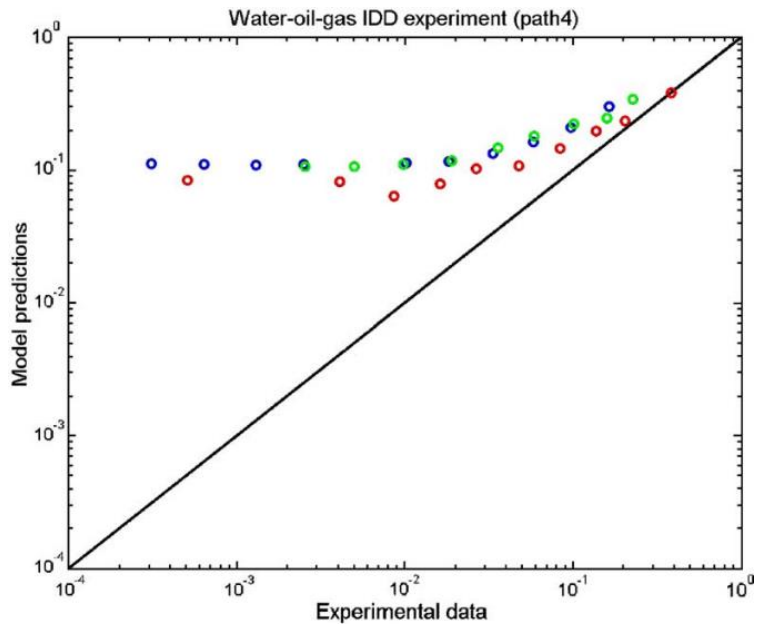

Figure 2.9 Gas relative permeability predicted by the WAG three-phase hysteresis of a three-phase water-flood, path 4 model's scatter plot, by Spiteri and Juanes, 2006.

They also used numerical simulations to show that the recovery results differ remarkably by considering different hysteresis models. It was also reported that models without hysteresis tend to underestimate the recovery in comparison with models using hysteresis. The results of numerical simulations done on a quarter five-spot pattern in a homogenous, two-dimensional reservoir are presented in the following table. They used the commercial black-oil simulator Eclipse 100 (Schlumberger Geo-Quest, 2003).

Table 2.1 Synthetic reservoir test case simulation results adapted from Spiteri and Juanes, 2006.

Case	Recovery Scheme	Hysteresis Model	Interpolation Model	Land Parameter (C)	% Recovery	% Difference From Base Case
1	Waterflood (Base Case 1)	None	None	N/A	49.0%	0.0%
2	WAG (Base Case 2)	None	Baker	N/A	50.8%	0.0%
3	WAG (Base Case 2)	None	Stone I	N/A	57.9%	0.0%
4	WAG (Base Case 2)	None	Stone II	N/A	55.9%	0.0%
5	WAG	Carlson	Baker	0.78	53.2%	4.7%
6	WAG	Carlson	Stone I	0.78	63.4%	9.5%
7	WAG	Carlson	Stone II	0.78	60.1%	7.5%
8	WAG	Killough	Baker	0.78	53.3%	4.9%
9	WAG	Killough	Stone I	0.78	62.8%	8.5%
10	WAG	Killough	Stone II	0.78	60.0%	7.3%
11	WAG	3-Phase WAG	Baker	0.78	53.5%	5.3%
12	WAG	3-Phase WAG	Stone I	0.78	66.8%	15.4%
13	WAG	3-Phase WAG	Stone II	0.78	59.2%	5.9%
14	WAG	3-Phase WAG	Stone I	0.5	67.0%	15.7%
15	WAG	3-Phase WAG	Stone I	1	65.4%	13.0%
16	WAG	3-Phase WAG	Stone I	2	63.1%	9.0%

Later, they added more complexity to their numerical simulations by working on a three-dimensional heterogeneous reservoir modified from the PUNQ-S3 model with multiple injection and production wells. They mentioned in their paper that the PUNQ-S3 model is a well-known reservoir model originally developed as a test case for production forecasting under uncertainty.

Table 2.2 PUNQ-S3 test case simulation results for heterogeneous reservoir adapted from Spiteri and Juanes, 2006.

Case	Recovery Scheme	Hysteresis Model	Interpolation Model	Land Parameter (C)	% Recovery	% Difference From Base Case
1	WAG-PUNQS3 (Base Case)	None	None	N/A	53.9%	0.0%
2	WAG-PUNQS3 (Base Case)	None	Stone I	N/A	57.7%	0.0%
3	WAG-PUNQS3 (Base Case)	None	Stone II	N/A	53.0%	0.0%
4	WAG-PUNQS3	Carlson	Stone I	N/A	59.3%	2.8%
5	WAG-PUNQS3	3P WAG Model	Stone I	0.78	62.9%	9.0%

As a result of Spiter and Juanes research it is very important to consider hysteresis of the relative permeability in the WAG processes but also the choice of an interpolation model and hysteresis plays a big role in prediction results, because the recovery results in the simulations without hysteresis model are highly underestimated and also the recovery results vary depending on the combination of different interpolation and hysteresis models.

There has been much research done later conforming Spiteri and Juanes' investigation. Below the research done by Shahrokhi in 2006 (Shahrokhi et al., 2014) is discussed.

The two-phase relative permeability and capillary pressure data in this study was from three WAG core-flooding experiments (Shahrokhi et al., 2014).

Table 2.3 Comparing different relative permeability models for WAG experiments adapted from Shahrokhi et al., 2014.

Test	Wettability	Direction
WAG-1	Water-Wet	IDIDID
WAG-2	Mixed-Wet	IDIDID
WAG-3	Mixed-Wet	DIDIDIDIDI

They used numerical simulations by different combination of relative permeability correlations and hysteresis models to reproduce their experimental WAG process results under different wettability conditions.

The results did not reproduce the experimental data and they identified the simulation errors comparing the predictions in oil recovery with the experimental oil recovery. Basically, the simulation models either overestimated or underestimated the oil recovery in both water-wet and mixed-wet wettability characteristics. The following figures show their results for each experiment WAG-1, WAG-2 and WAG-3.

WAG-1, water-wet system:

Table 2.4 WAG-1 simulation results- water-wet core starting with water injection adapted from Shahrokhi et al., 2014.

Case	Three-Phase Interpolation Model	Including Hysteresis	Oil Recovery (%S_{orw})	% Error (R_{Sim}-R_{Exp})
1	Stone I	None	34.5	-49.3
2	Stone II	None	54.5	-83.3
3	SWI	None	82.8	-1.0
4	Stone I	Carlson	39.1	-44.7
5	Stone I	Jargon	41.4	-42.4
6	Stone I	Killough	44.0	-39.8
7	SWI	Carlson	98.7	14.9
8	SWI	Jargon	99.2	15.4
9	SWI	Killough	99.9	16.1
10	Stone I	WAG Hysteresis with Constant Parameters	45.6	-38.2
11	Stone I	WAG Hysteresis with Updated Parameters	79.1	-4.7

WAG-2, mixed-wet system:

Table 2.5 WAG-2 - mixed-wet core starting with water injection adapted from Shahrokhi et al., 2014.

Case	Three-Phase Interpolation Model	Including Hysteresis	Oil Recovery (%S_{orw})	% Error (R_{Sim}-R_{Exp})
12	Stone I	None	67.1	-14.5
13	Stone II	None	1.3	-80.3
14	SWI	None	44.2	-37.4
15	Stone I	Carlson	71.3	-10.3
16	Stone I	Jargon	85.3	3.7
17	Stone I	Killough	87.8	6.2
18	SWI	Carlson	57.2	-24.4
19	SWI	Jargon	77.5	-4.1
20	SWI	Killough	75.7	-5.9
21	Stone I	WAG Hysteresis with Constant Parameters	86.9	5.3
22	IKU	None	54.2	-27.4

WAG-3, mixed-wet system:

Case	Three-Phase Interpolation Model	Including Hysteresis	Oil Recovery (%S_{orw})	% Error (R_{Sim}-R_{Exp})
23	Stone I	None	73.1	-8.7
24	Stone II	None	31.7	-50.1
25	SWI	None	61.8	-20.0
26	Stone I	Carlson	95.2	13.4
27	Stone I	Jargon	99.9	18.1
28	Stone I	Killough	100.0	18.2
29	SWI	Carlson	86.7	4.9
30	SWI	Jargon	96.0	14.2
31	SWI	Killough	100.0	18.2
32	Stone I	WAG Hysteresis with Constant Parameters	100.0	18.2
33	IKU	None	71.8	-10.0

Table 2.6 WAG-3 - mixed-wet core starting with gas injection adapted from Shahrokhi et al., 2014.

Based on this literature, errors of different hysteresis models oil recovery from the real oil recovery are not small and it is not sufficient to rely on the relative permeability hysteresis models currently used in the commercial software. In addition, among these models, the Larsen and Skauge model seems to have better performance, which is the hysteresis model used in this study's simulations.

Chapter 3: Properties of the Reservoir Models and Fluids

The base model in this research was created using PVT data included in the material of "CO_2 EOR Modeling Using GEM" presented in a Computer Modeling Group (CMG) Course. The oil properties in this course were used for models with low viscosity oil, and modified versions of them were applied for models with high viscosity oil. The relative permeability curves for both water-wet and oil-wet characteristics were provided by Dr. Shawket Ghedan. Compositional simulation software GEM was used for numerical simulations of this study, and units are considered in field.

3.1 Properties of the Reservoir Models

3.1.1 Reservoir Base Models Gridding

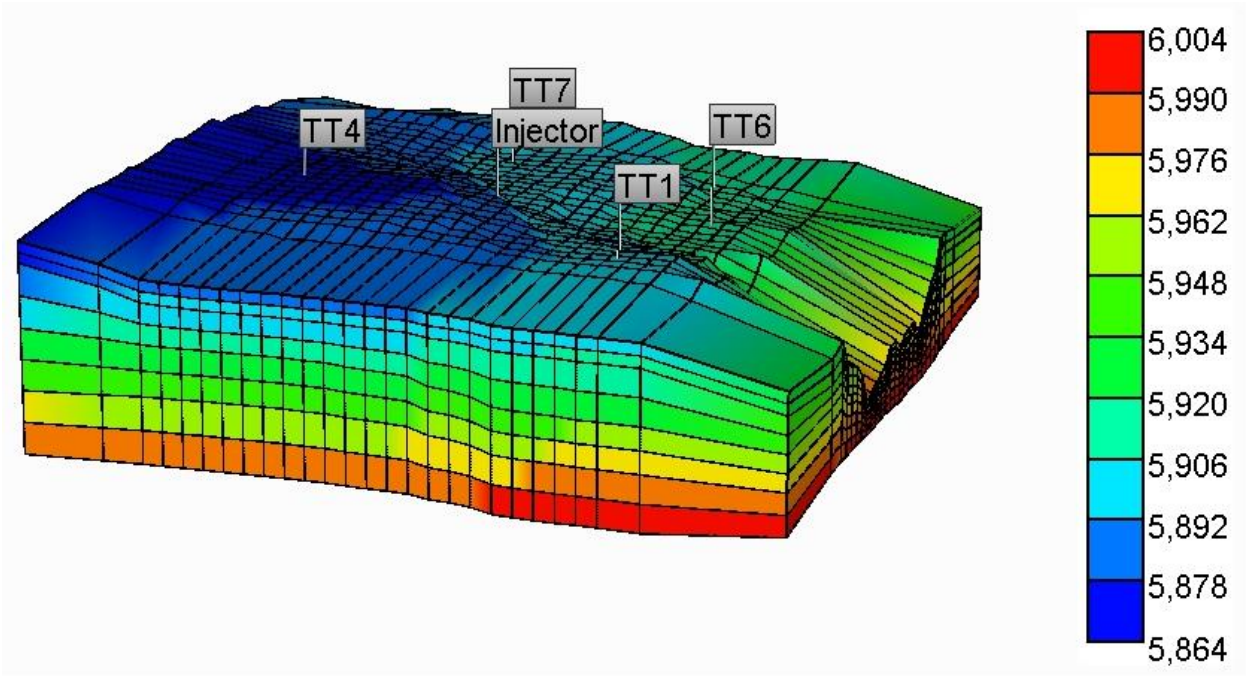

Figure 3.1 Base models 3D grid top.

Orthogonal corner point gridding was applied for a reservoir of eight layers with a thickness of 140 ft.

In the models with a coarse grid size, there are 26*26 blocks in each layer:

I-direction block widths (ft): 1554 460 22*230 460 920

J-direction block widths (ft): 1858 460 22*230 460 1534

In the models with a fine grid size, there are 130*130 blocks in each layer:

I-direction block widths (ft): 5*310.8 5*92 110*46 5*92 5*184

J-direction block widths (ft): 5*371.6 5*92 110*46 5*92 5*306.8

Grid thickness varies from block to block and layer to layer, and it is in the range of 2.4-21.7 feet for both fine and coarse grid size models.

Layer 1 and layer 2 thickness (ft): 2.6-9.5

Layer 3 and layer 4 thickness (ft): 2.4-21.7

Layer 5 and layer 6 thickness (ft): 3.1-20.4

Layer 7 and layer 8 thickness (ft): 3.2-21.2

3.1.2 Reservoir Base Models' Porosity

Reservoir models in this research are heterogeneous, their porosity is in the range of 0.189-0.296, and the average porosity is 0.26. Layers 1-2 have the same porosity as well as layers 3-4, layers 6-5 and layers 7-8. The following figures show the reservoir models porosity for each layer:

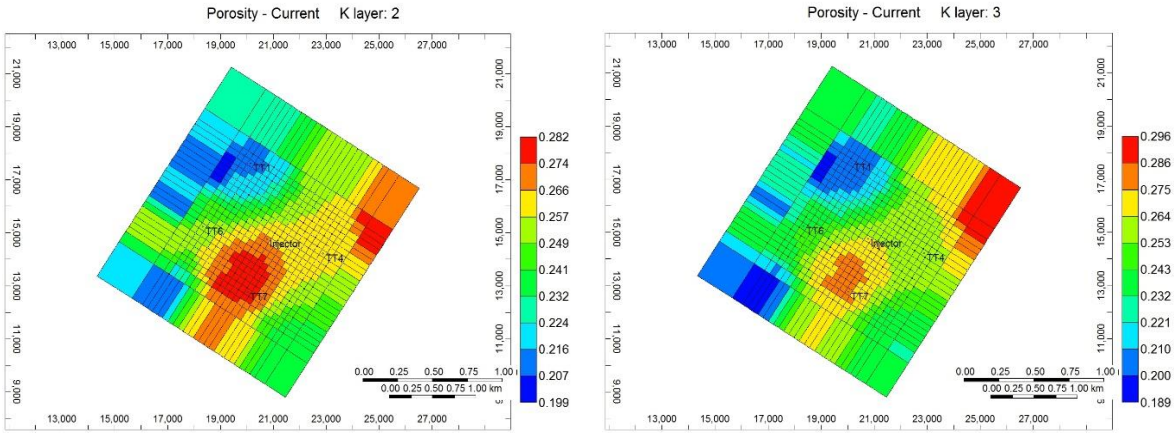

Figure 3.2 Porosity of layers 1 and 2 on the left and layers 3 and 4 on the right.

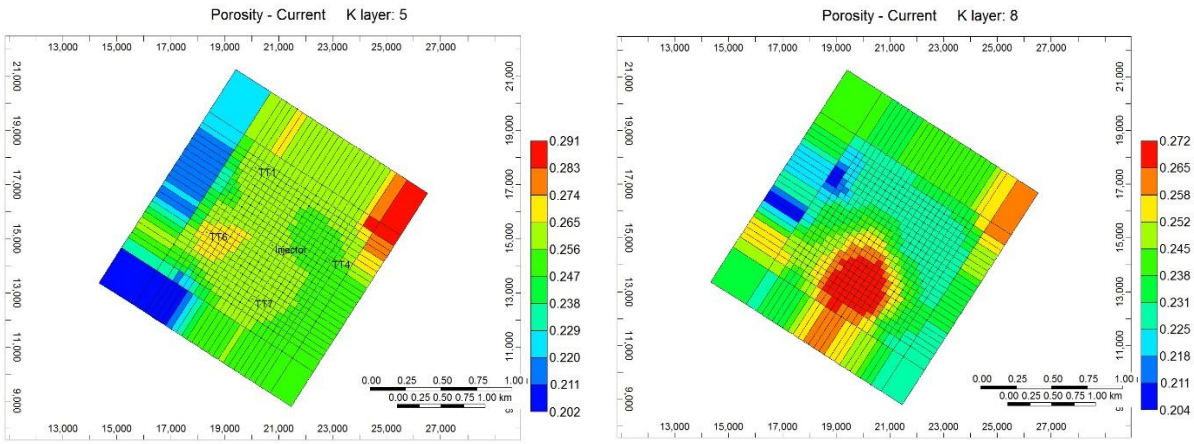

Figure 3.3 Porosity of layers 5 and 6 on the left and layers 7 and 8 on the right.

3.1.3 Reservoir Base Models' Permeability

The reservoir models permeability in the I and J directions are equal and in the range of 0-10,000 md and the vertical permeability is in the range of 0-7,200 md.

The following figures show the permeability for each layer:

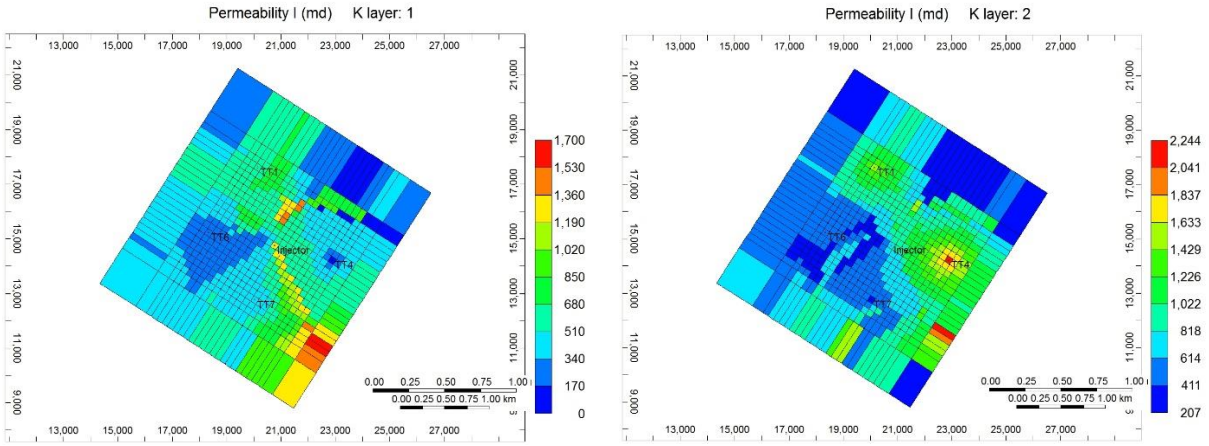

Figure 3.4 Permeability of layer 1 on the left and layer 2 on the right.

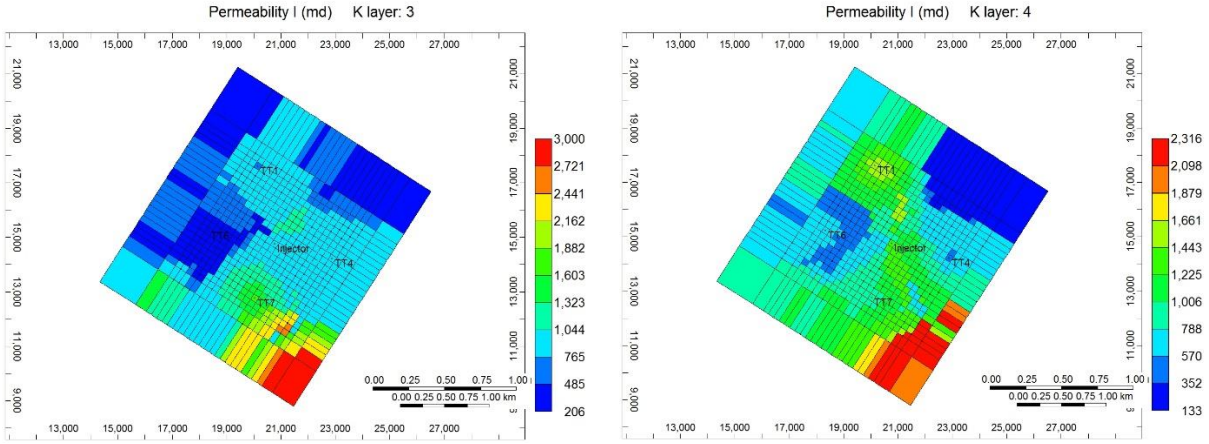

Figure 3.5 Permeability of layer 3 on the left and layer 4 on the right.

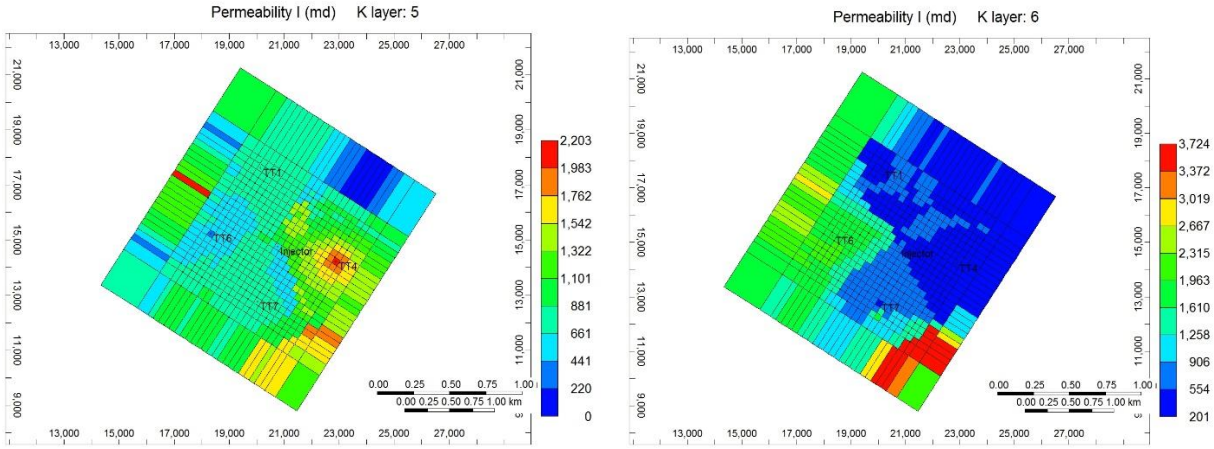

Figure 3.6 Permeability of layer 5 on the left and layer 6 on the right.

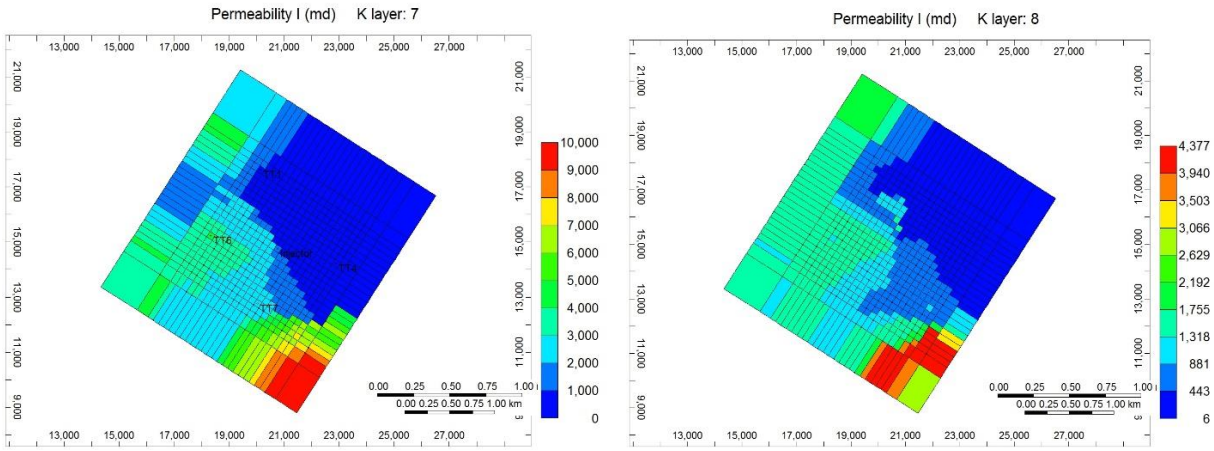

Figure 3.7 Permeability of layer 7 on the left and layer 8 on the right.

3.2 Properties of the Fluids

The models PVT packages were prepared using WinProp CMG software. WinProp is an equation of state (EOS) based fluid behavior and PVT modelling package by CMG Ltd. The laboratory data for fluids can be imported into WinProp and an EOS can be tuned to match its physical behavior. Then using WinProp fluid interactions will be predicted and a fluid model will be created for use in CMG software.

The following steps have been done to create the PVT packages for this study using WinProp:

- Lumping the fluid components into 7 pseudo-components
- Matching saturation pressure for the lumped fluids
- Predicting laboratory experiments
    - Differential liberation
    - CCE (constant composition expansion)
    - CVD (constant volume depletion)
    - Separator GOR
    - Swelling tests

- Matching viscosity data
- Determining minimum miscibility pressure
- Tuning EOS for laboratory-determined MMP

The initial reservoir pressure and temperature are 3,500 psi and 160 F, respectively, and the experimental saturation pressure used for matching is 740 psi.

The next table shows the lab fluid properties:

Table 3.1 Reservoir fluid properties.

API	32
FVF	1.18
GOR	247

The reservoir oil pseudo-components composition was found as:

Table 3.2 Fluid composition.

CO_2	0.011829992
N_2 - C_1	0.11702013
C_2 - nC4	0.12482148
iC_5 - C_7	0.13955734
C_8 - C_{12}	0.065135016
C_{13} - C_{19}	0.31304433
C_{20} - C_{30}	0.22859171

The following table is the oil density data used for the CCE experiment:

Table 3.3 Data used in CCE experiment.

Pressure (psi)	Oil Density (lbm/cf)
2515	49.567
2015	49.442
1515	49.193
1015	49.005
740	48.881
615	48.943
465	49.505

The following table presents the data used in the Diff Lib experiment:

Table 3.4 Data used in Diff Lib experiment.

Pressure (psi)	Oil SG	Oil Viscosity (cP)
740	0.782	2.65
615	0.783	2.68
465	0.792	2.72
315	0.806	2.83
130	0.843	2.89
15	0.853	3.65

The first contact minimum miscibility is above 5,000 psi which is the limit on the facilities. Therefore, there will be no first contact miscibility but multiple contact miscibility can be achieved at 2,750 psi found in the lab.

The models with a lower viscosity fluid, with API 40, have the following pseudo-components composition:

Table 3.5 Lower viscosity fluid composition.

CO_2	0.011829992
N_2 - C_1	0.11702013
C_2 - nC4	0.19453823
iC_5 - C_7	0.22025311
C_8 - C_{12}	0.28150612
C_{13} - C_{19}	0.093977503
C_{20} - C_{30}	0.080874910

3.3 Rock-Fluids' Properties

The following figures are the relative permeability and capillary pressure data used in the simulations for water-wet models.

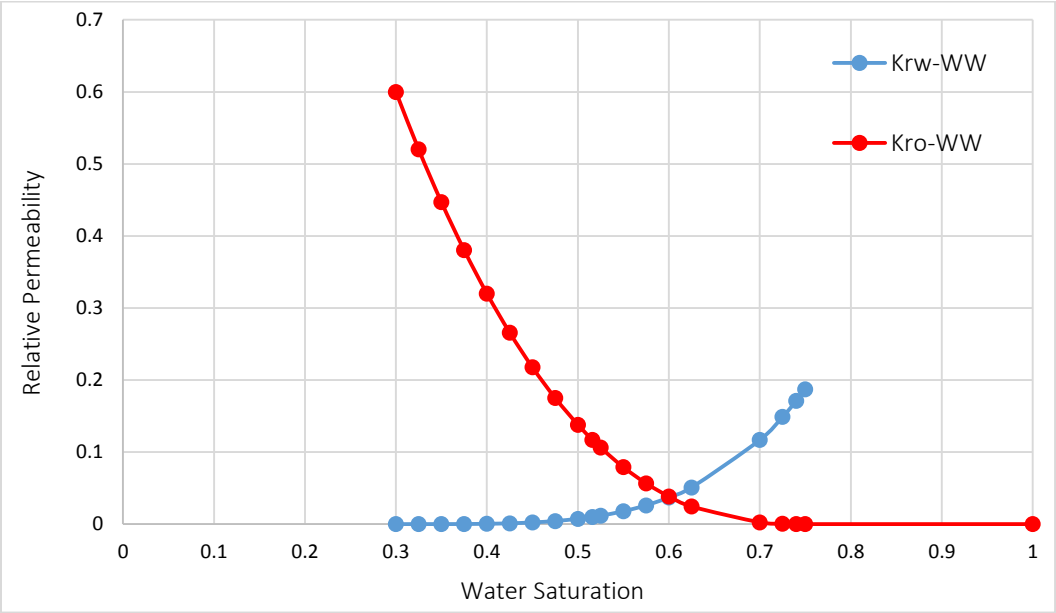

Figure 3.8 Relative permeability curves, water/oil, water-wet system.

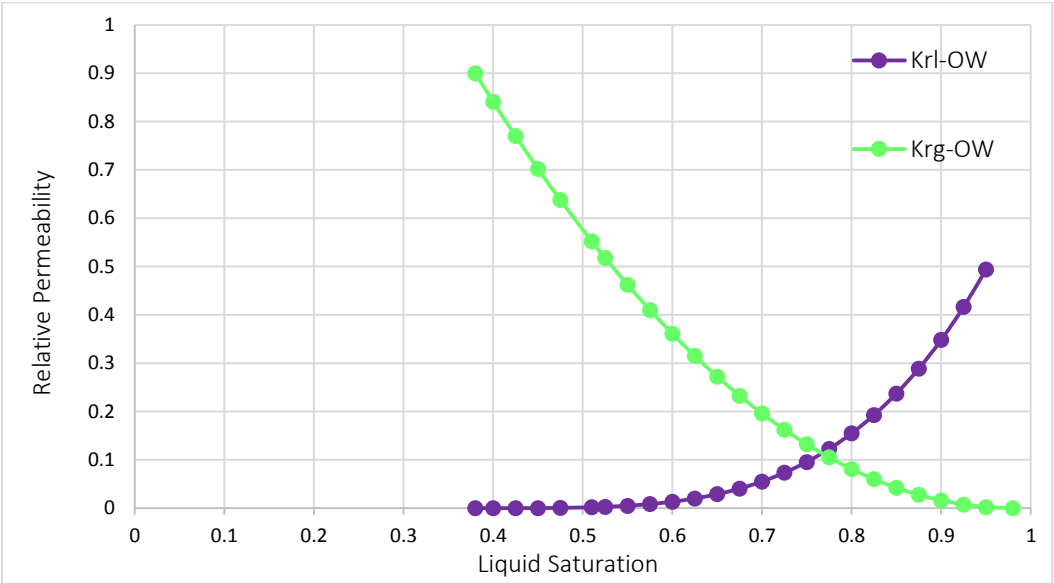

Figure 3.9 Relative permeability curves, liquid/gas, water-wet system.

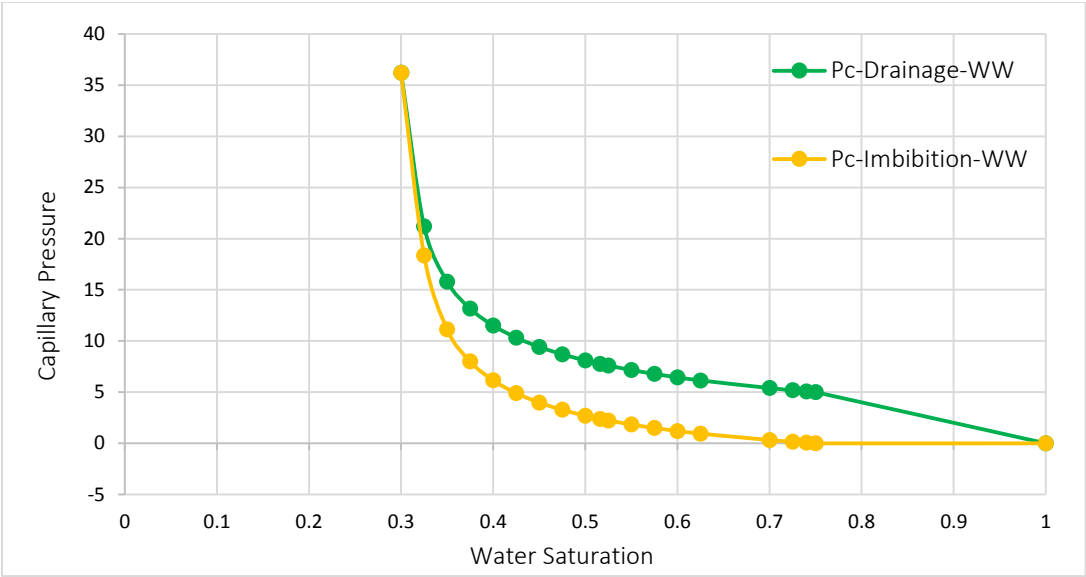

Figure 3.10 Capillary pressure curves, water-wet system.

The following figures represent the relative permeability and capillary pressure curves used in the oil-wet system simulation models.

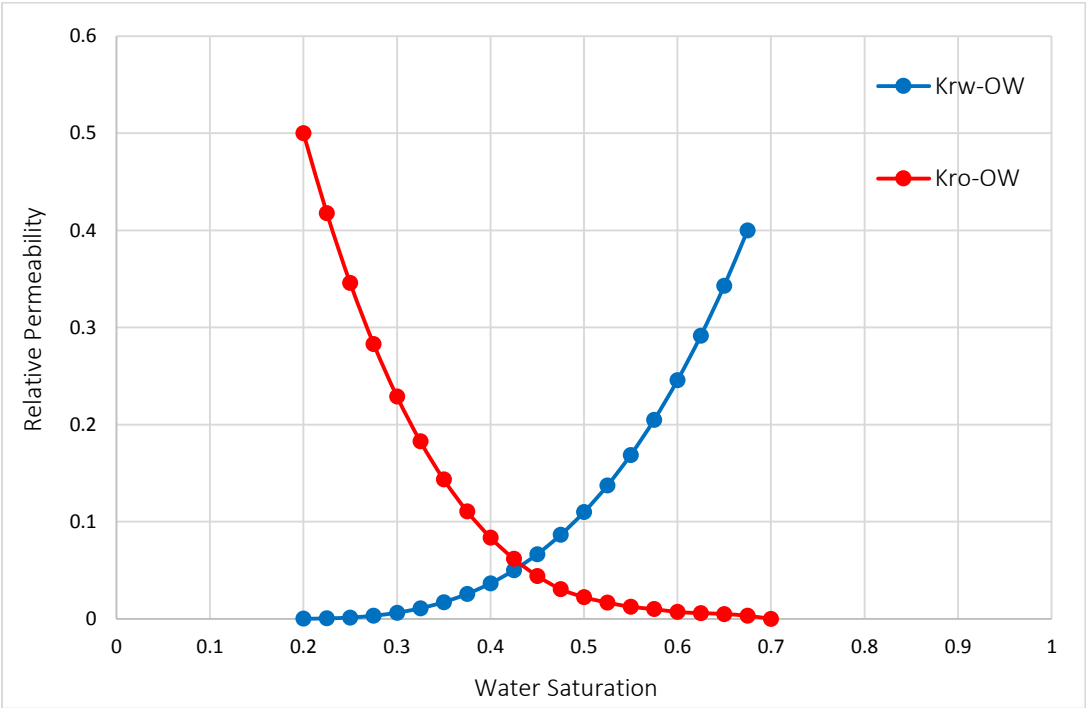

Figure 3.11 Relative permeability curves, water/oil, oil-wet system.

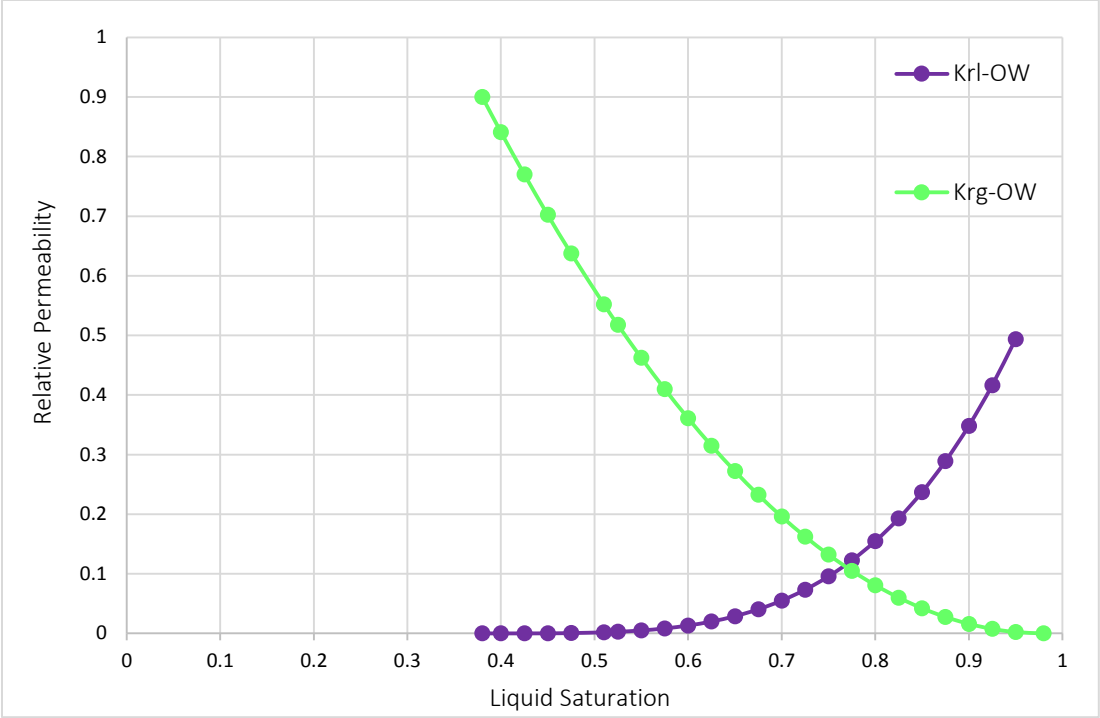

Figure 3.12 Relative permeability curves, liquid/gas, oil-wet system.

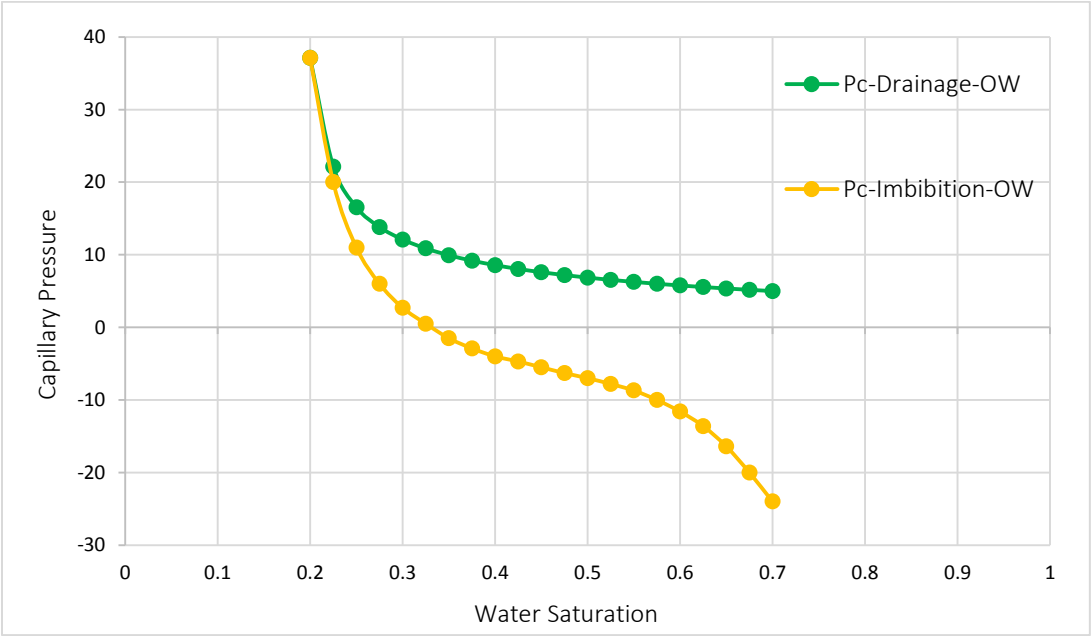

Figure 3.13 Capillary pressure curves, oil-wet system.

3.4 Method of Comparison

All the simulations are done for 5-well pattern reservoirs with one injector and 4 producers perforated in all 8 layers. The facility limitations are considered as the following constraints:

- Injector Max BHP 5,000 psi
- Producers Min BHP 2,500 psi
- Producers Max STL 5,000 bbl/d
- Producers Min STO 10 bbl/d
- Producers Max WCUT 97%
- Producers Max GOR 20,000 cf/bbl

In order to have a fair comparison, all the models' reservoir pressure was kept around 3,300 psi. Different scenarios of water flooding, CO_2 flooding and water alternating CO_2 flooding were studied on both water-wet and oil-wet reservoirs. Scenarios were based on considering fluids with different API and reservoirs with different rock wettability characteristics and also reservoirs with different permeability distribution in their layers. Then the effect of including hysteresis model in a WAG process numerical simulation was studied.

3.5 Relative Permeability Models

The relative permeability models used in this research are Stone I (Stone, 1970) and Stone II (Stone, 1973).

The original Stone's first model was modified by Aziz and Settari in 1979 for end point relative permeability as in the formula below:

$$\boldsymbol{k_{ro} = \frac{S_o^* * k_{row} * k_{rog}}{k_{rocw}(1 - S_w^*)(1 - S_g^*)}}$$

where $\boldsymbol{k_{rocw}}$ is the oil relative permeability at connate water $\boldsymbol{S_{wc}}$. Also, $\boldsymbol{S_o^*}$, $\boldsymbol{S_w^*}$, and $\boldsymbol{S_g^*}$ are calculated as below, when $\boldsymbol{S_o > S_{om}}$ and $\boldsymbol{S_w > S_{wc}}$:

$$\boldsymbol{S_o^* = \frac{S_o - S_{om}}{1 - S_{wc} - S_{om}}}$$

$$\boldsymbol{S_o^* = \frac{S_w - S_{wc}}{1 - S_{wc} - S_{om}}}$$

$$\boldsymbol{S_o^* = \frac{S_g}{1 - S_{wc} - S_{om}}}$$

$\boldsymbol{S_{om}}$ is the minimum residual oil saturation retained during three-phase flow.

Stone's second model is a modification of the first model for mixed-wet rocks and it is described by:

$$\boldsymbol{k_{ro} = k_{rocw}\left[\left(\frac{k_{rw}}{k_{rocw}} + k_{rw}\right)\left(\frac{k_{rg}}{k_{rocw}} + k_{rg}\right) - k_{rw} - k_{rg}\right]}$$

where $\boldsymbol{k_{rw}}$ and $\boldsymbol{k_{rg}}$ are read from two-phase oil/water and oil/gas systems' relative permeabilities.

3.6 Hysteresis Models

The relative permeability of a given phase is a function of saturations as well as many other rock and fluid characteristics such as wettability, a flow rate, interfacial tension and saturation history. The dependence of the relative permeability on the saturation path is referred to as hysteresis. Carlson's (Carlson 1981) hysteresis model, which is based on the Land (Land 1980) trapping equation, is the most common two-phase hysteresis model used in commercial simulators. This method presents a model for a scanning imbibition curve and assumes that to be representative of any subsequent drainage process.

The two-phase hysteresis models are not accurate in modeling processes such as water alternating gas injection (WAG) where simultaneous flow of all three phases occurs. The relative permeability of a given phase in this process should be considered as a function of the saturation history of not only its own phase but also other phases as well. Also, the assumption of the reversibility of drainage and imbibition scanning curves should be removed.

As indicated in the literature review, unfortunately investigation results show that the common hysteresis models are not very reliable. This research was done using hysteresis models by Larsen and Skauge (Larsen and Skauge, 1998), which is explained in the literature review chapter. Below the Carlson model is explained briefly. Next, it is briefly explained how Carlson model works and why it was not used in this study.

3.6.1 Carlson Hysteresis Model

The Carlson hysteresis model is applied for the gas phase using the Land trapping model:

$$\boldsymbol{S_{gt} = S_{gc} + \frac{S_{g,hy} - S_{gc}}{1 + C(S_{g,hy} - S_{gc})}}$$

where the free gas saturation $\boldsymbol{S_{gf}}$ is calculated from Land's equation as:

$$\boldsymbol{S_{gf} = S_{gc} + \frac{1}{2}\left\{(S_g - S_{gt}) + \sqrt{(S_g - S_{gt})^2 + \frac{4}{C}(S_g - S_{gt})}\right\}}$$

The gas relative permeability on the drainage to imbibition scanning curve and vice versa is given by (the scanning curve is considered reversible):

$$\boldsymbol{k_{rg}(S_g) = k_{rg}^{d}(S_{gf})}$$

Unlike the Larsen and Skauge (Larsen and Skauge, 1998) model, the same flowing saturation is used to calculate relative permeability for gas saturation increasing or decreasing while on a scanning curve. This assumption of the reversibility of drainage and imbibition scanning curves is not realistic. Therefore, Larsen and Skauge model is a more reliable model to be used in the numerical simulation of WAG.

Chapter 4: Results and Discussion

4.1 CO_2-WAG Recovery and Effects of Hysteresis on CO_2-WAG Models

After primary operation declines, secondary recovery methods will be applied to maintain the depleted reservoir pressure by injecting water or gas. The injected water or gas displaces the oil toward producing wells. In tertiary recovery operations one or more fluids will be injected into an oil reservoir to recover the remaining oil left behind the primary and secondary processes.

The reservoir base model in this study was producing by primary depletion from 1965-07-01 till 1966-02-01 when oil production dropped to 4,214.65 bbl/day. Then secondary recovery of water flooding was done in the reservoir and it improved the oil production up to 19,837.2 bbl/day. However, after 9 years of water flooding the oil production dropped to 3,451.82 bbl/day on 1975-01-01. Therefore, some EOR methods were needed to improve the oil production. Hence, tertiary recovery operations of CO_2 flooding and CO_2-WAG were considered. Water alternating gas (CO_2) or CO_2-WAG injection is an EOR technique for improving oil recovery by combining effects of water flooding and gas flooding. In Section 4.1.1, water flooding, CO_2 flooding and a CO_2-WAG process are compared and CO_2-WAG flooding was the most economical operation with the highest production. Note that the producer bottom-hole pressure is set higher than the bubble point pressure and less than the MMP pressure so that around the producers, CO_2 is not miscible with the reservoir oil.

As explained in Chapter 2, it is necessary to consider relative permeability hysteresis effects in the WAG process. Basically, a saturation direction change in a CO_2-WAG process must be included in relative permeability calculations. In Section 4.1.2 relative permeability hysteresis effects are

added into the WAG simulation models. Results indicated the importance of considering hysteresis in the prediction of oil production, which increases substantially.

Rock wettability impacts the rock main attributes of multi-phase properties such as capillary pressure and relative permeability curves and as a result fluid movement and distribution in pores. Most of reservoir rocks are not completely water-wet or oil-wet, and they have mixed-wettability. Previous studies of the effect of hysteresis on WAG were done for water-wet systems. In this study both water-wet and oil-wet reservoirs are investigated.

4.1.1 WAG Performance in Comparison with Water Flooding and CO_2 Flooding

First, we compare the results of different oil recovery methods after reservoir primary operation and water flooding as a secondary operation. The following three approaches were studied: (1) continuing with water flooding (2) switching to CO_2 flooding (3) switching to CO_2-WAG flooding.

The following constraints were considered in both the oil-wet and water-wet reservoir simulation models. WAG cycles of water injection and CO_2 injection were both considered for 90 days, starting with CO_2 injection. In order to have a fair comparison of the WAG process with CO_2 flooding, the maximum amount of the gas injection rate was limited to 30 MMscf for both the WAG process and CO_2 flooding. A water injection rate was controlled by keeping the average reservoir pressure around 3,300 psia in both the oil-wet and water-wet reservoirs.

Comparing the CO_2 flooding and CO_2-WAG flooding simulation results, there were $8.8*10^{10}$ scf and $4.4*10^{10}$ scf less CO_2 injected into the reservoir during CO_2-WAG flooding for the oil-wet and water-wet reservoirs, respectively (Figure 4.1). The amounts of CO_2 injected into the reservoir during the WAG process in the water-wet and oil-wet models are equal.

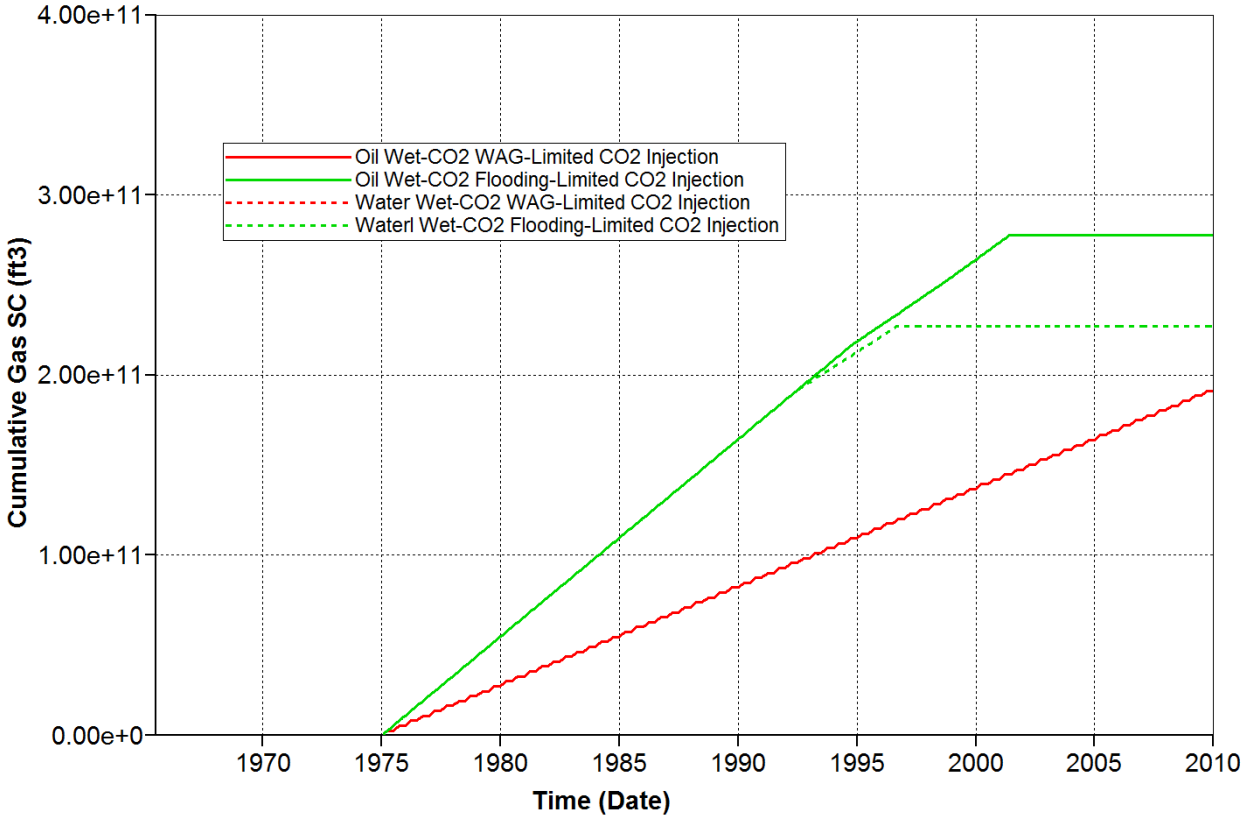

Figure 4.1 Cumulative CO_2 Injection, Oil-Wet and Water-Wet Models.

Comparing water flooding with CO_2-WAG flooding, the amount of the cumulative water injected into the reservoir in water flooding is higher than the amount of the cumulative water injected during CO_2-WAG flooding for both the oil-wet and water-wet models. Figure 4.2 shows that the cumulative water injection in the CO_2-WAG process is about 30 million bbl fewer than the cumulative water injection in the water flooding for both the oil-wet and water-wet reservoirs.

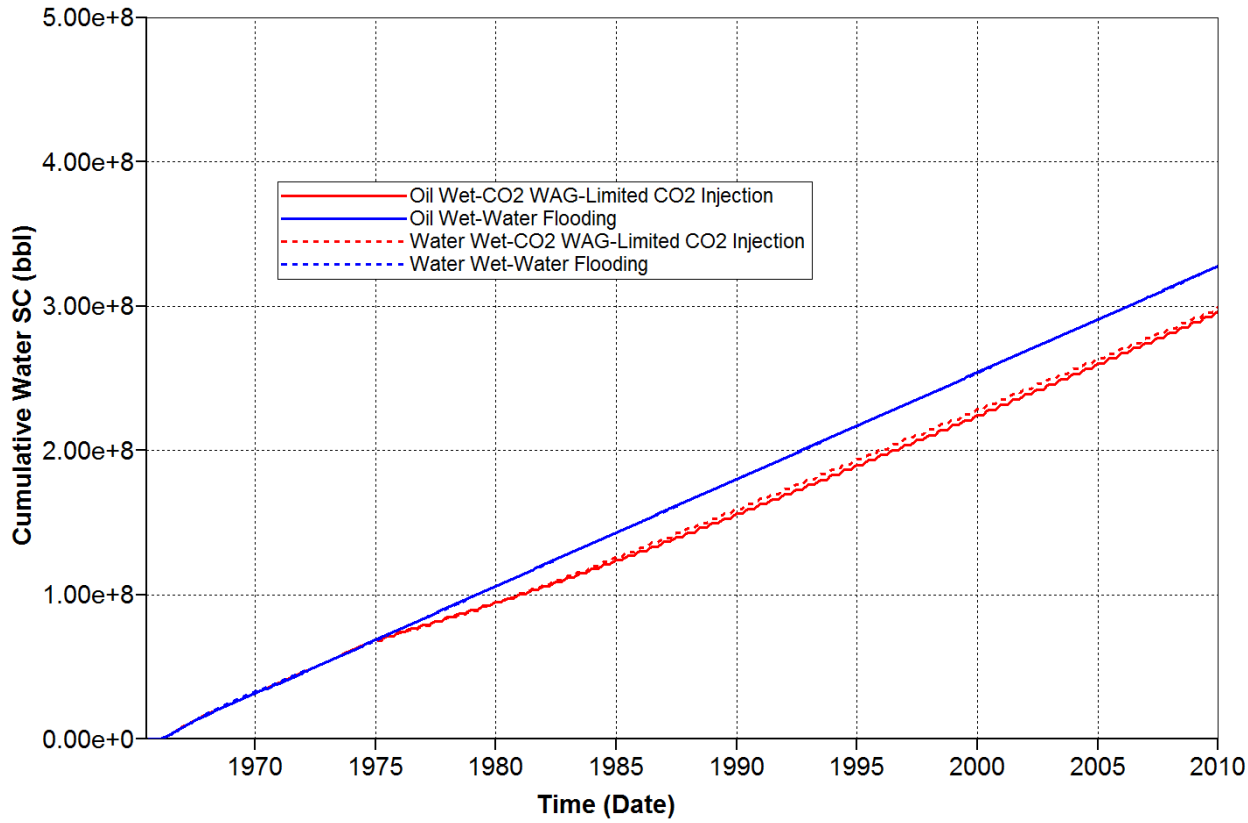

Figure 4.2 Cumulative Water Injection, Oil-Wet and Water-Wet Models.

Simulation results also show that the oil production rate in CO_2-WAG flooding is much higher than the oil production rate in CO_2 flooding or water flooding in both the oil-wet and water-wet reservoirs (Figure 4.3). Figure 4.3 is presented in the next page.

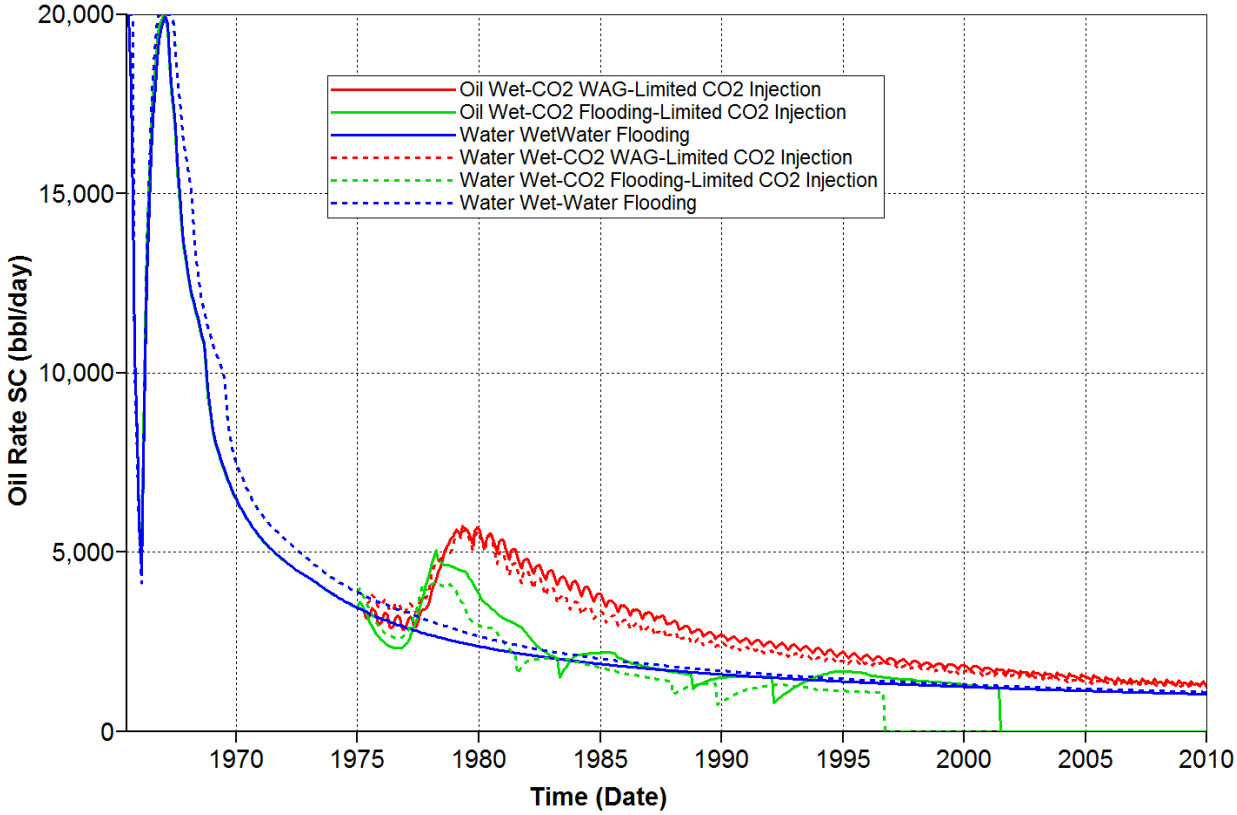

Figure 4.3 Oil Production Rate, Oil-Wet and Water-Wet Models.

Simulation results show that in both reservoir characteristics, the CO_2-WAG process will result in higher oil production by injecting less water and CO_2 into the reservoir compared to the water flooding and CO_2 flooding processes (Figures 4.1- 4.3).

Looking at the cumulative oil results for CO_2 flooding and water flooding, CO_2 flooding may work slightly better at the beginning of flooding, but as a result of early gas breakthrough, water flooding works much better later on, specifically in the water-wet model (Figure 4.4, next page).

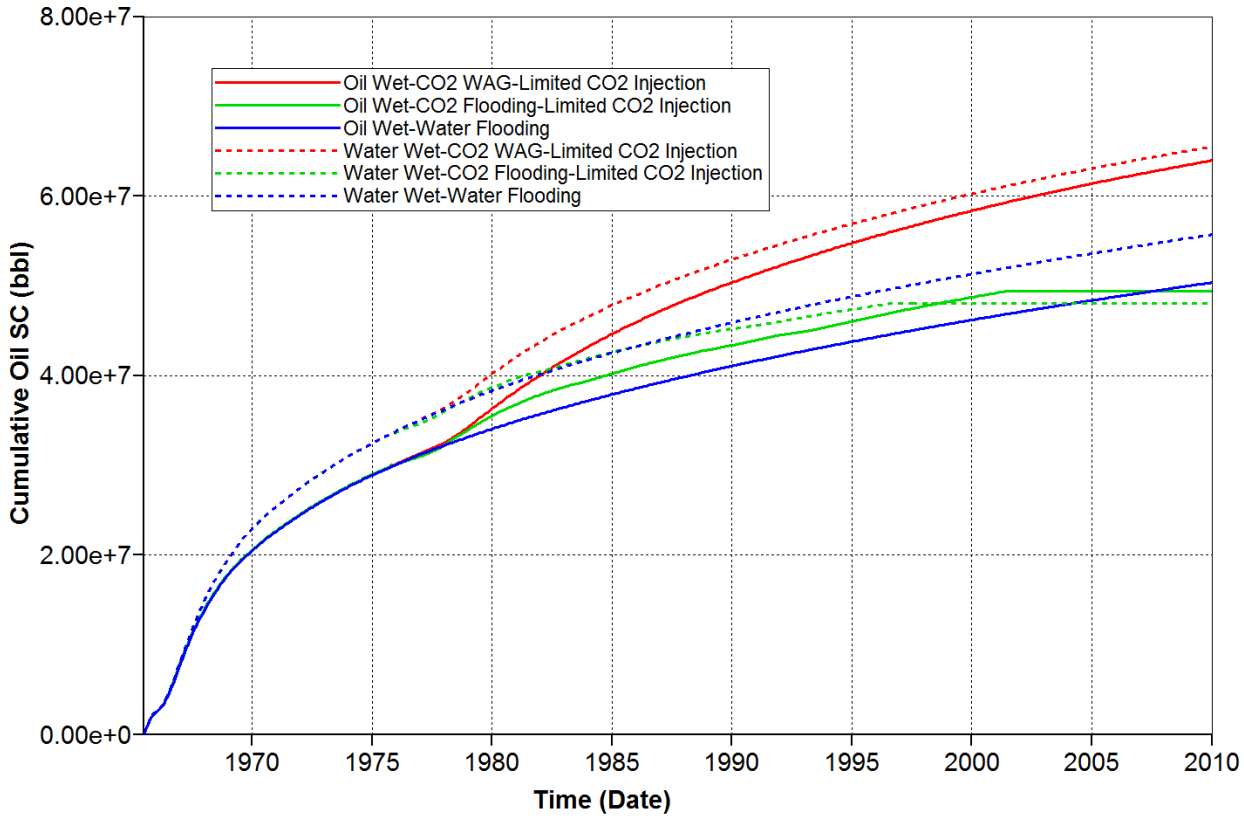

Figure 4.4 Cumulative Oil Production Oil-Wet and Water-Wet Models.

Figure 4.5 represents that not only CO_2 flooding has lower oil production compared to the CO_2-WAG flooding but also the gas-oil ratio is much higher in CO_2 flooding for both the oil-wet and water-wet reservoirs, which is another disadvantage of CO_2 flooding compared to the CO_2-WAG flooding. After 21 years of CO_2 flooding in the water-wet reservoir and 25 years of CO_2 flooding in the oil-wet reservoir, the GOR (gas-oil ratio) reached 20,000 scf/bbl because of CO_2 breakthrough. This corresponds to the producing well limitation constraint and, therefore, CO_2 injection was stopped (Figure 4.5, next page).

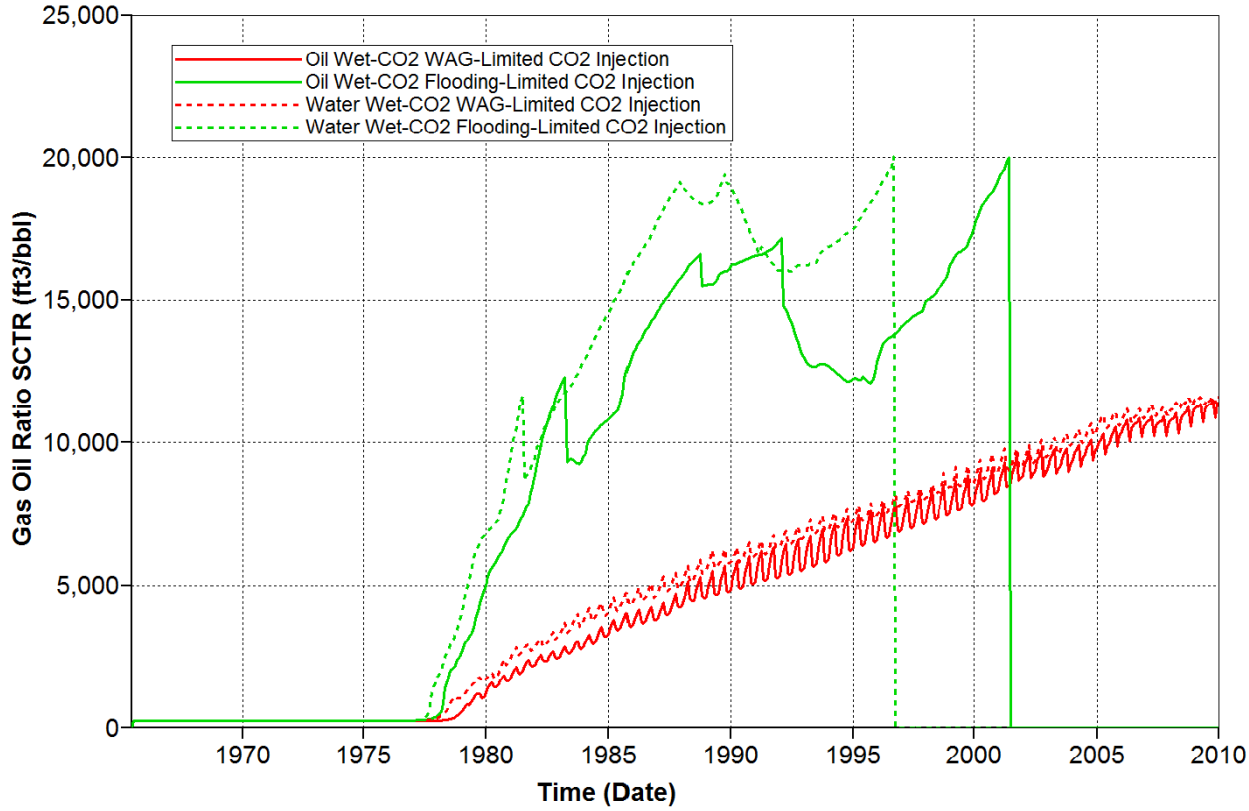

Figure 4.5 Gas Oil Ratio, Oil-Wet and Water-Wet Models.

Also, water cut (WCUT) during the CO_2-WAG process is lower than the WCUT for water flooding for both reservoir characteristics (Figure 4.6). This is another advantage of the WAG over water flooding.

Therefore, not only was there less water and CO_2 injection into the reservoir for WAG flooding but also there was less water and CO_2 production, which makes the WAG process more desirable than water flooding and CO_2 flooding.

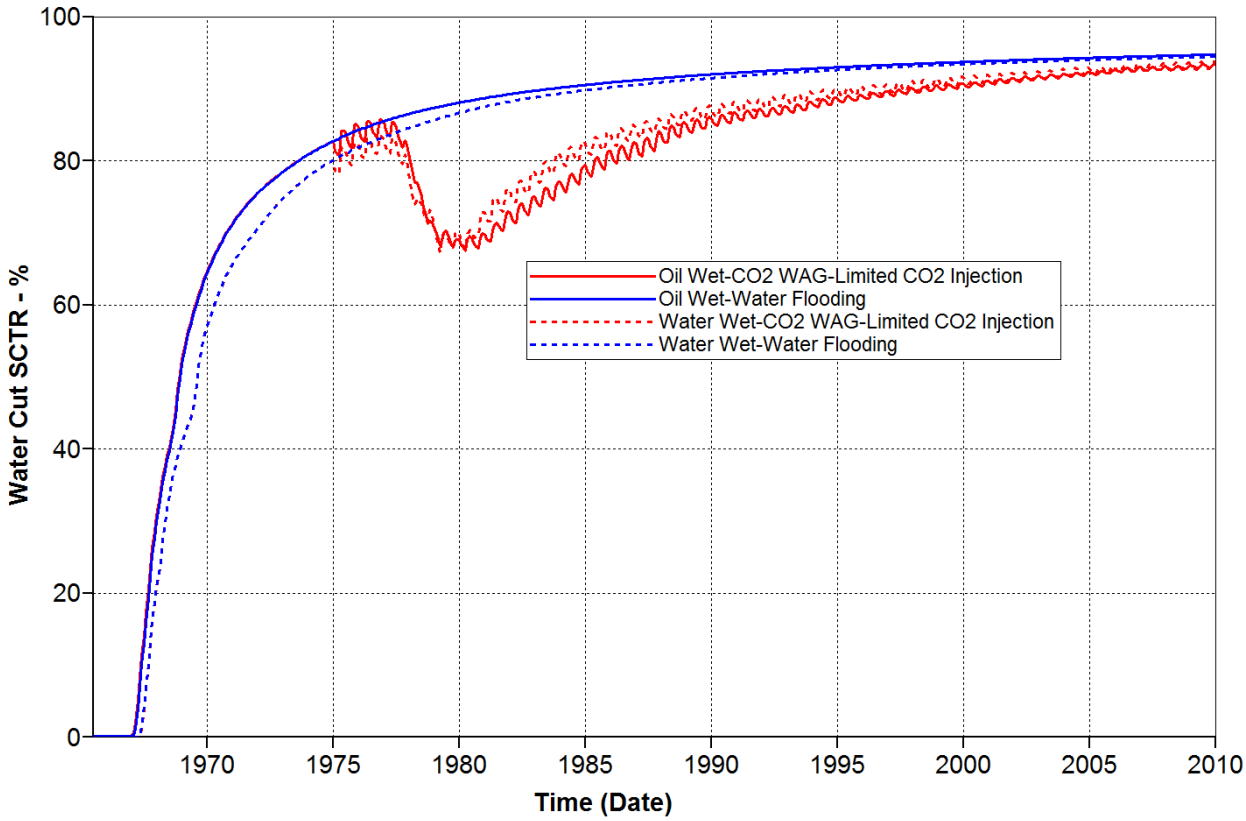

Figure 4.6 Water Cut, Oil-Wet and Water-Wet Models.

Because of the gravity segregation effect, injected water migrates towards the lower layers of the formation, the injected gas rises to the top of the reservoir, and CO_2-WAG flooding takes advantage of both CO_2 injection and water injection and sweeps all the layers of the reservoir.

Recalling some definitions from Chapter 2 regarding mobility concept, we explain why CO_2-WAG worked the best in both the water-wet and oil-wet models compared to water flooding and CO_2 flooding. Essentially, WAG injection improved oil recovery by modifying a mobility ratio and sweep efficiency. A mobility ratio is defined by S. Thomas (Green and Willhite, 1998) as the mobility of the displacing fluid (λ_D) divided by the mobility of the displaced fluid (λ_d):

$$\boldsymbol{M = \lambda_D / \lambda_d}$$

Also, mobility is defined as relative permeability divided by viscosity:

$$\boldsymbol{\lambda_D} = \frac{\boldsymbol{k_D}}{\boldsymbol{\mu_D}} \text{ and } \boldsymbol{\lambda_d} = \frac{\boldsymbol{k_d}}{\boldsymbol{\mu_d}}$$

Considering a gas-oil system we have:

$$\boldsymbol{\lambda_g} = \frac{\boldsymbol{k_{rg}}}{\boldsymbol{\mu_g}} \text{ and } \boldsymbol{\lambda_o} = \frac{\boldsymbol{k_{ro}}}{\boldsymbol{\mu_o}}$$

where k_{rg} and k_{ro} are the relative permeabilities of gas and oil and μ_g and μ_o are the viscosities of gas and oil, respectively. Therefore, gas has a higher mobility due to its low viscosity.

Displacement efficiency *E* is considered as the product of microscopic and macroscopic displacement efficiencies:

$$\boldsymbol{E} = \boldsymbol{E_{Macro}} * \boldsymbol{E_{Micro}}$$

where *E* is the volume of oil recovery by EOR divided by the amount of the initial oil in place at the beginning of injection (Green and Willhite, 1998).

Microscopic sweep efficiency refers to the effect of the displacing fluid in mobilizing the oil at the pore scale. The volumetric or macroscopic displacement efficiency is displacing fluids in a volumetric scale which refers to the vertical and horizontal sweep efficiencies of the displacing fluid in sweeping out a volume of a reservoir (Green and Willhite, 1998):

$$\boldsymbol{E_{Macro}} = \boldsymbol{E_v} * \boldsymbol{E_h}$$

Gas microscopic efficiency of oil is normally better than the water microscopic displacement at the pore scale, because there is lower IFT (interfacial tension) in a gas-oil system compared to an oil-water system. However, gas low viscosity and high mobility result in gas fingering and early gas breakthrough, and, therefore, water has better macroscopic sweep efficiency. Hence, it is essential to control a gas-oil mobility ratio in the WAG injection process (Green and Willhite, 1998).

As a result, injecting too much water will result in poor microscopic efficiency and injecting large amounts of gas will reduce the macroscopic sweep efficiency. CO_2-WAG flooding takes advantages of both good microscopic sweep efficiency of CO_2 injection and macroscopic sweep efficiency of water injection and improves the oil production.

It should be mentioned that the comparison between different methods of water flooding CO_2 flooding and CO_2-WAG flooding was based on the assumption that reservoir pressure is kept at 3,300 psi. Checking the results for both the oil-wet and water-wet models, reservoir pressure during water flooding was almost stable at 3,300 psi. However, in the CO_2-WAG process reservoir pressure changes between 3,100 psi to 3,300 psi and in CO_2 flooding it dropped drastically (Figures 4.7 and 4.8). This is caused by limiting the CO_2 injection rate in CO_2 flooding and CO_2-WAG flooding.

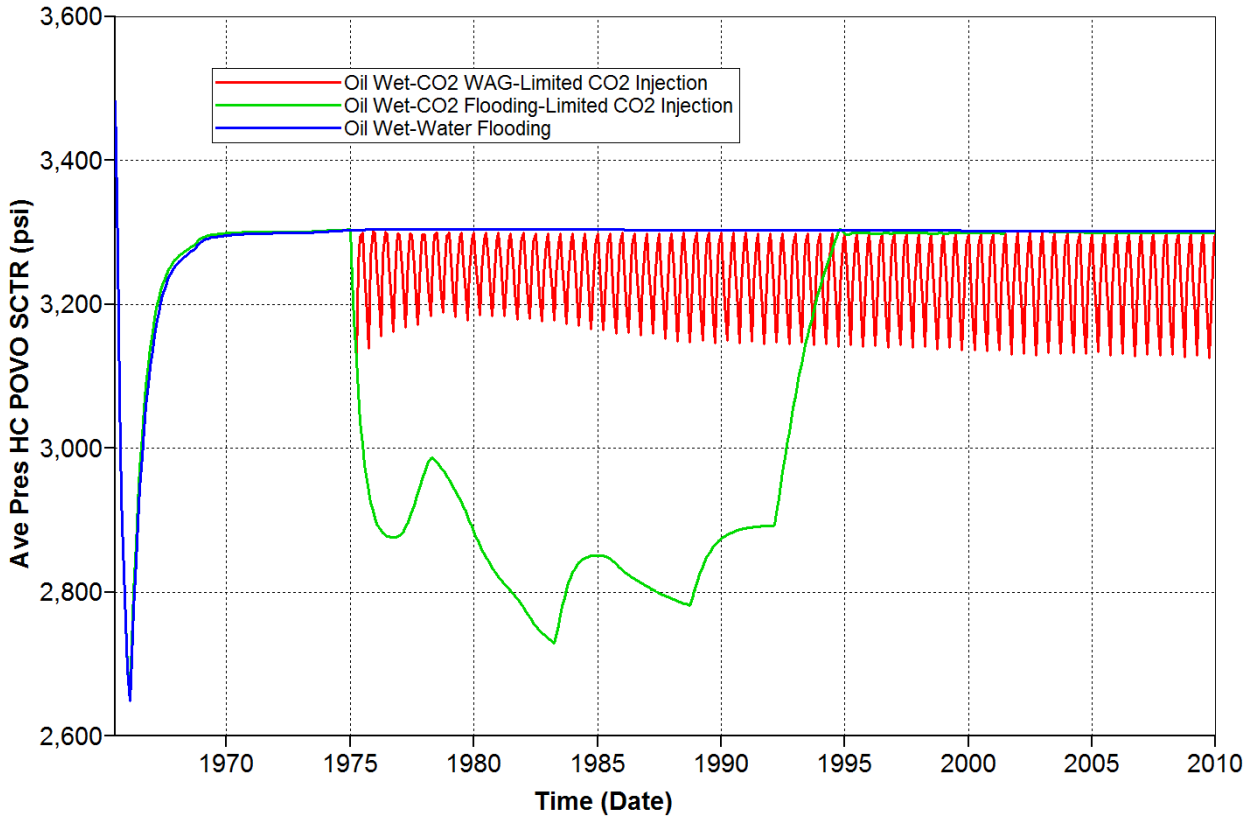

Figure 4.7 Reservoir Pressure, Oil-Wet Model.

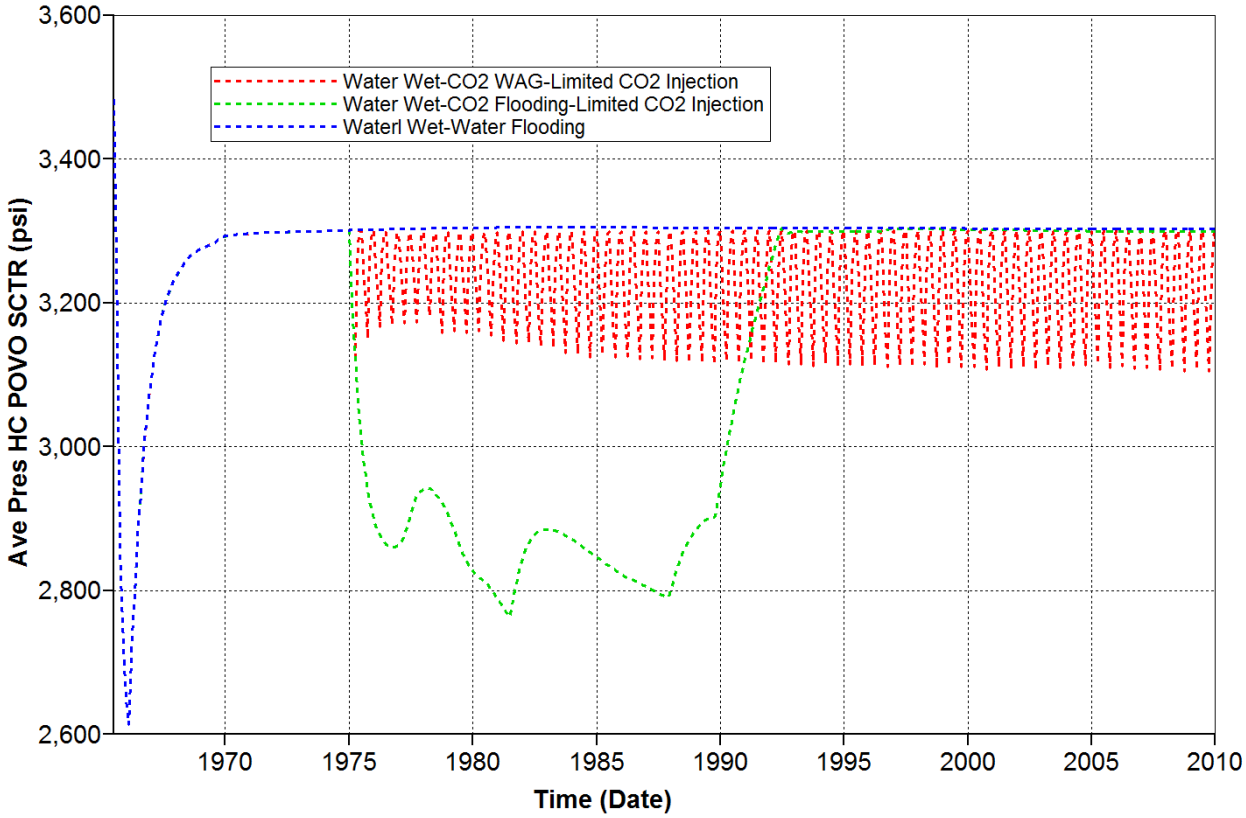

Figure 4.8 Reservoir Pressure, Water-Wet Model.

Therefore, in the next step, the CO_2 injection limit was removed to resolve the reservoir pressure dropping issue in the CO_2 flooding and WAG injection for both the water-wet and oil-wet models. As a result of removing the limit for a CO_2 injection rate, reservoir pressure is stable around 3,300 psi during CO_2 flooding and WAG injection (Figures 4.9 and 4.10).

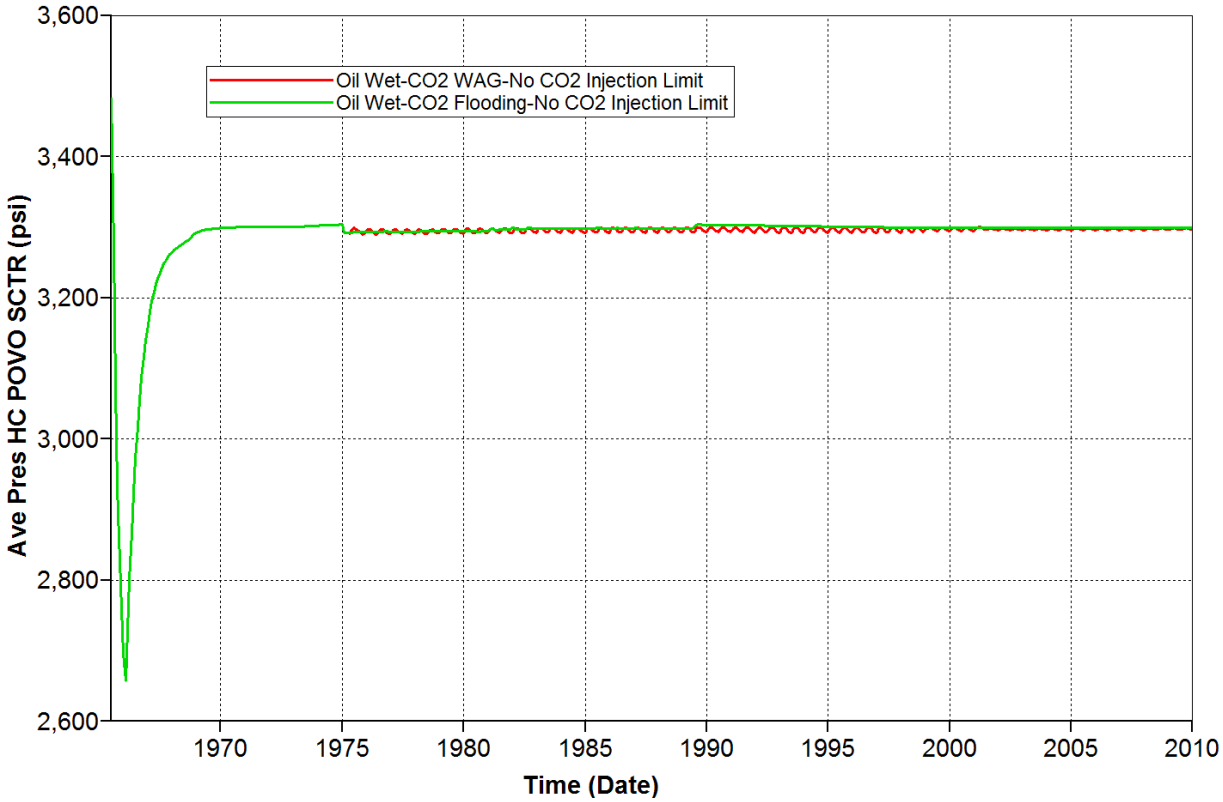

Figure 4.9 Reservoir Pressure, Oil-Wet Model.

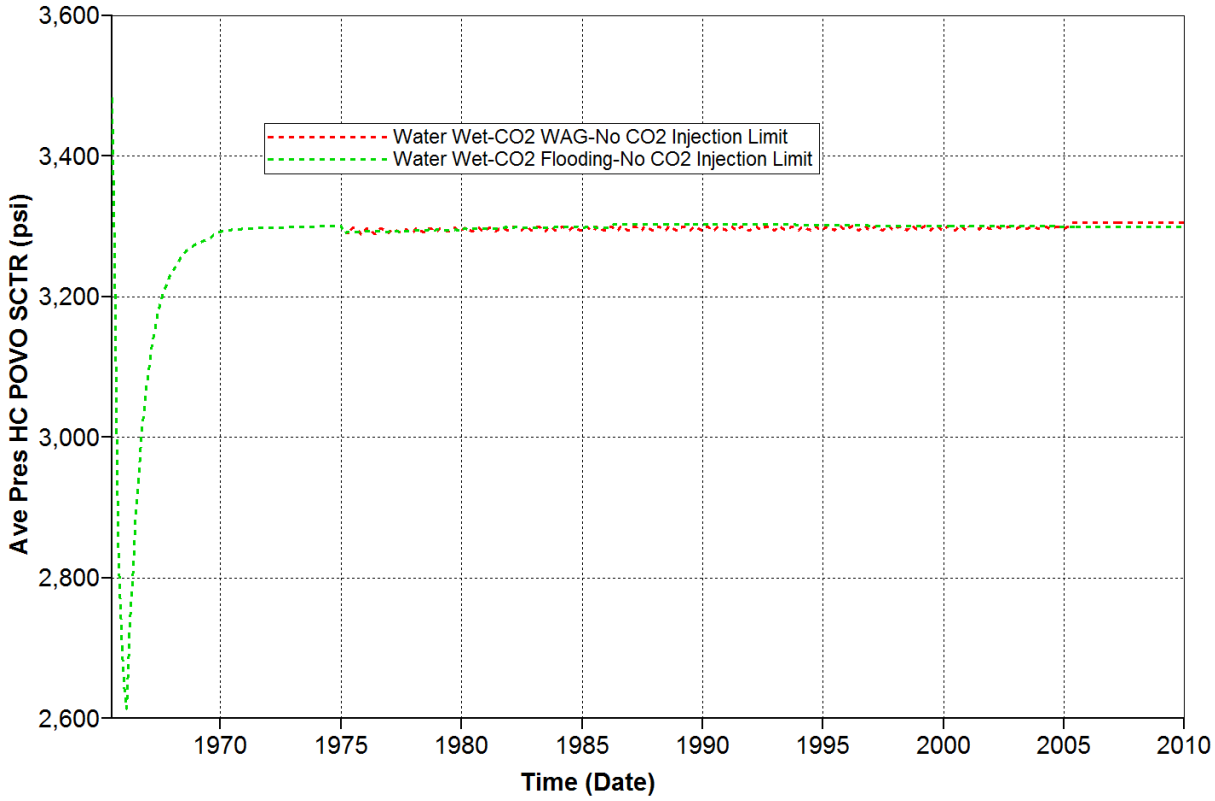

Figure 4.10 Reservoir Pressure, Water-Wet Model.

Although removing the limit for the CO_2 injection rate in CO_2 flooding and WAG flooding improved the oil production rate for the first 5 years, later the oil production rate dropped drastically because of the early breakthrough of CO_2 specially in the CO_2 flooding (Figures 4.11 and 4.12).

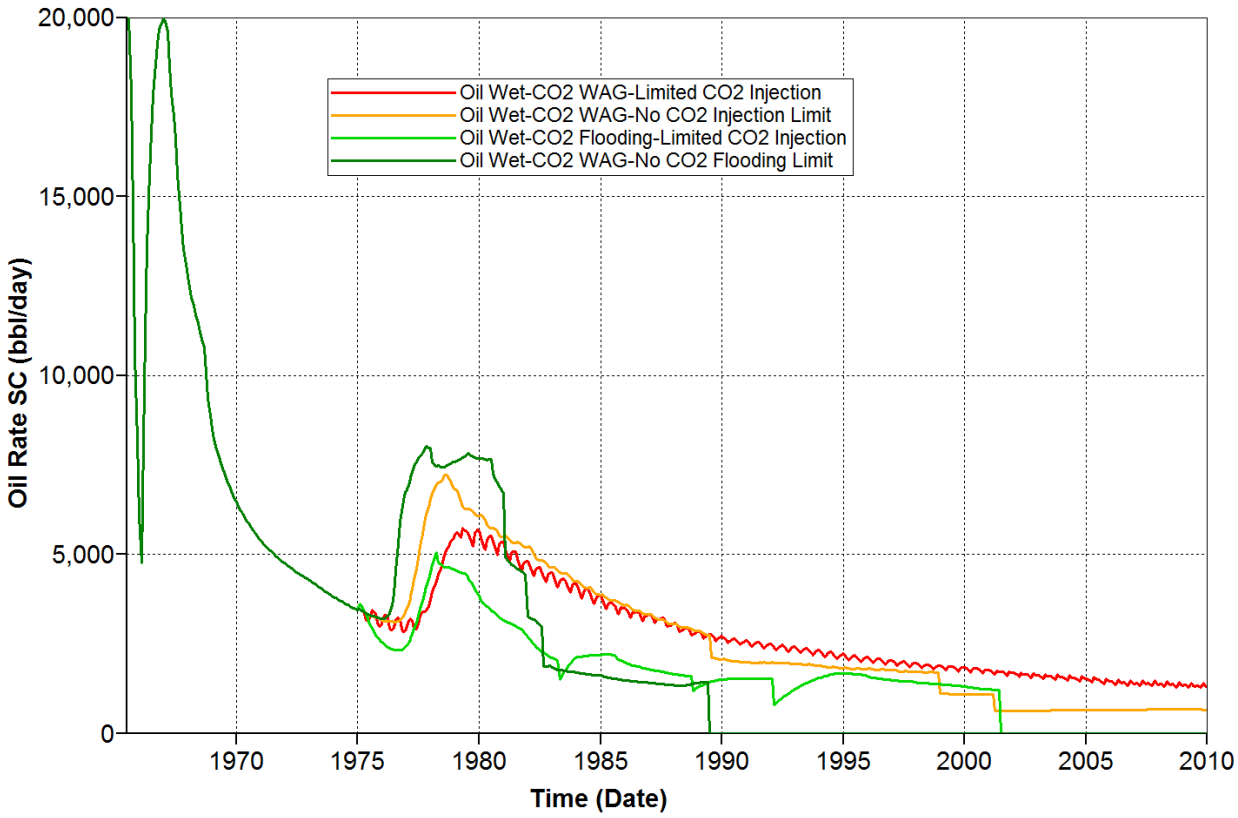

Figure 4.11 Oil Production Rate, Oil-Wet Model.

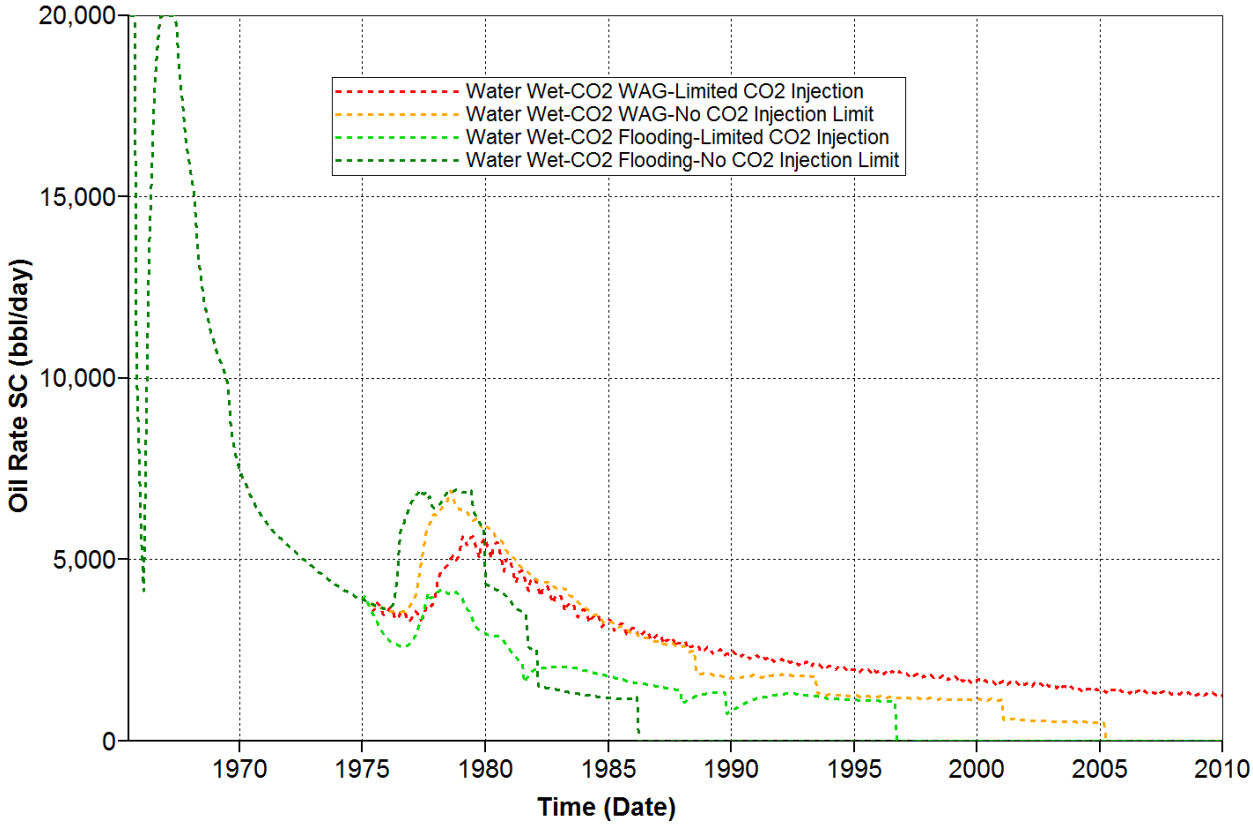

Figure 4.12 Oil Production Rate, Oil-Wet Model.

Note that WAG injection still works better than CO_2 flooding for both the water-wet and oil-wet models. In addition, injecting more CO_2 in the WAG process did not result in much more oil production by the end of the simulation time for both wettability characteristics (Figures 4.13 and 4.14).

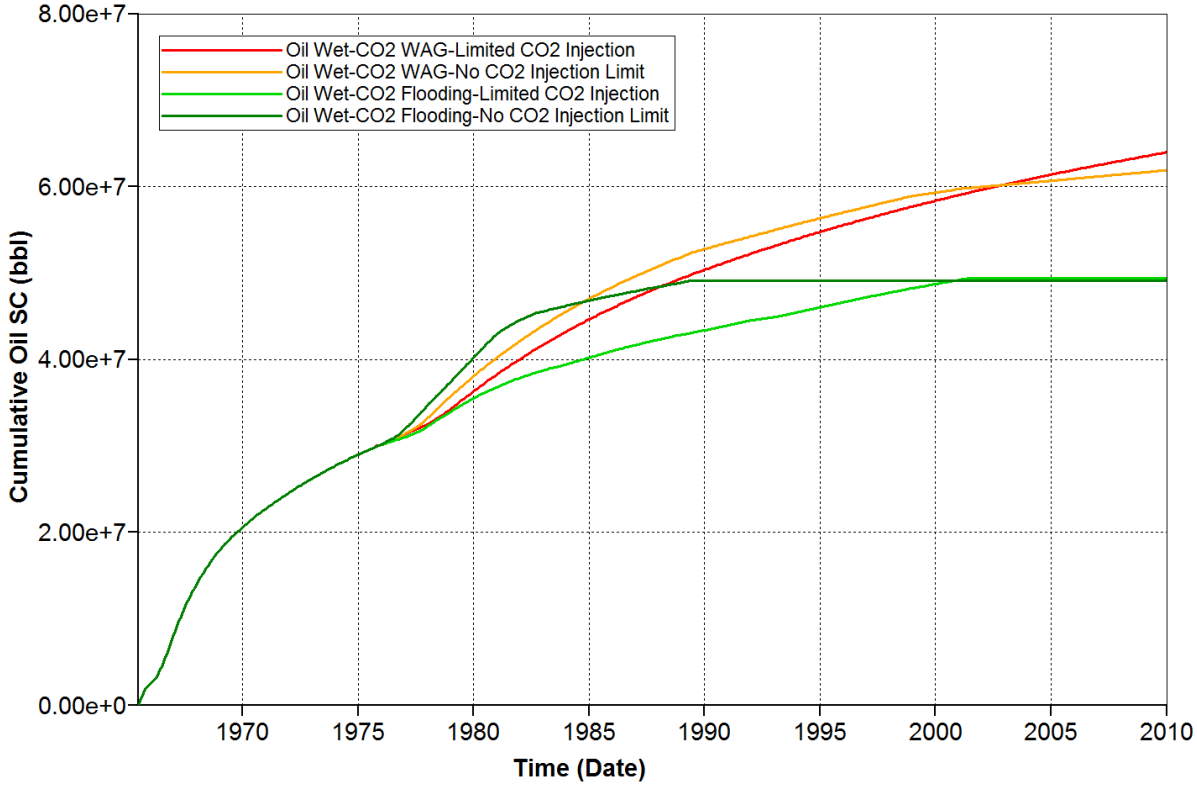

Figure 4.13 Cumulative Oil Production, Oil-Wet Model.

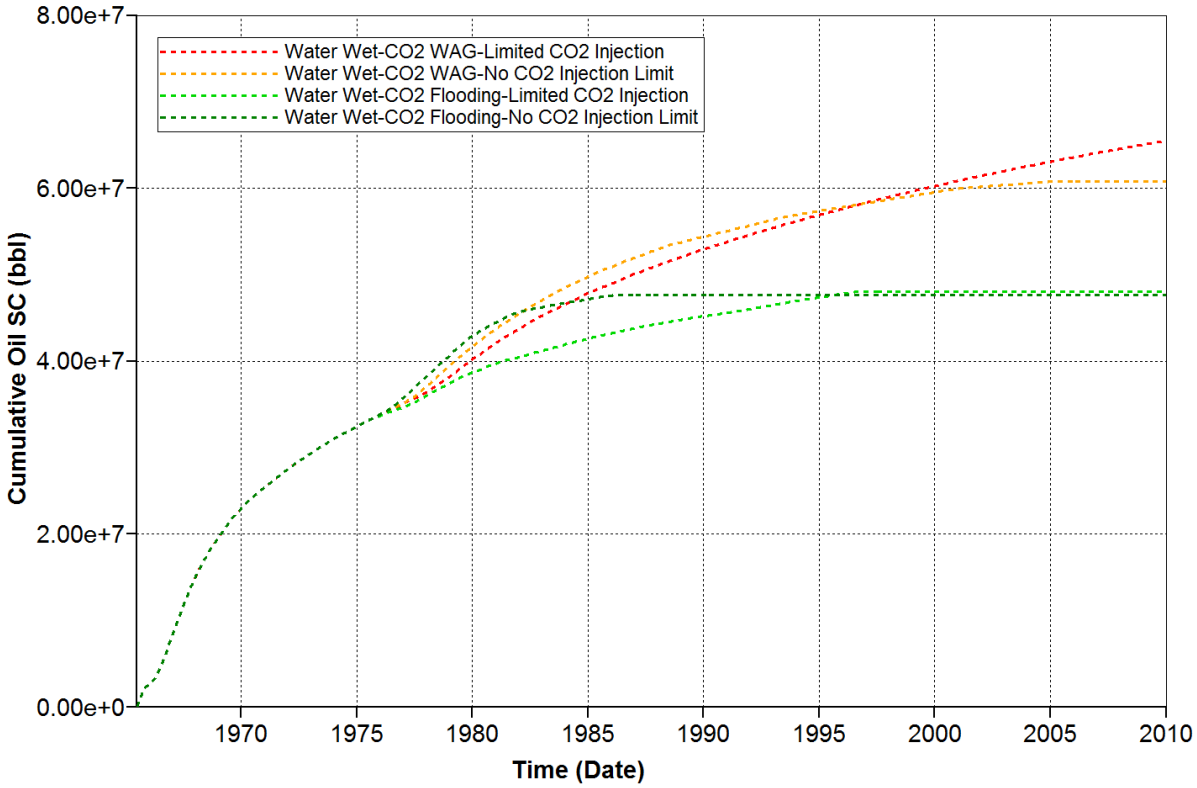

Figure 4.14 Cumulative Oil Production, Water-Wet Model.

Although removing the limit for a CO_2 injection rate resulted in earlier CO_2 breakthrough in CO_2 flooding and WAG flooding, it also resulted in a lower water injection rate (Figures 4.15 and 4.16) and water cut in the WAG process (Figure 4.17) for both the water-wet and oil-wet models.

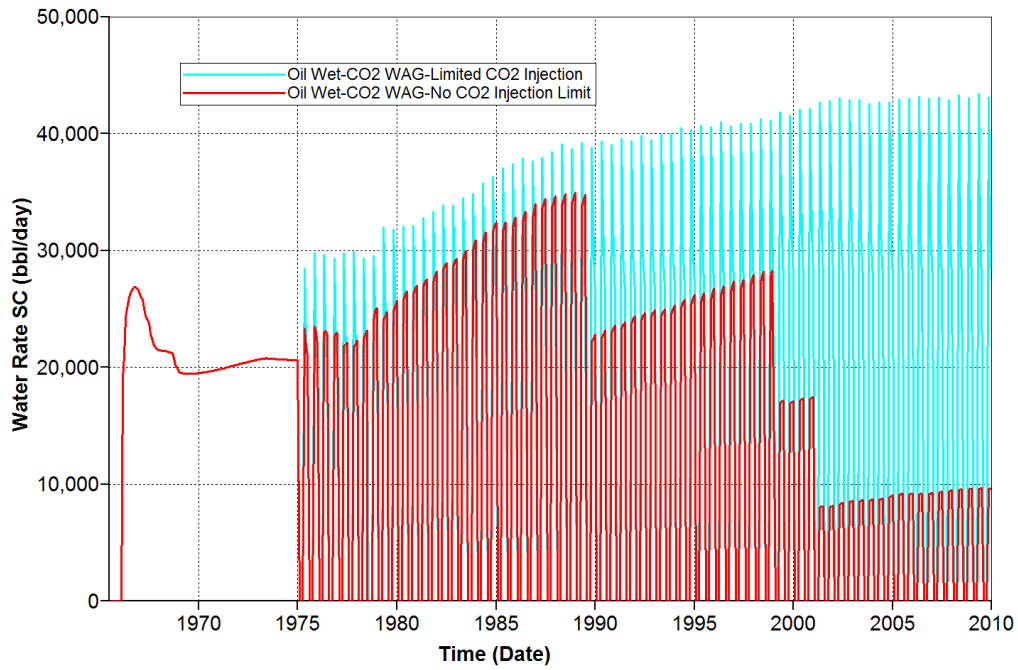

Figure 4.15 Water Injection Rate, Oil-Wet Model.

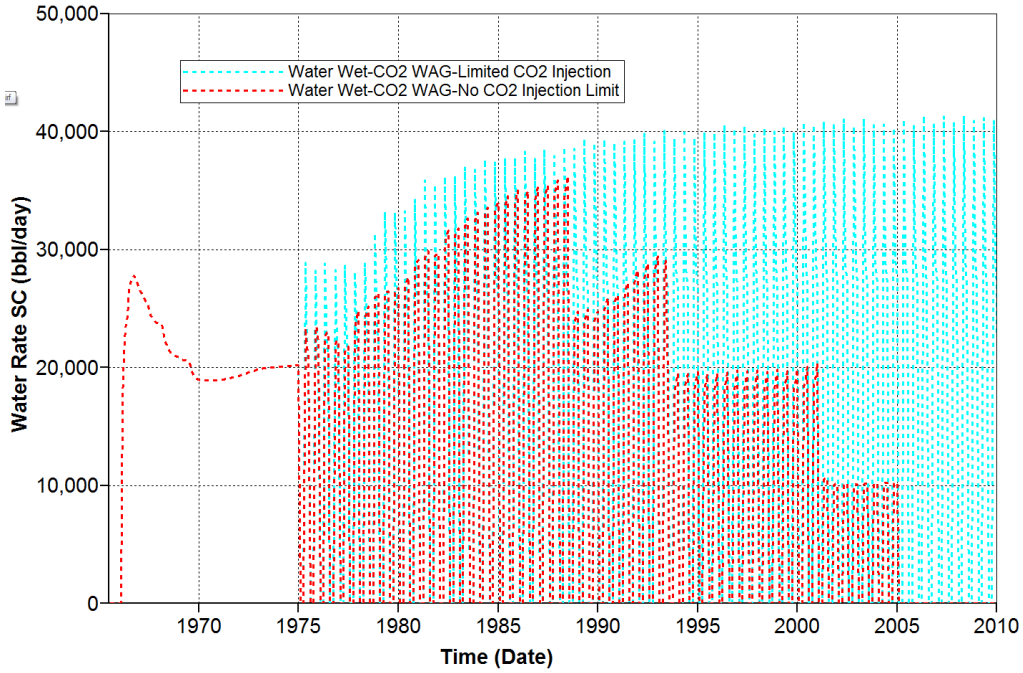

Figure 4.16 Water Injection Rate, Water-Wet Model.

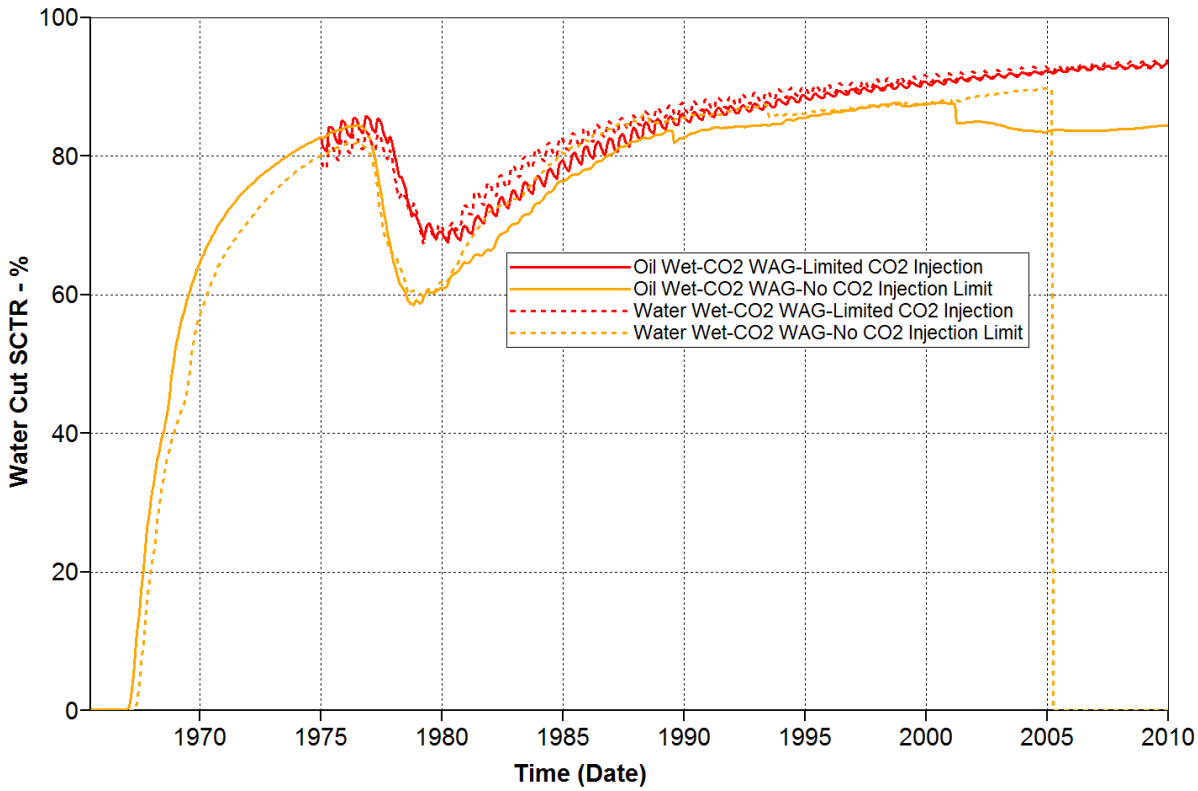

Figure 4.17 Water Cut, Oil-Wet Model.

In summary, the simulation results indicate that CO_2-WAG injection works much better than CO_2 flooding and water flooding in both the oil-wet and water-wet reservoirs. Also, water flooding works better than CO_2 flooding specifically in the water-wet reservoir, because of the early breakthrough of CO_2 due to having some pores and layers with high permeability. In addition, CO_2 flooding is not fully miscible in this study's simulations.

WAG injection increases the oil recovery factor of water flooding by 2.4 in the water-wet model and 4.7 in the oil-wet reservoir. Note that the oil recovery factors for CO_2-WAG flooding and CO_2 flooding in Table 4.1 belong to the simulations with no limit on a CO_2 injection rate. As discussed earlier having no limit on a CO_2 injection rate results in stable average reservoir pressure around 3,300 psi during CO_2-WAG flooding and CO_2 flooding. Therefore, we have a fair comparison between different recovery methods.

Table 4.1 Oil Recovery Factor.

Oil Recovery Factor	Water-Wet System	Oil-Wet System
Water Flooding	26.4	20.9
CO_2-flooding	22.6	20.4
CO_2-WAG	28.8	25.6

Note that water flooding worked better in a water-wet reservoir in comparison with an oil-wet system. This can be explained by the definition of the rock wettability. In a rock/oil/water system, wettability is defined as the tendency of a fluid to preferentially adhere to (or wet) the surface of a rock in the presence of other immiscible fluids.

In a water-wet system, water occupies small pores and contacts the rock surface in large pores and oil is in the middle of large pores. Therefore, during water flooding in a water-wet reservoir water displaces the oil in the middle of large pores.

However, in an oil-wet system, the location of the two fluids is partly reversed from the water-wet system. Water usually fills very small pores but oil contacts majority of the rock surface in large pores. On the other hand, the water also presents in the middle of large pores and does not contact the large pore throat surface, and it is usually present in small amounts. Even in the oil-wet reservoir, water fills the smallest pores since oil never enters the small pores due to capillary forces. Therefore, during water flooding water cannot displace the oil presented in the large pores completely because oil contacts the rock surface. Hence, the oil recovery factor during water flooding in a water-wet system is higher than that in oil-wet system.

4.1.2 Effect of Hysteresis on CO_2-WAG Models

Hysteresis usually refers to the reversing of saturation changes from increasing to decreasing or vice versa. This hysteresis effect in relative permeability can be considered between two consecutive injections when they are carried out in the same direction which is the case in CO_2-WAG flooding. Therefore, good knowledge of three-phase relative permeability accounting for cyclic hysteresis effects is needed for the numerical simulation of a WAG process. Below the impact of relative permeability hysteresis effects on the WAG simulation are studied using the famous Larsen-Skauge model. As a result, considering hysteresis improved the oil production very much in both oil-wet and water-wet reservoirs (Figures 4.18 and 4.19). Two scenarios for WAG flooding were considered: (1) a limited CO_2 injection rate and (2) no limitation for a CO_2 injection rate.

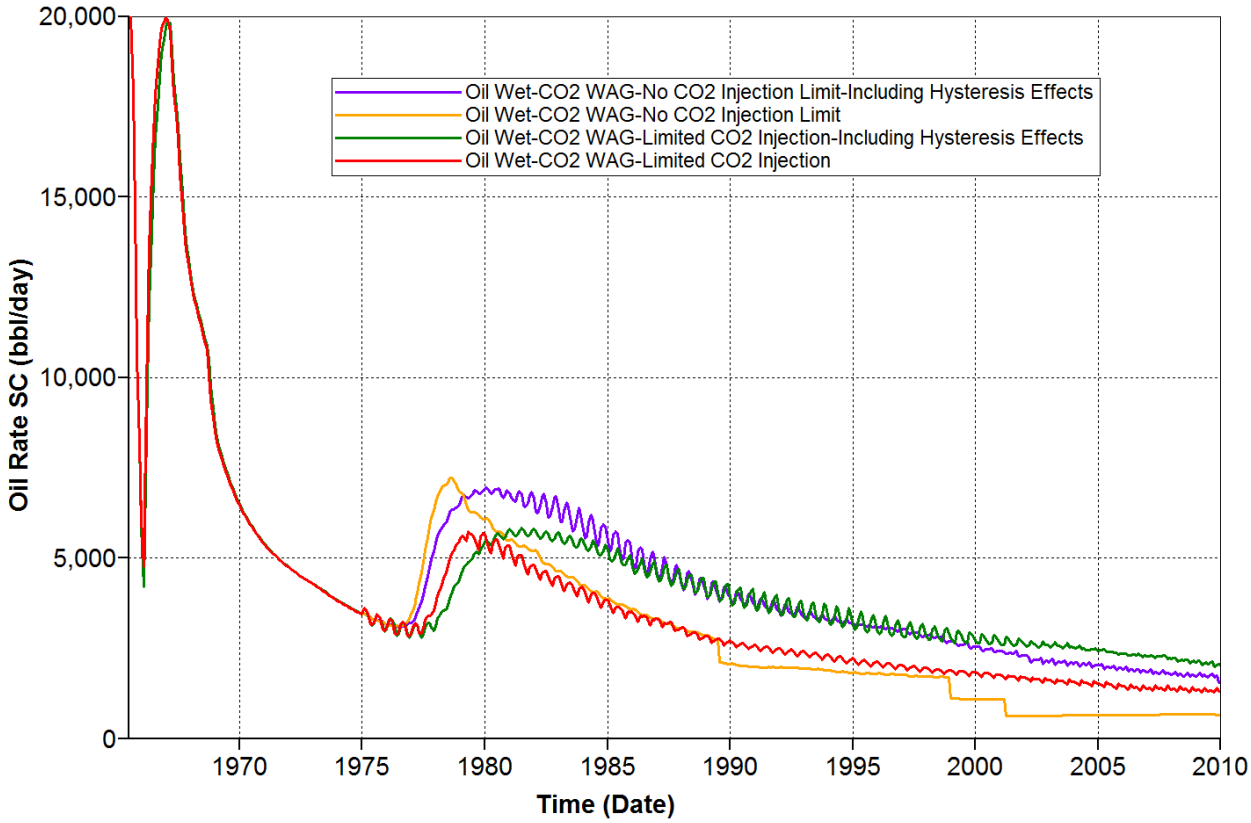

Figure 4.18 Oil Production Rate, Oil-Wet Model.

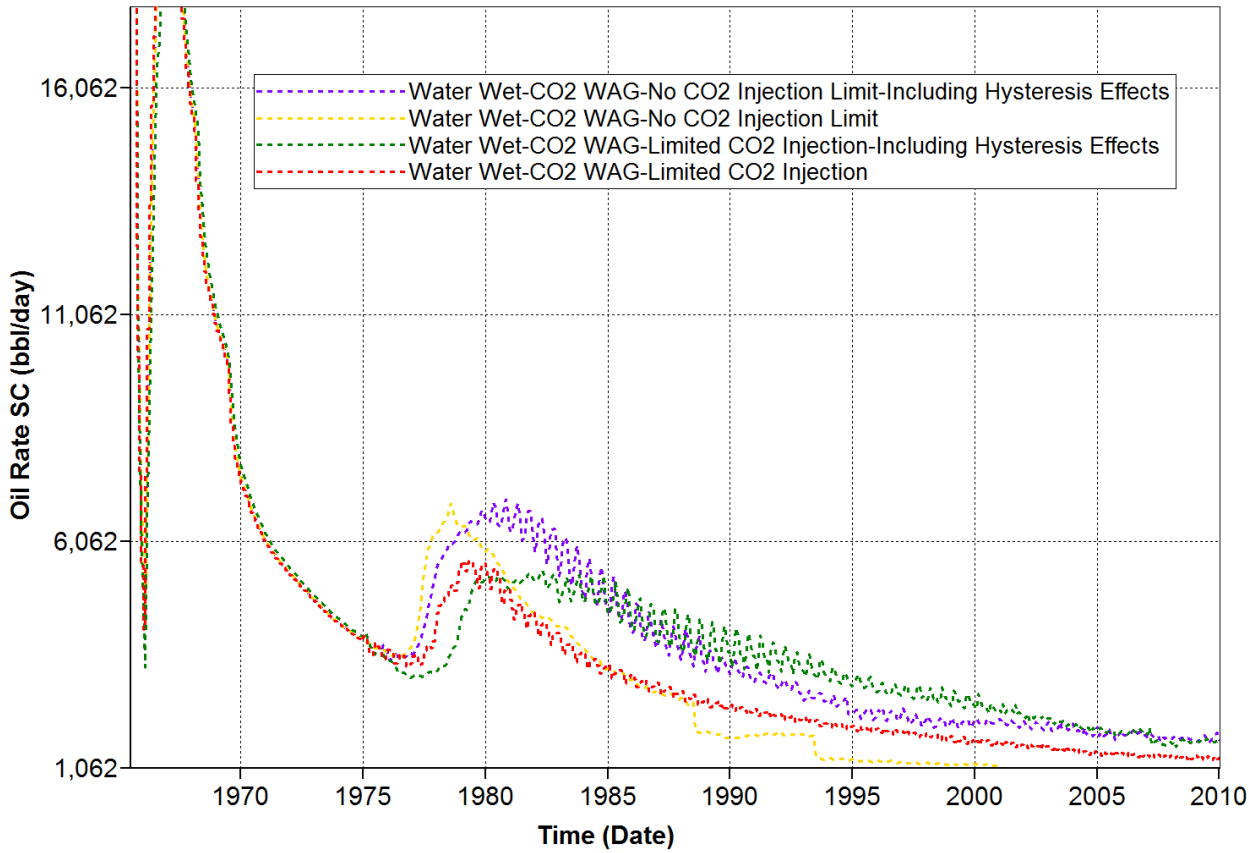

Figure 4.19 Oil Production Rate, Water-Wet Model.

In short term production, injecting more CO_2 improved the oil production. However, in long term production, with less amounts of CO_2 injection almost the same oil production was achieved for both wettability characteristics (Figures 4.20 and 4.21), because injecting more CO_2 in the scenario of a non-limited CO_2 injection rate resulted in earlier CO_2 breakthrough. Therefore, after 35 years of WAG flooding, cumulative oil production is almost the same in both scenarios.

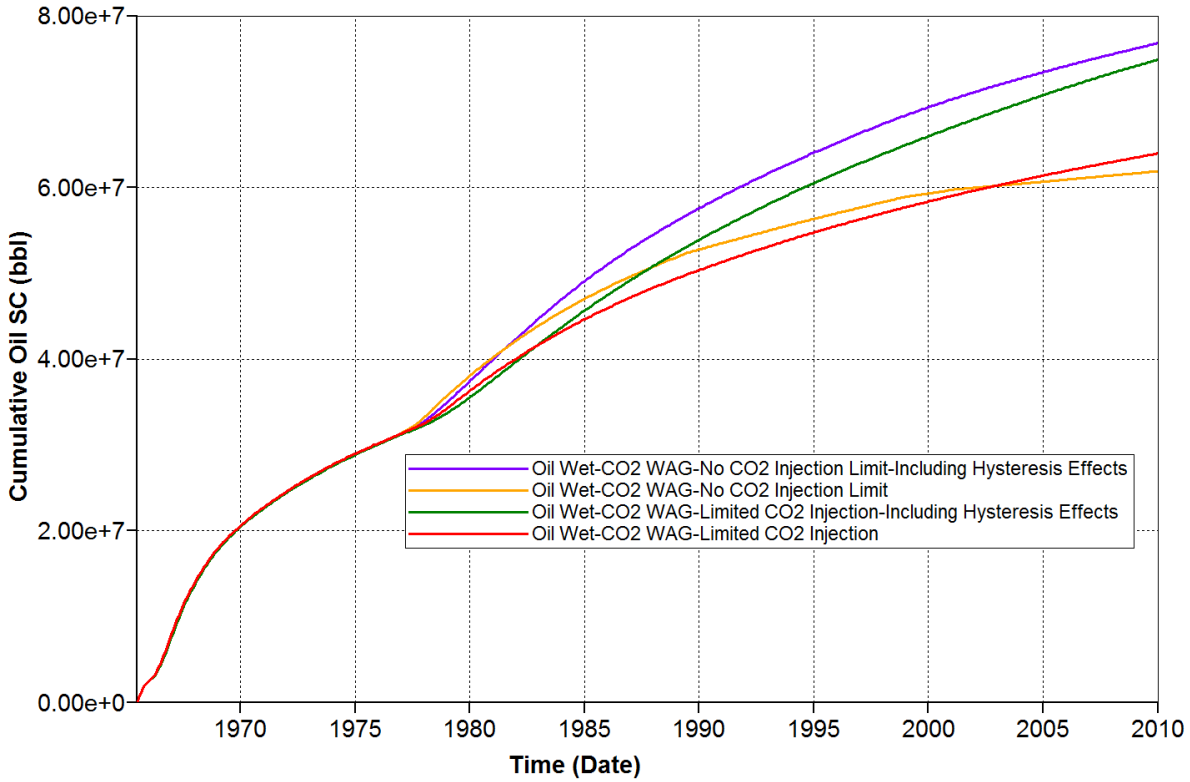

Figure 4.20 Cumulative Oil Production, Oil-Wet Model.

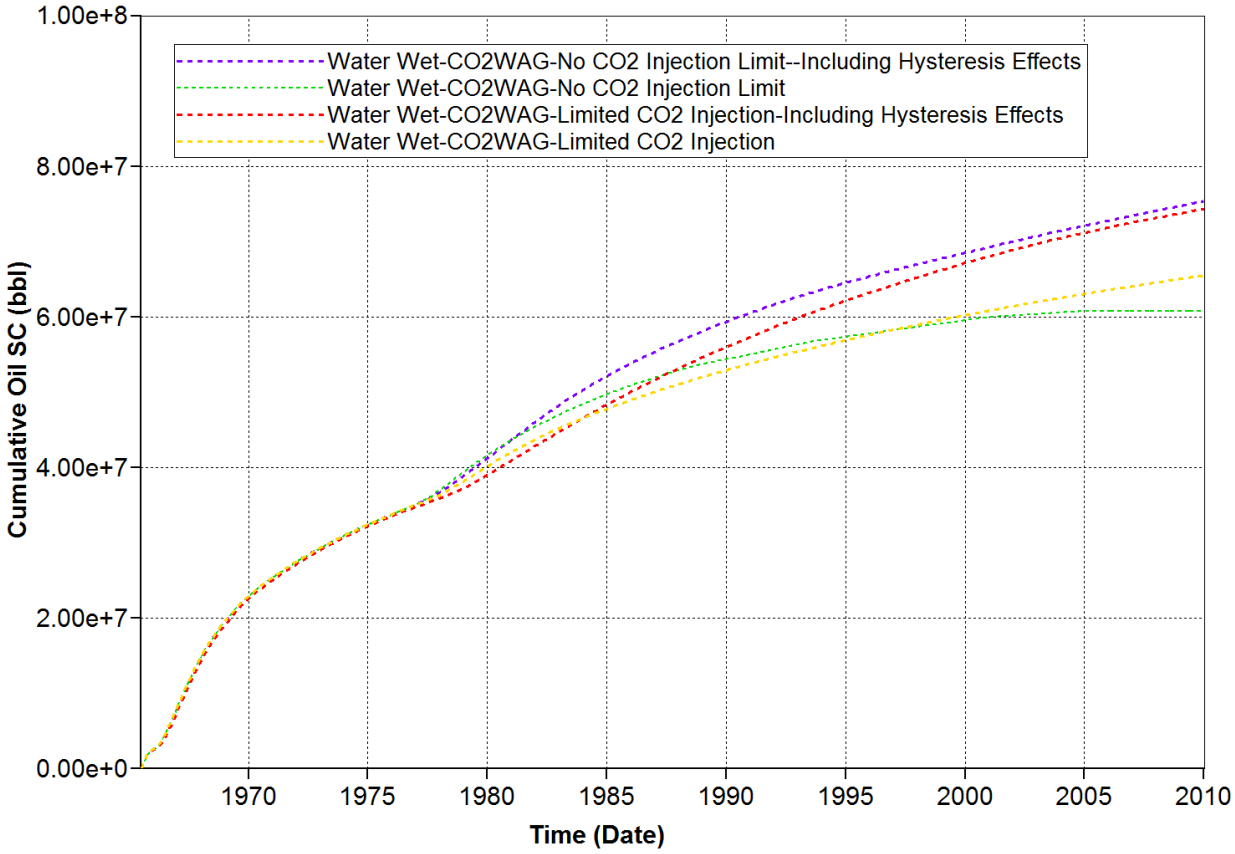

Figure 4.21 Cumulative Oil Production, Water-Wet Model.

Additionally, the amounts of the CO_2 injection rate and the water injection rate in the WAG process decreased a lot considering hysteresis effects; also, there were less gas production and water production compared to the models without including hysteresis effects. Considering the scenario with no limit for a CO_2 injection rate, there were almost 211 MMscf more CO_2 injected in the simulation without considering hysteresis effects in the water-wet model and 51100MMscf in the oil-wet model (Figure 4.22).

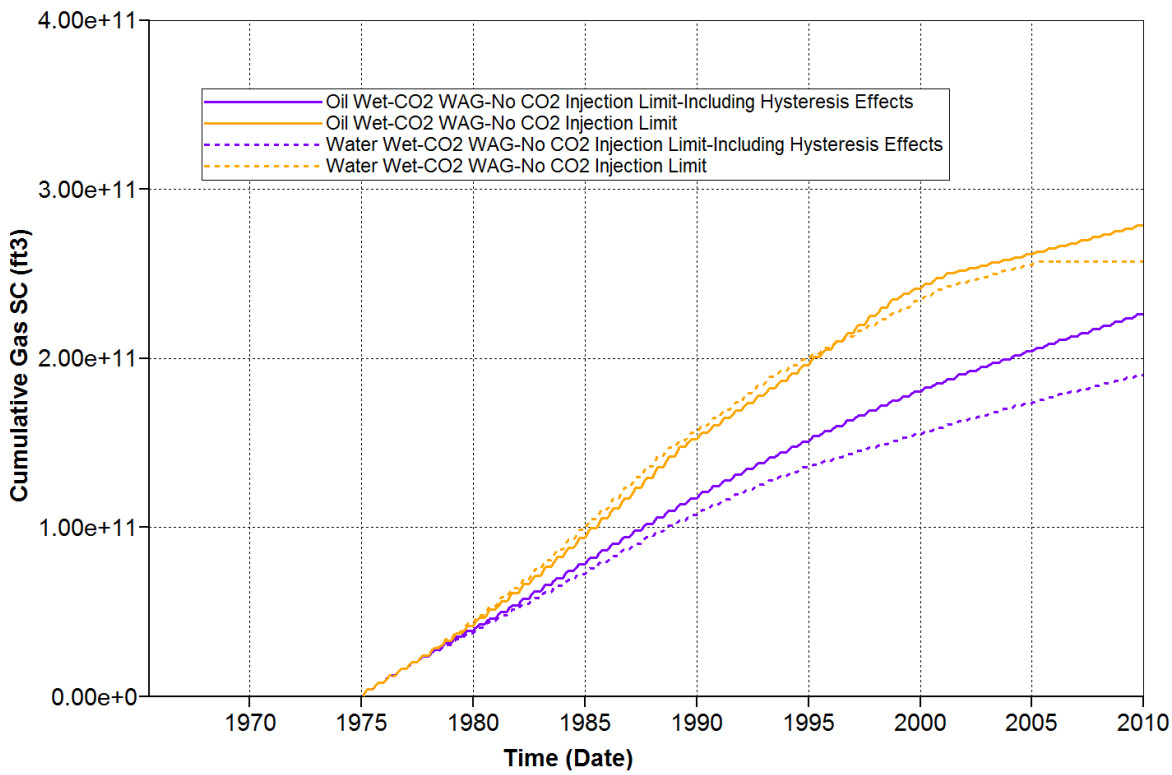

Figure 4.22 Cumulative Gas Injection, Oil-Wet and Water-Wet Models.

Considering hysteresis effects resulted in a much lower GOR in all the simulation models for both oil-wet and water-wet characteristics. In the scenarios of limiting a CO_2 injection rate, there was the same amount of CO_2 injected into the reservoir for both simulations including and excluding hysteresis effects; however, the GOR decreased a lot in the models including the hysteresis effects (Figure 4.23, next page).

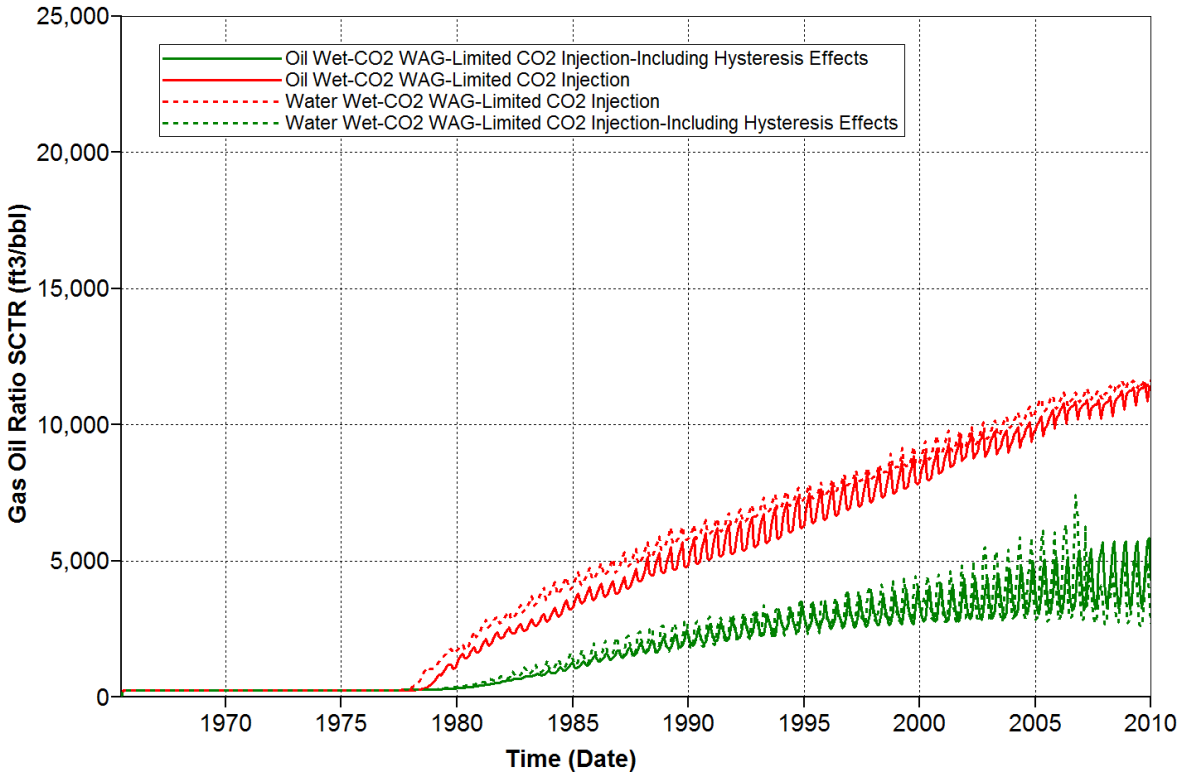

Figure 4.23 Gas Oil Ratio, Oil-Wet and Water-Wet Models.

Note that in the water-wet WAG flooding model without hysteresis when there was no limit for a CO2 injection rate, CO2 injection was stopped on 2005-03-02 due to a very high GOR, and considering a hysteresis effect resolved the issue and resulted in a lower GOR (Figure 4.24). In the models including hysteresis effects GOR decreased because there was more CO2 trapped into the reservoir which will be explained later in this section.

From the above discussions, a decrease in the GOR, for the WAG flooding simulations including a hysteresis effect, was independent from the amount of the CO_2 injection rate. Therefore, we can continue discussing the results by only considering the scenario of no limit on a CO_2 injection rate. This way the average reservoir pressure is stable around 3,300 psi during CO_2-WAG flooding. Therefore, we have a fair comparison between different simulations and recovery methods.

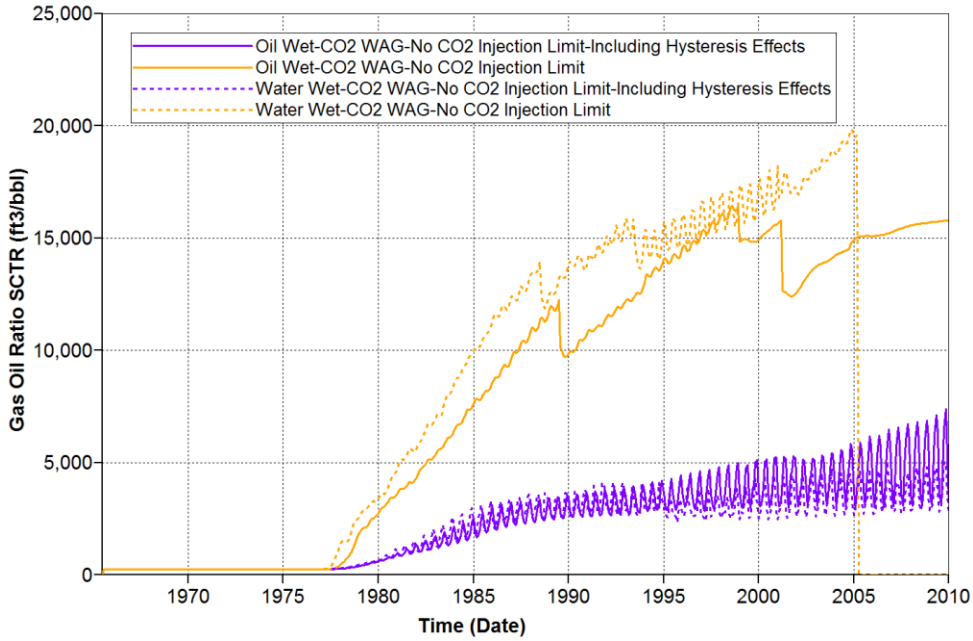

Figure 4.24 Gas Oil Ratio, Oil-Wet and Water-Wet Models.

A water injection rate and WCUT in production are decreased a lot as well by involving hysteresis effects (Figures 4.25 and 4.26). Therefore, considering the hysteresis effect results in much more realistic economical calculations for the WAG injection in both reservoirs with oil-wet and water-wet wettability characteristics.

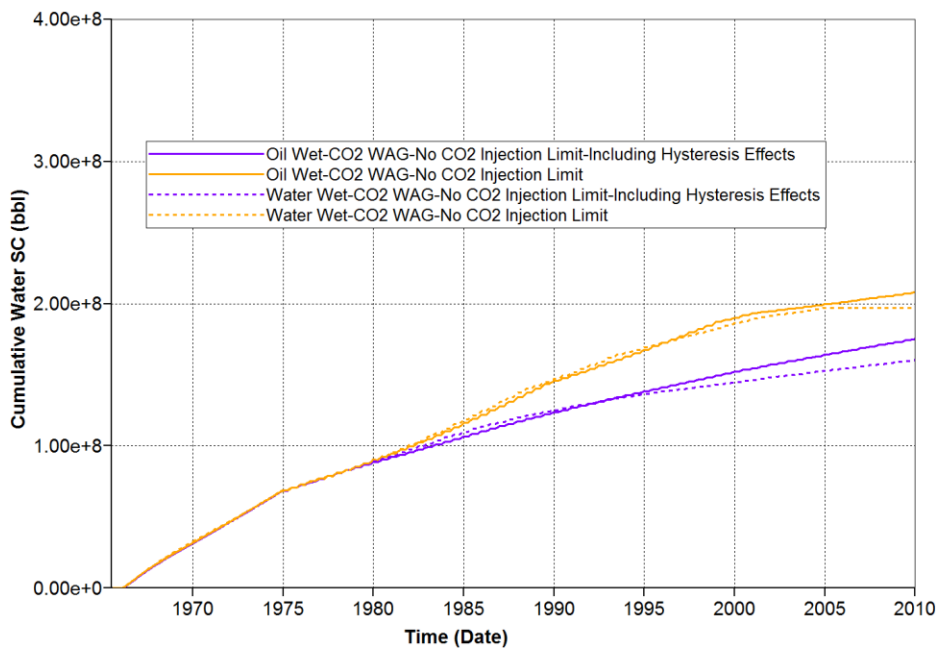

Figure 4.25 Cumulative Water Injection Oil-Wet and Water-Wet Models.

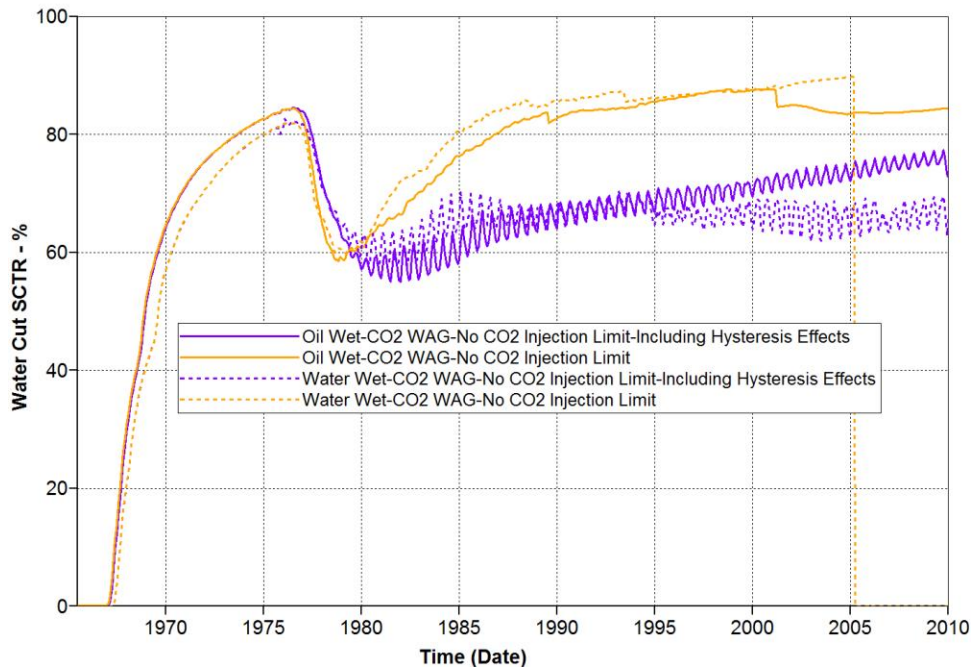

Figure 4.26 Water Cut Oil-Wet and Water-Wet Models.

It was discussed earlier that the average reservoir pressure should be around 3,300 psi in order to have a fair comparison between simulations. By involving hysteresis effects in the simulations with no limit for a CO_2 injection rate, reservoir pressure was still stable around 3,300 psi for both the oil-wet and water-wet reservoirs (Figure 4.27).

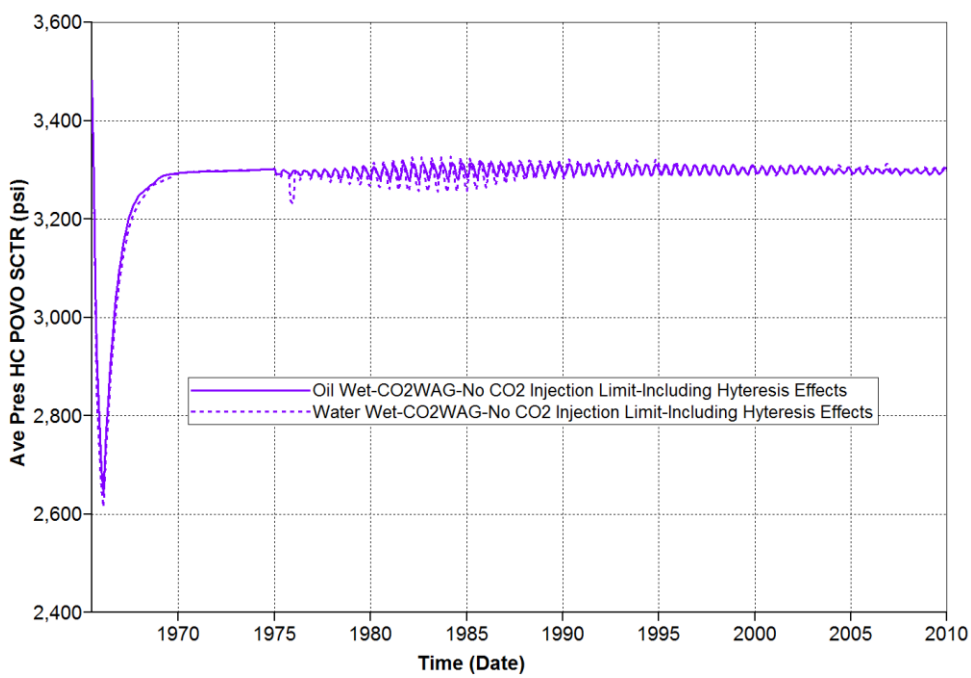

Figure 4.27 Reservoir Pressure, Oil-Wet and Water-Wet Models.

Three-phase relative permeabilities are critical in determining the phase mobility, and, therefore, they have a strong impact on oil recovery. The hysteresis effects must be included in the WAG flooding simulations in order to have the correct values of three-phase relative permeabilities. By involving the hysteresis effects, we are essentially considering the impact of the trapped CO_2 in a reservoir. More trapped CO_2 in the reservoir means lower gas relative permeability and thus higher oil relative permeability which results in better oil mobility and more oil production. When there is more CO_2 trapped into the reservoir, there is less CO_2 production and also there is less potential for injecting CO_2 into the reservoir as it is already stored in the reservoir. Hence, by not including hysteresis effects in the simulations, we are considering less trapped gas (CO_2) in the reservoir and, therefore, our prediction of the oil production is non-realistic and much lower than its actual value.

The following figures compare the CO_2 concentration in layer 3 of the reservoir models for CO_2-WAG injection for both water-wet and oil-wet reservoirs. The top figures refer to the WAG simulations excluding the hysteresis effects and the bottom figures refer to the WAG simulations including hysteresis effects. As we can see, there is more CO_2 trapped into the reservoir while considering hysteresis effects. The same pattern has been seen in the other layers of the reservoirs.

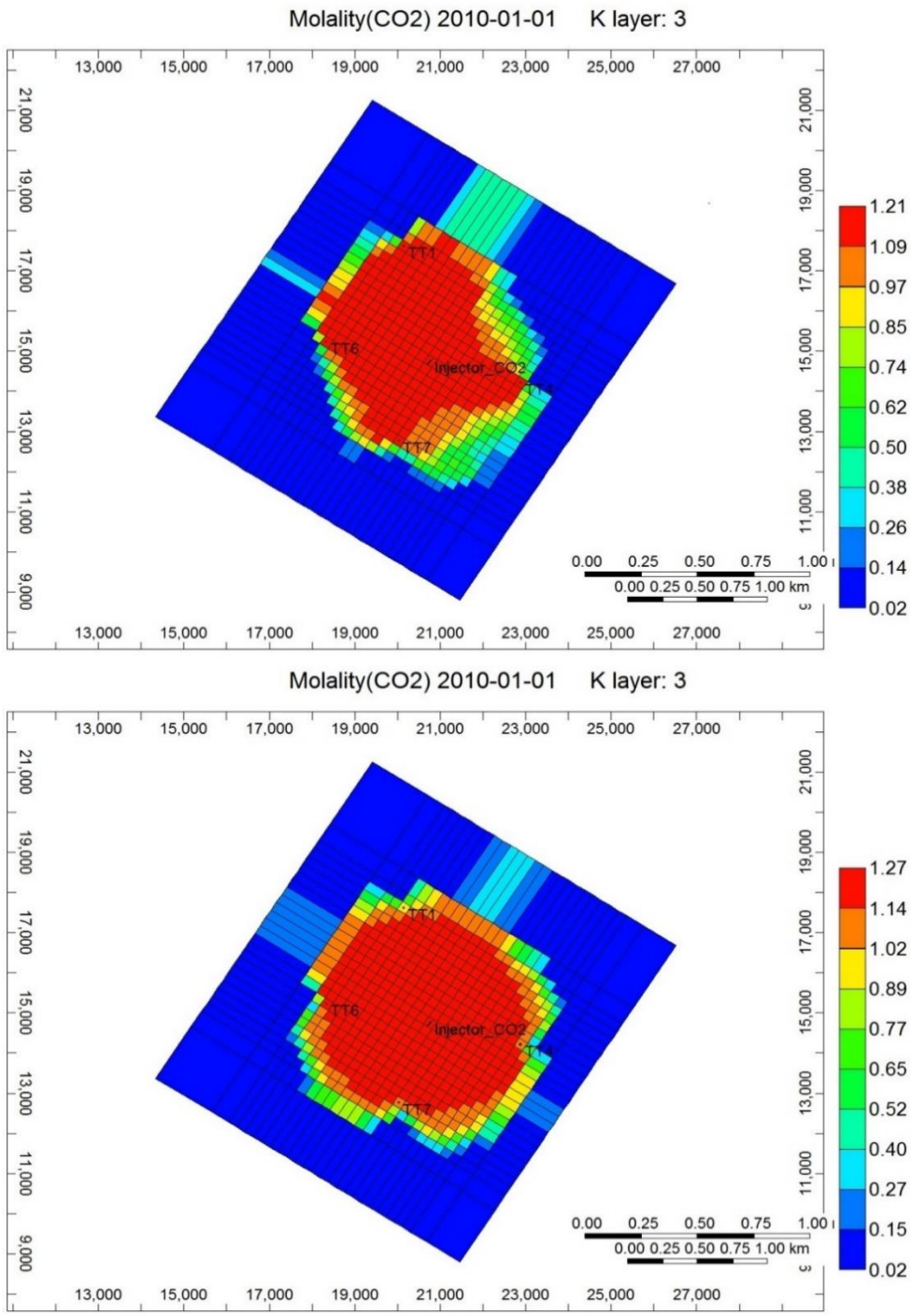

Figure 4.28 CO_2 Molality Layer 3, Oil-Wet.

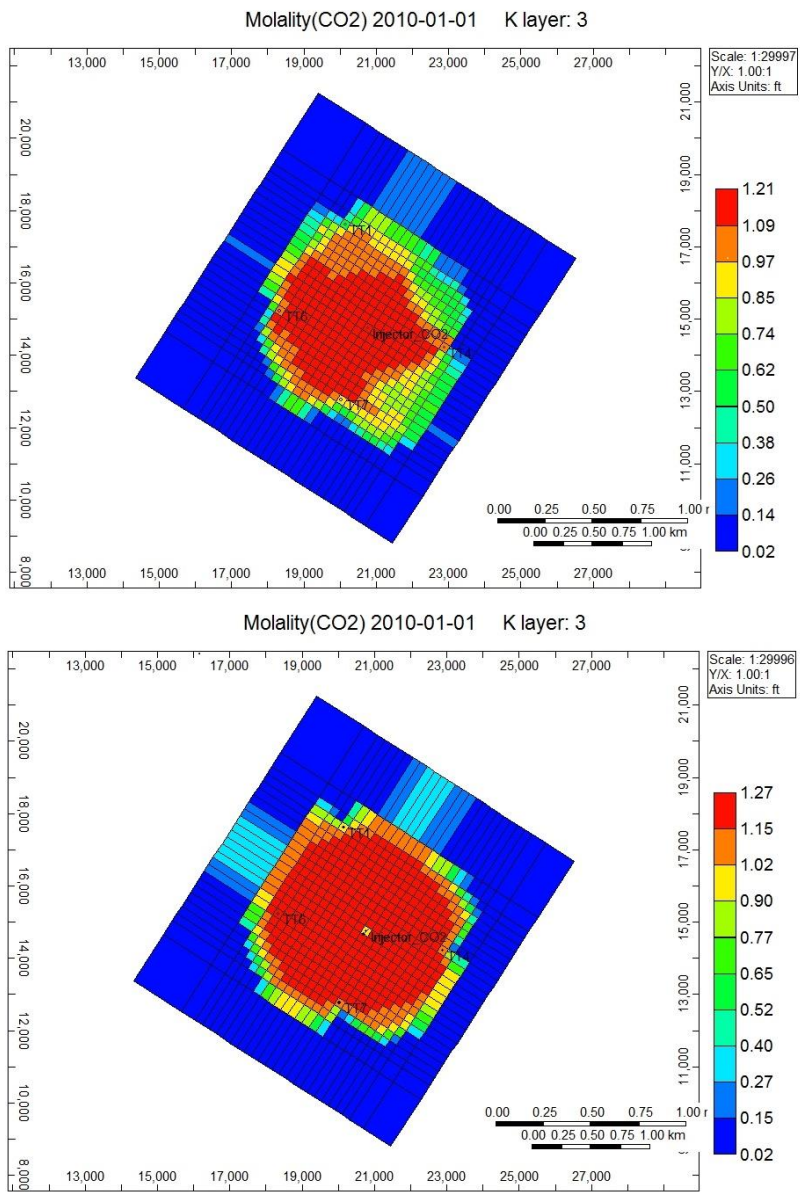

Figure 4.29 CO_2 Molality Layer 3, Water-Wet.

Considering the hysteresis effects, there was less CO_2 injected into the reservoir and also the oil recovery factor was increased by 6.9 in the water-wet reservoir and by 6.2 in the oil-wet reservoir.

Table 4.2 Oil Recovery Factor.

Oil Recovery Factor	Water-Wet System	Oil-Wet System
CO_2 WAG No Hysteresis	28.8	25.6
CO_2 WAG with Hysteresis	35.7	31.8

4.2 Fine Gridding Effect on CO_2-WAG Simulation

Simulations of WAG models with finer grids require more running time, especially for CO_2-WAG flooding considering hysteresis effects. Hence, in this study the simulation models with coarse grids were considered first and then results were confirmed using fine gridding models. Fine gridding models are considered with grid block sizes of one fifth (1/5) of the block sizes in the coarse gridding models.

Below the results of an oil-wet model are presented, although it should be mentioned that the same results were achieved for a water-wet model. As Figure 4.30 shows, the oil production was overestimated using the coarse gridding model during the WAG process. The solid curves represent CO_2-WAG flooding using fine gridding and the dot curves present the coarse models. Fine gridding simulation models confirm that considering a hysteresis effect makes a big difference in oil production during the WAG process by increasing the oil production.

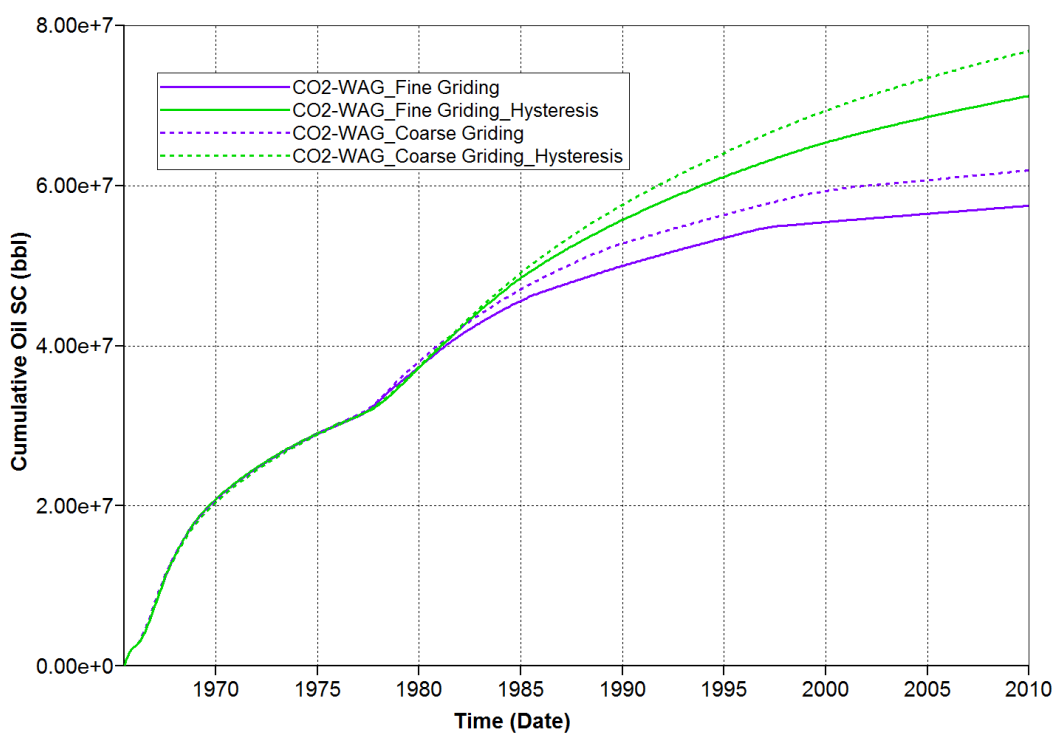

Figure 4.30 Cumulative Oil Production.

Looking at the oil rate curves, oil production rates of coarse and fine gridding models are almost the same for the first 6 years of oil production by CO_2-WAG flooding. Therefore, the length of the oil production is an important factor in choosing a gridding size for a simulation model (Figure 4.31).

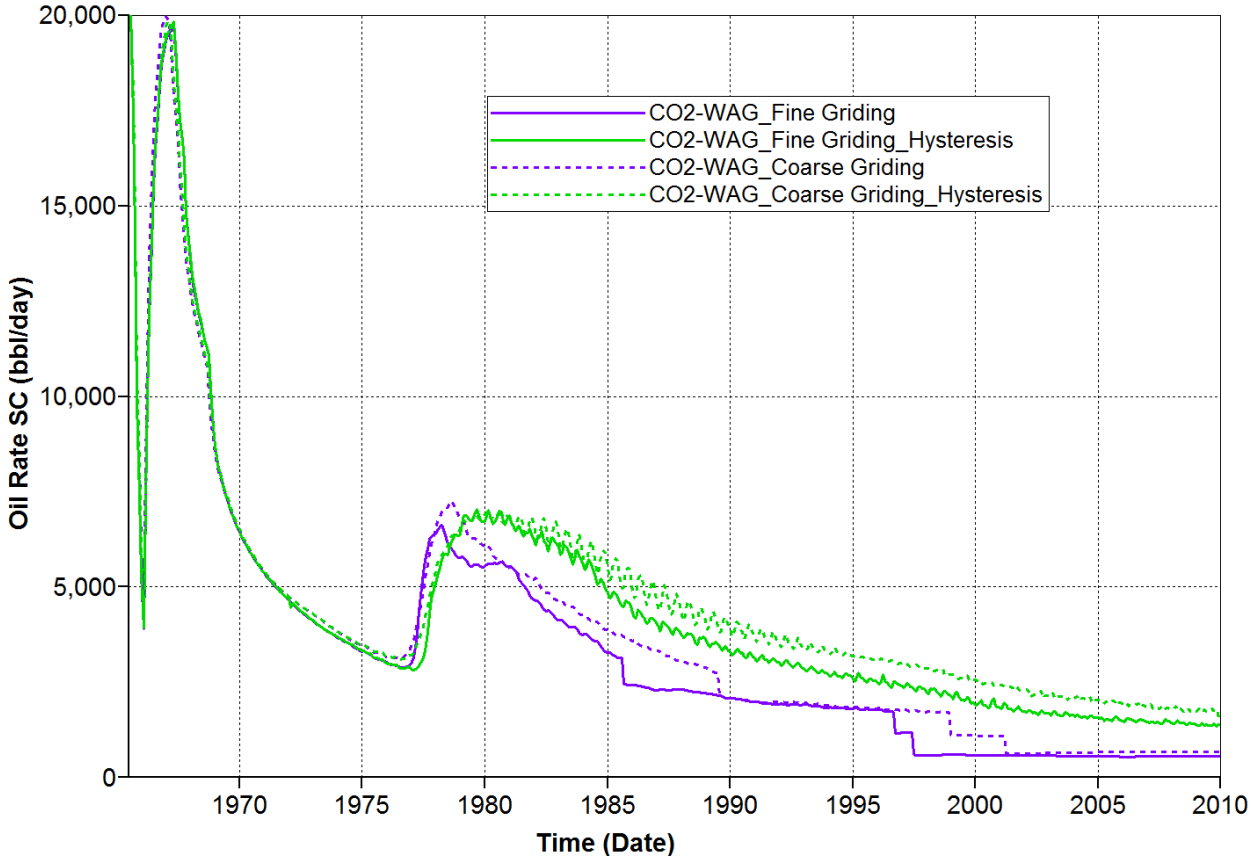

Figure 4.31 Oil Production Rate.

A smaller grid size simulation model also confirms that the models considering a hysteresis effect yield more oil production by injecting less water and CO_2 into the reservoir. Results also show that in the models using finer grids there is less potential for CO_2 and water injection and as a result less oil production (Figures 4.32 and 4.33).

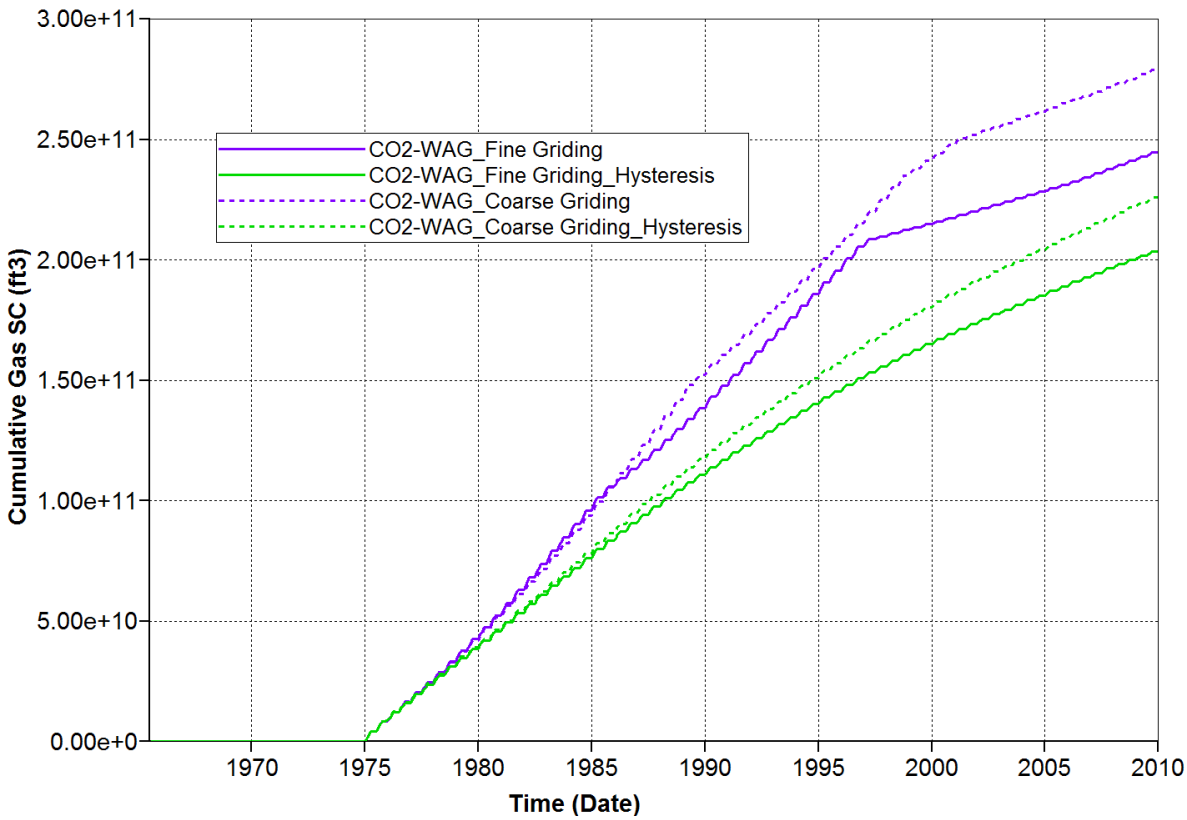

Figure 4.32 Cumulative CO_2 Injection.

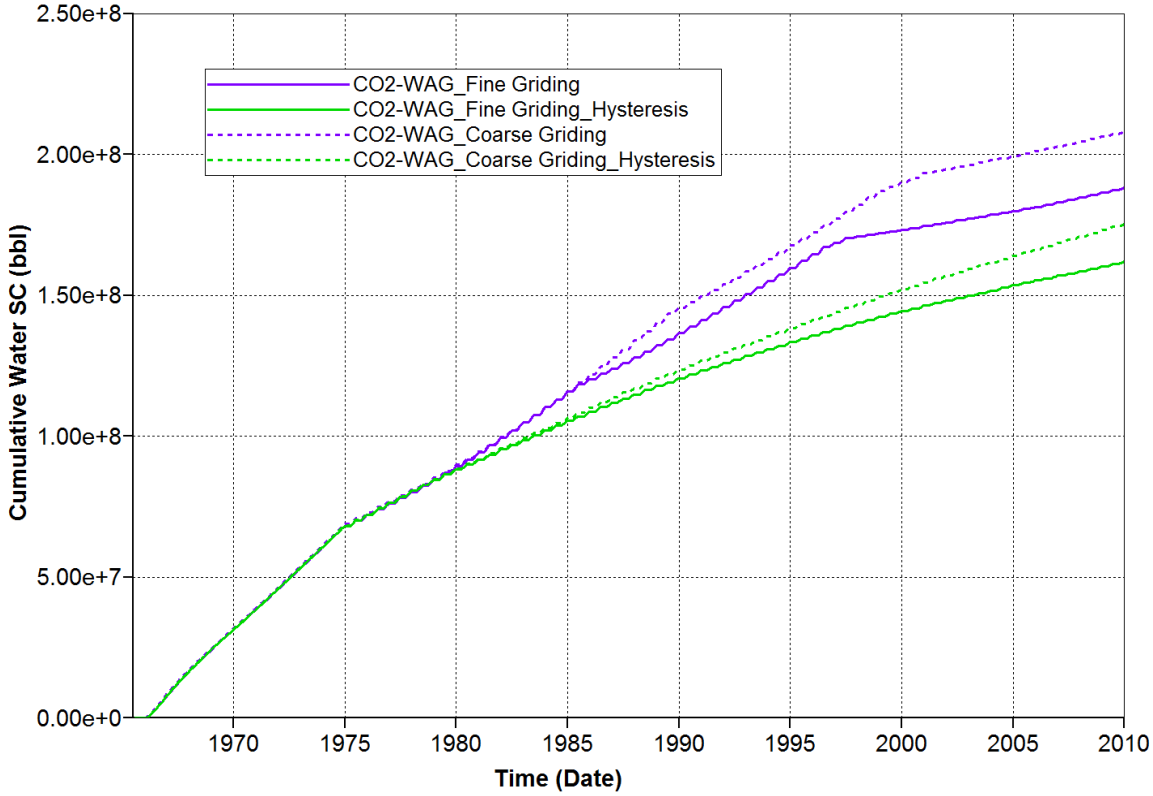

Figure 4.33 Cumulative Water Injection.

4.3 Effect of Hysteresis and Oil Viscosity on CO_2-WAG Models

In the original model which was discussed earlier the oil API is 32. In this section results of a lighter oil with API 40 will be discussed.

The figures in this section are all considered for the oil-wet reservoir, although the same behavior was seen in the water-wet reservoir. At the end of this section the values of an oil recovery factor for both the oil-wet and water wet models are presented.

Figure 34 indicates that the oil production in the WAG model is higher than that in water flooding and CO_2 flooding although WAG flooding production decreases to less than water flooding production later in 1990 because of a high GOR which will be discussed later. Also, the oil production in the WAG model considering hysteresis effects of relative permeabilities is much more than in the WAG model excluding hysteresis effects, which confirms the conclusion discussed earlier using oil with API 32 in Section 4.1.2.

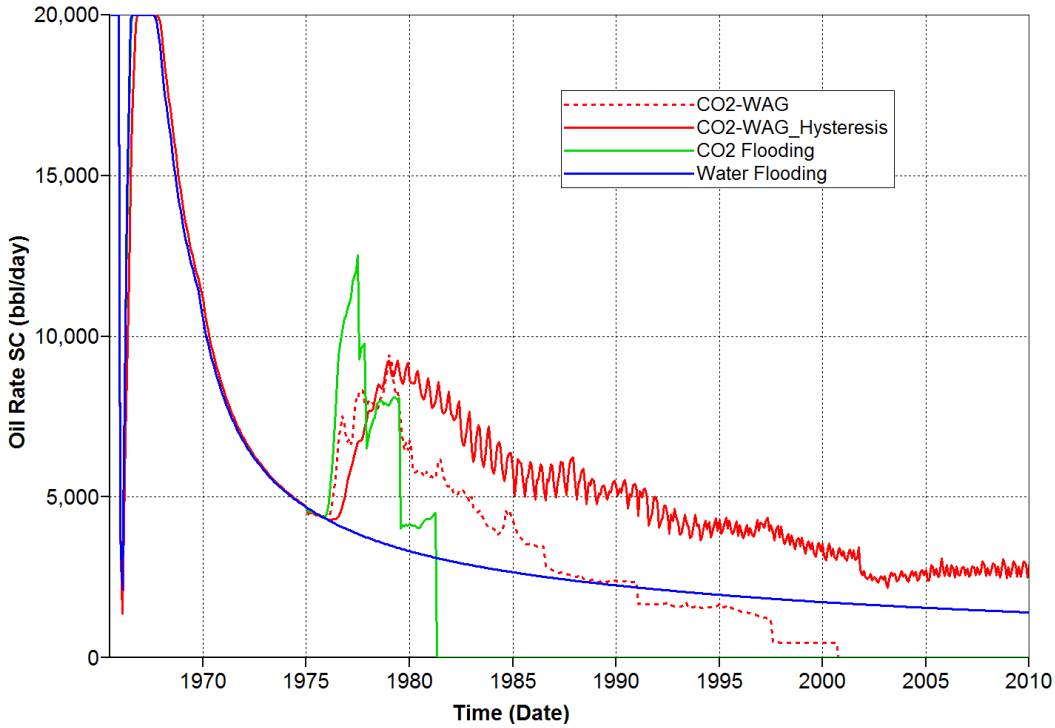

Figure 4.34 Oil Production Rate, Oil-Wet Model.

The simulation results for cumulative oil production show that considering the hysteresis effects in the simulation for the lighter oil (i.e., API 40) results in a larger difference in oil production, in comparison with the case for heavier oil (i.e., API 32).

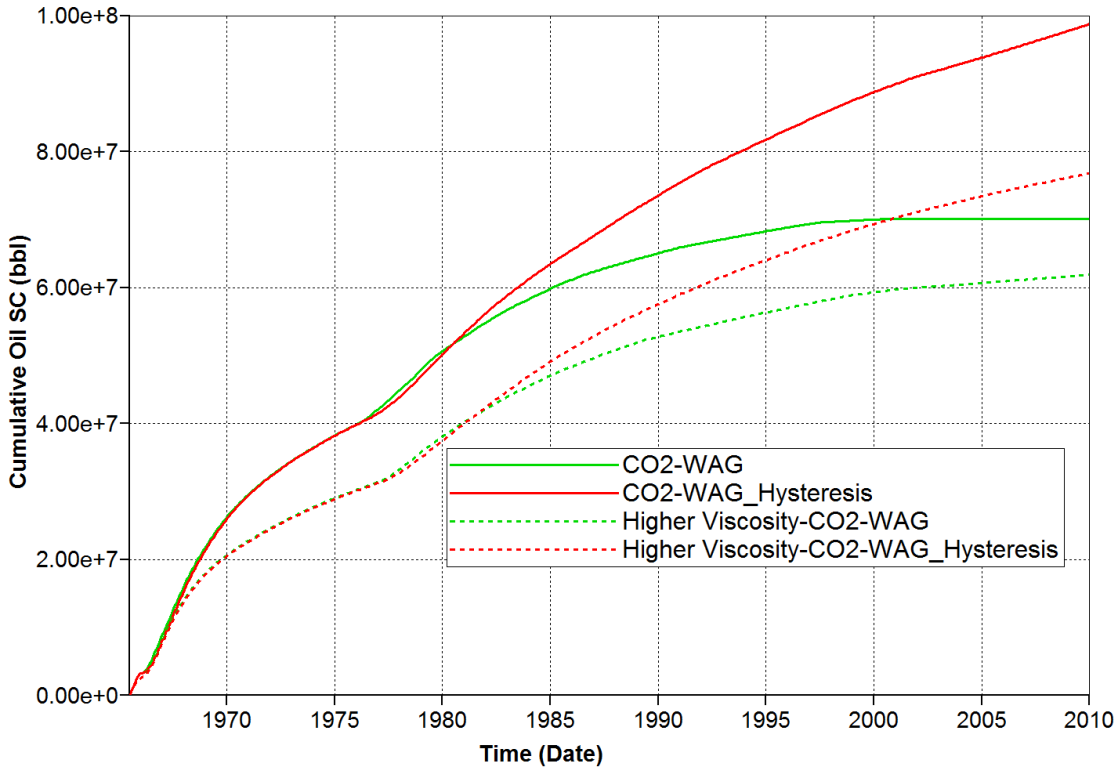

Figure 4.35 Cumulative Oil Production, Oil-Wet Model.

That is because of more CO_2 trapped into the reservoir in the case of lower oil viscosity which resulted in more oil production (Figure 4.36). Recall the mobility ratio formula:

$$\boldsymbol{M = \lambda_D/\lambda_d = \lambda_g/\lambda_o = \frac{k_{rg}}{\mu_g} * \frac{\mu_o}{k_{ro}}}$$

Lighter oil has less viscosity, and, therefore, higher mobility which results in a lower mobility ratio and more CO_2 trapped into the reservoir resulting in more oil production.

The following figure shows that there is much higher trapped CO_2 in layer 3 of the reservoir while considering hysteresis effects. This difference in the amount of trapped CO_2 is more than what was seen in the models with higher oil viscosity (Figure 4.36).

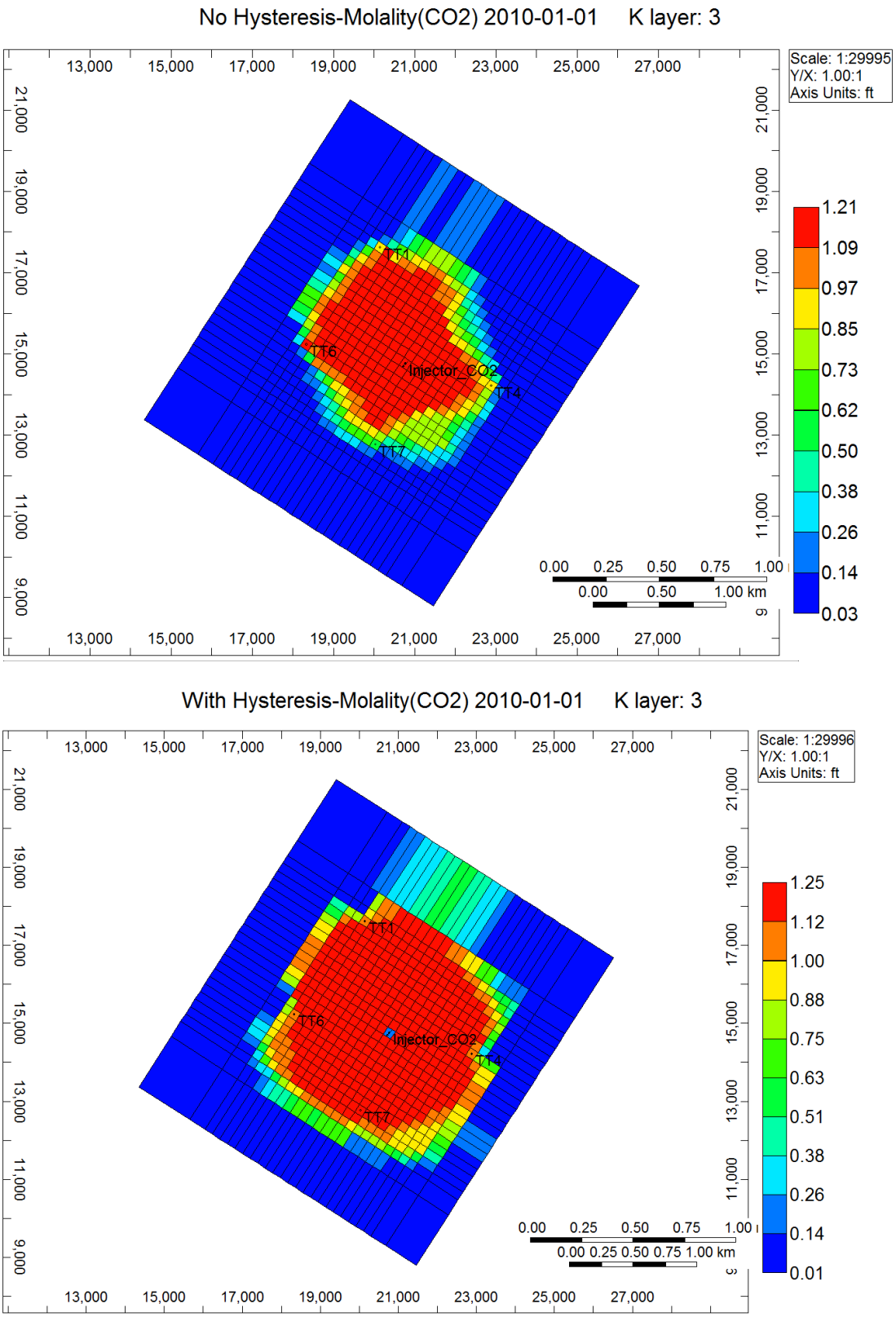

Figure 4.36 CO_2 Molality in Layer 3, Oil-Wet Model.

Not considering hysteresis effects in WAG resulted in a much higher GOR and earlier breakthrough for CO_2 and a wrong comparison between water flooding and CO_2-WAG flooding. Hence, it is even more necessary to consider relative permeability hysteresis effects in WAG simulation models with lower oil viscosity.

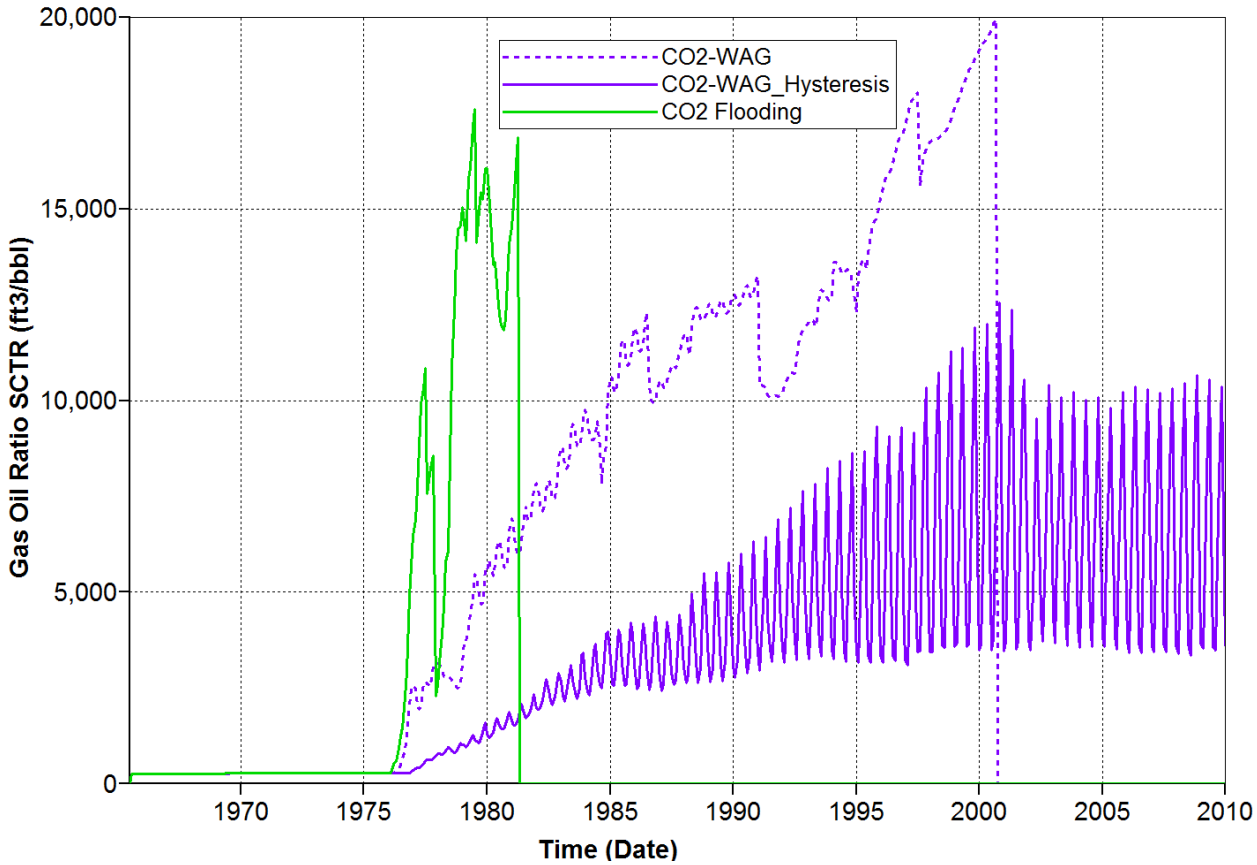

Figure 4.37 Gas Oil Ratio, Oil-Wet Model.

The average reservoir pressure is pretty stable around 3,300 psi during WAG flooding, which makes the comparison pretty fair.

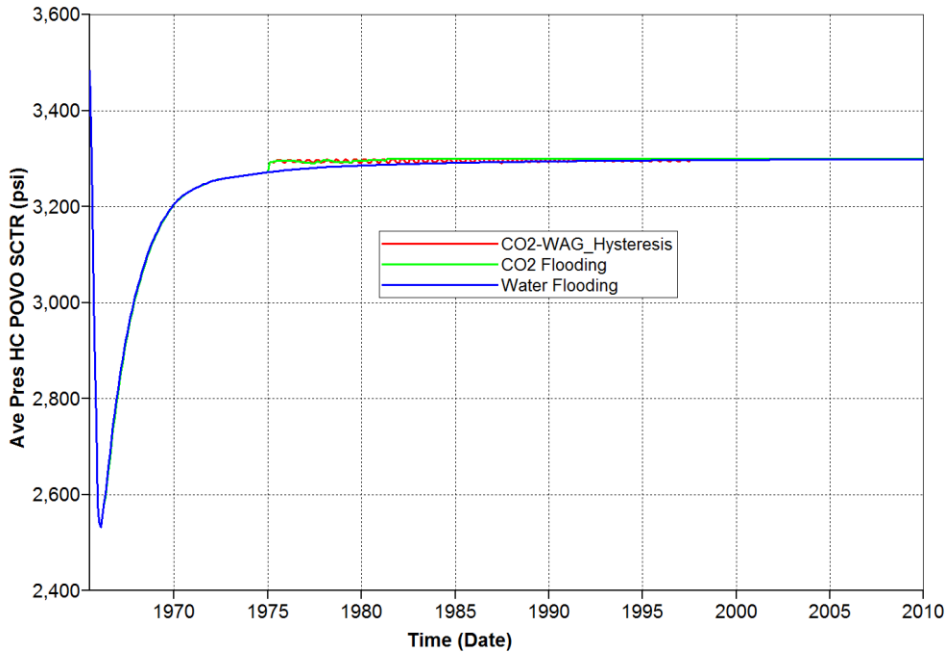

Figure 4.38 Average Reservoir Pressure, Oil-Wet.

As presented below, the oil recovery factor by using hysteresis in WAG is increased by 9.2 in the water-wet system and 11.9 in the oil-wet system. Basically, considering correct WAG simulations (WAG simulations including hysteresis effects) the oil recovery factor was increased from 31.6% in water flooding to 43.5% in CO_2-WAG injection in the water-wet system. Also, in the oil-wet system correct CO_2-WAG simulations increased the oil recovery factor from 28.3% in water flooding to 41.1% CO_2-WAG flooding.

Table 4.3 Oil Recovery Factor.

Oil Recovery Factor	Water-Wet System	Oil-Wet System
Water Flooding	31.6	28.3
CO_2 Flooding	20	22.3
CO_2 WAG No Hysteresis	34.3	29.2
CO_2 WAG with Hysteresis	43.5	41.1
Oil Recovery Improvement Using Hysteresis	9.2	11.9

4.4 Effect of Hysteresis and High Permeability Contrast on WAG Models

In this scenario, the reservoir model has a high permeability contrast in its layers, meaning that some layers of the reservoir have very low permeability and some layers have very high permeability. The following figure describes the permeability distribution in different layers. Layers 1, 3 and 5 have low permeability, layers 2, 4, 6 and 8 have high permeability, and layer 7 has the highest permeability compared to the other layers of the reservoir.

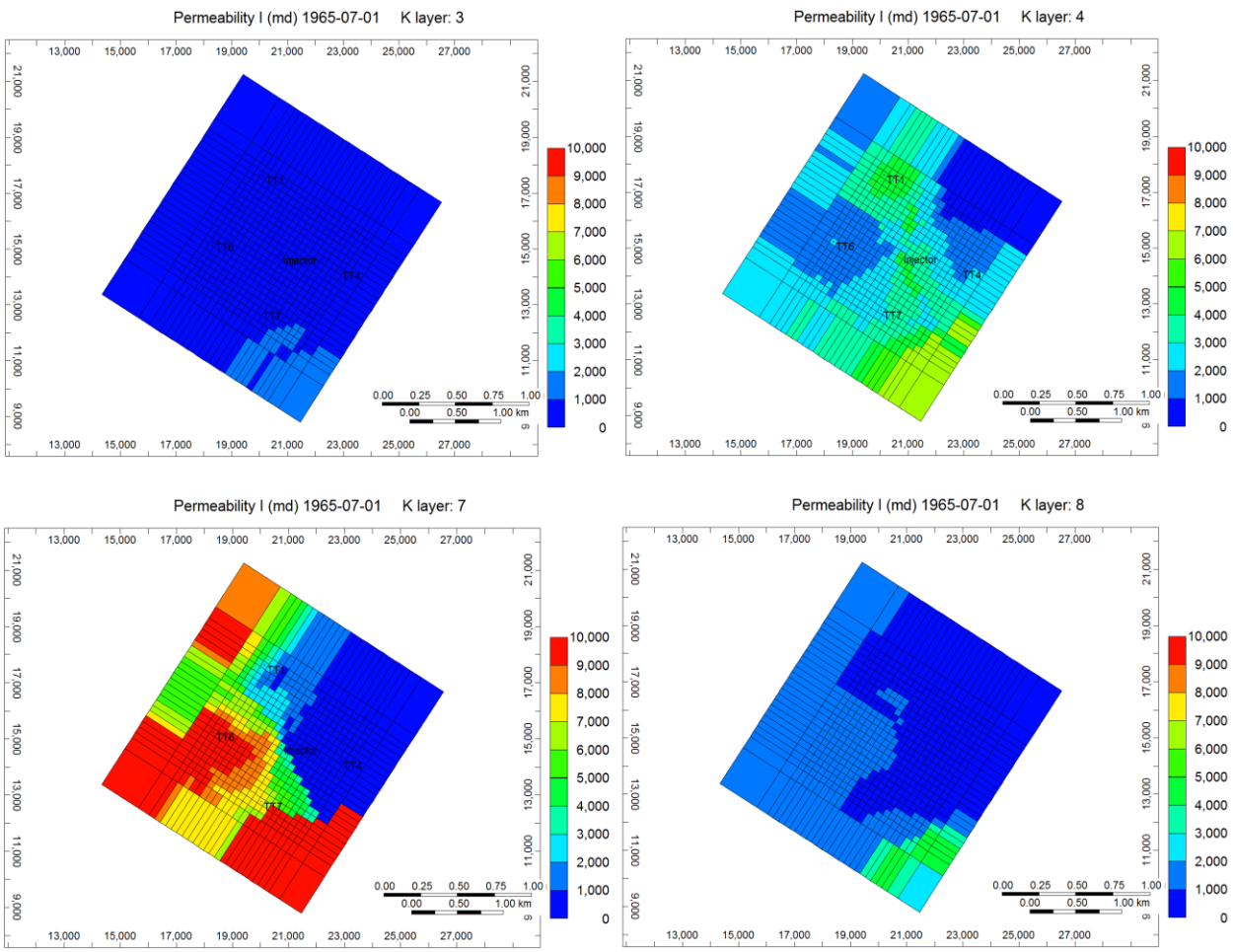

Figure 4.39 Permeability of layers 3 and 7 on the left and layer 4 and 8 on the right.

The figures in this section are all considered for the oil-wet reservoir, although the same behavior was seen in the water-wet reservoir. At the end of this section the values of an oil recovery factor for both the oil-wet and water wet models are presented.

Results indicate that due to having some very high permeable layers CO_2 breakthrough happens very early in CO_2 flooding simulation. Therefore, WAG flooding improves the oil production a lot.

Figure 4.40 shows that GOR is really high in the WAG model without considering hysteresis in the oil-wet system. Therefore, considering hysteresis has an even more impact on the model with a high permeability contrast compared to the original model.

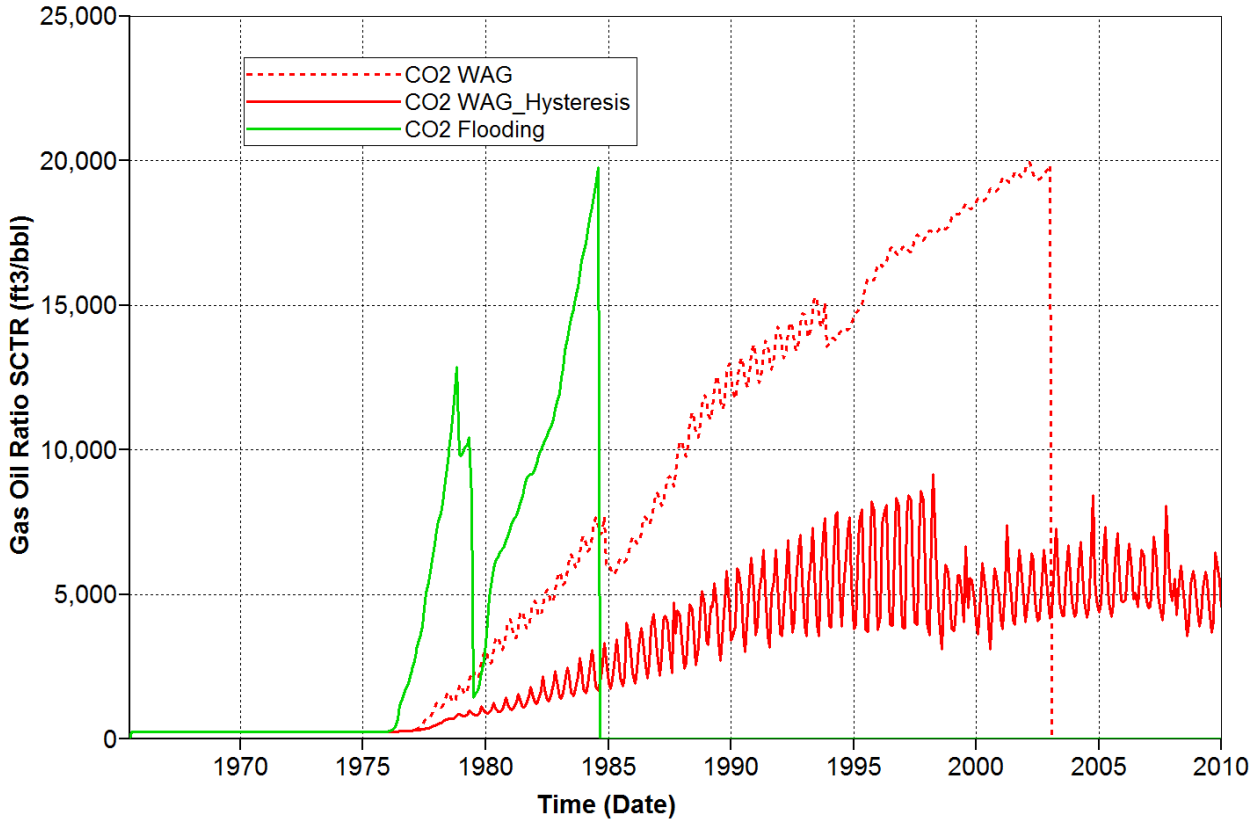

Figure 4.40 Oil-Wet Model Gas Oil Ratio.

The following figures show a big difference in oil production considering a hysteresis effect in WAG flooding (Figures 4.41). Therefore, the impact of using relative permeability hysteresis in WAG simulation of a high permeability contrast reservoir is bigger compared to the original reservoir model. This bigger impact is the result of the higher permeability in some layers of the

reservoir which have bigger potential of storing CO_2 into the reservoir. By not considering hysteresis effects in the WAG simulation, less CO_2 is trapped in high permeable layers of the reservoir and more CO_2 is produced, resulting in very high GOR and much lower oil production.

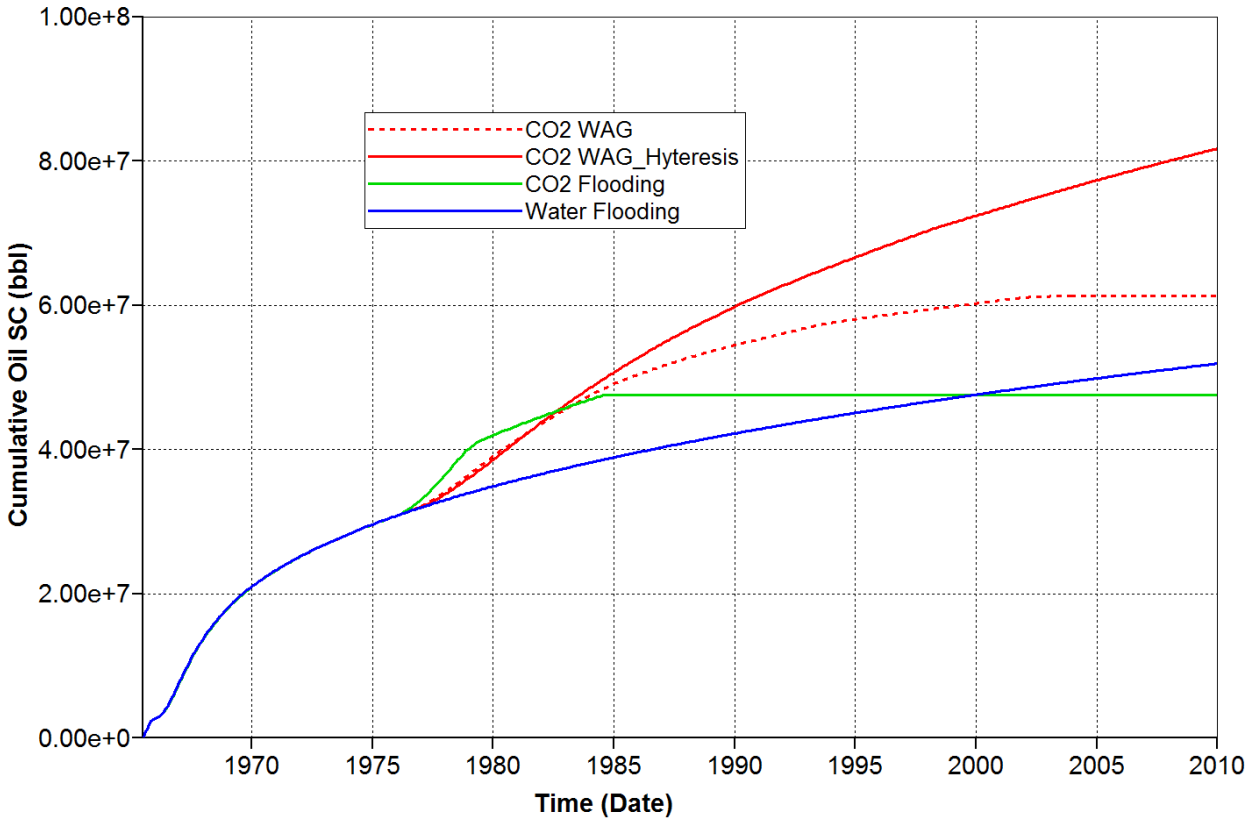

Figure 4.41 Cumulative Oil Production for Oil-Wet Model.

The average reservoir pressure was very stable around 3,300 psi during CO_2-WAG flooding (Figure 4.42), which confirms the importance of considering a relative permeability hysteresis effect in WAG injection for a reservoir with a high permeability contrast.

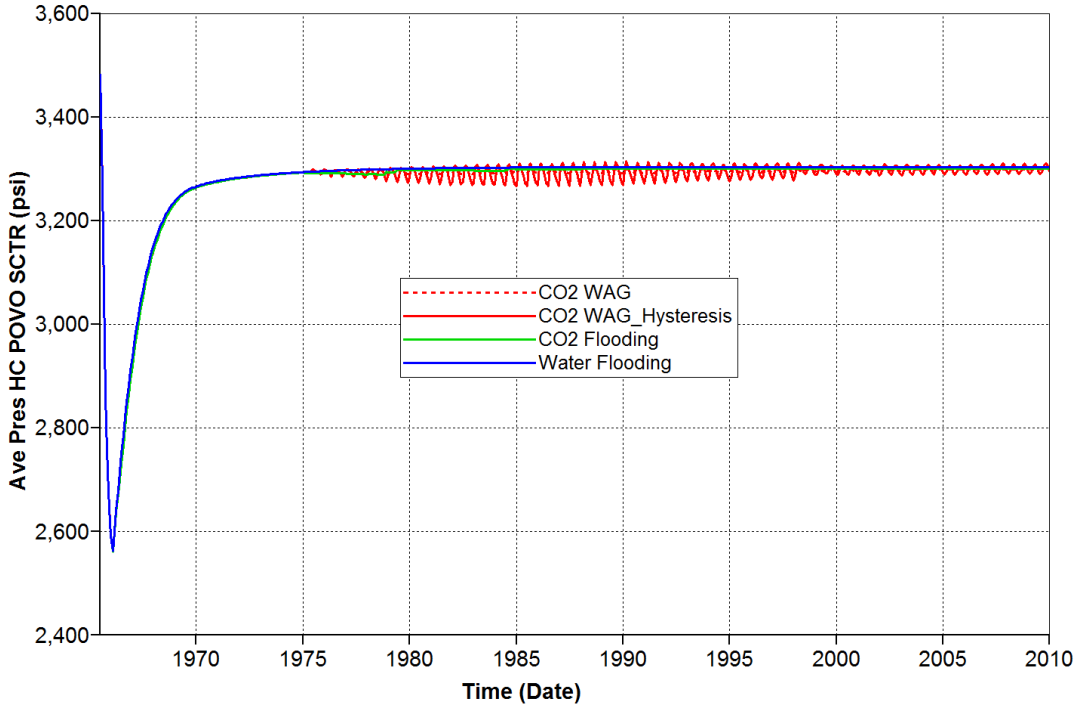

Figure 4.42 Average Reservoir Pressure in Oil-Wet Model.

Thus, WAG simulations considering hysteresis effects increase the oil recovery factor by 10.9 in water-wet and 12.3 in the oil-wet model. Compared to water flooding, WAG flooding without considering hysteresis effects did not increase the oil recovery factor very much, which is because of the early breakthrough of CO_2 injected into the reservoir. But including the hysteresis effects in the CO_2-WAG flooding simulation did increase the oil recovery factor from 26.8% in water flooding to 37.2% in CO_2-WAG flooding for the water-wet system and from 21.5% in water flooding to 33.8% in CO_2-WAG flooding for the oil-wet system.

Table 4.4 Oil Recovery Factor.

Oil Recovery Factor	Water-Wet System	Oil-Wet System
Water Flooding	26.8	21.5
CO_2 Flooding	21.9	19.7
CO_2 WAG No Hysteresis	27.8	25.4
CO_2 WAG with Hysteresis	37.2	33.8
Oil Recovery Improvement Using Hysteresis	9.4	8.4

Chapter 5: Conclusions

As stated in the above results, CO_2-WAG improved the oil recovery for all investigated reservoirs in this study which have different rock and fluid properties. It was also shown that considering hysteresis effects in the simulation models is necessary. Estimated oil production in WAG simulations not including hysteresis effects is very much underestimated, and also the amounts of the gas injection and water injection are overestimated. The following tables state the oil recovery factors for different scenarios (reservoirs with high viscosity oil or low viscosity oil or a reservoir with layers having a high permeability contrast) in water-wet and oil-wet systems.

Water-wet models:

Table 5.1 Oil Recovery Factor for Water-Wet Model.

Oil Recovery Factor Water-Wet System	High Viscosity Oil	Low Viscosity Oil	High Permeability Contrast in Reservoir
Water Flooding	26.4	31.6	26.8
CO_2 Flooding	22.6	20	21.9
CO_2 WAG No Hysteresis	28.8	34.3	27.8
CO_2 WAG with Hysteresis	35.7	43.5	37.2
Oil Recovery Improvement Using Hysteresis in WAG	**6.9**	**9.2**	**9.4**

Oil-wet models:

Table 5.2 Oil Recovery Factor for Oil-Wet Model.

Oil Recovery Factor for Oil-Wet System	High Viscosity Oil	Low Viscosity Oil	High Permeability Contrast in Reservoir
Water Flooding	20.9	28.3	21.5
CO_2 Flooding	20.4	22.3	19.7
CO_2 WAG No Hysteresis	25.6	29.2	25.4
CO_2 WAG with Hysteresis	31.8	41.1	33.8
Oil Recovery Improvement Using Hysteresis in WAG	**6.2**	**11.9**	**8.4**

Results indicate that including the hysteresis effects in the simulation has more impact on the oil production improvement in the case of the low viscosity oil reservoir and the high permeability contrast reservoir.

In addition, it has been observed that water flooding and CO_2 flooding behave differently with respect to the rock and fluid properties, such as reservoir permeability distribution and oil viscosity. The following figures present the oil recovery factors for different scenarios in both the oil-wet and water-wet systems.

As future work one may check the reliability of these simulation results considering hysteresis effects for some reservoirs and compare the estimated oil production and gas and water injection against actual production and injection data. Then one may modify the common hysteresis models in commercial simulators to achieve more realistic results using simulations.

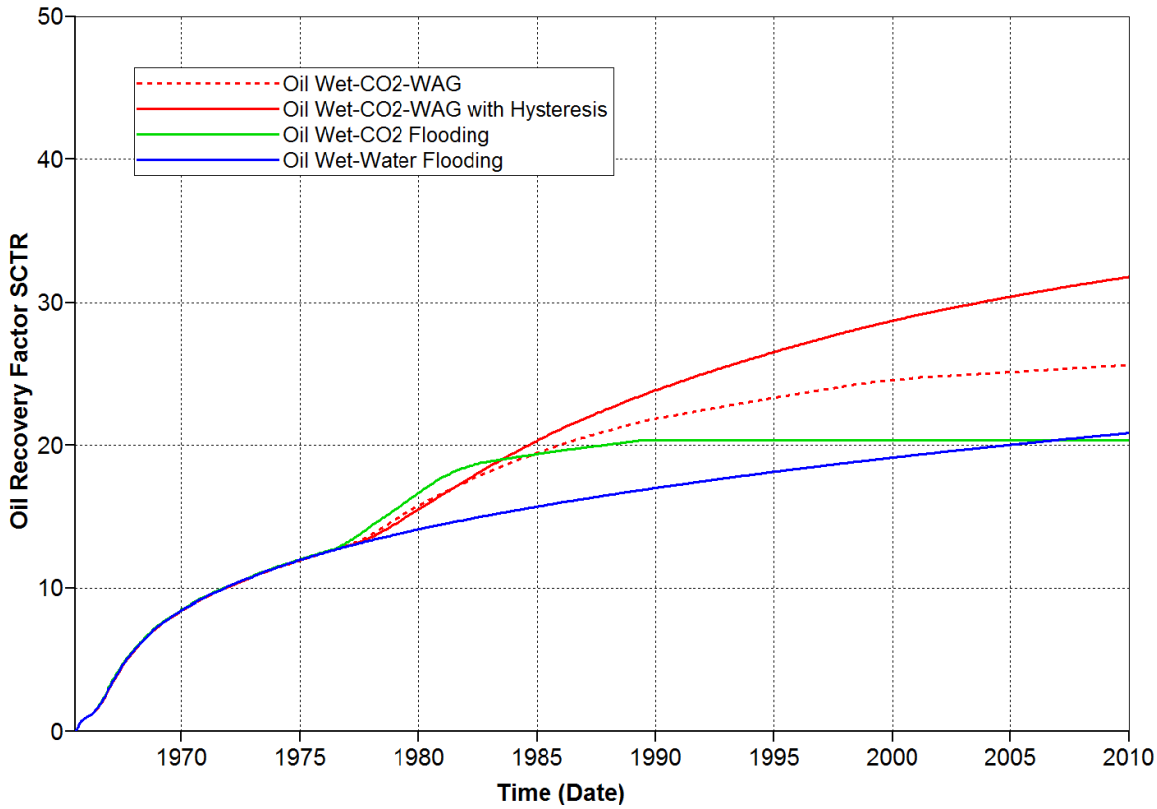

Figure 5.1 Oil Recovery Factor for Oil-Wet Model with Higher Oil Viscosity.

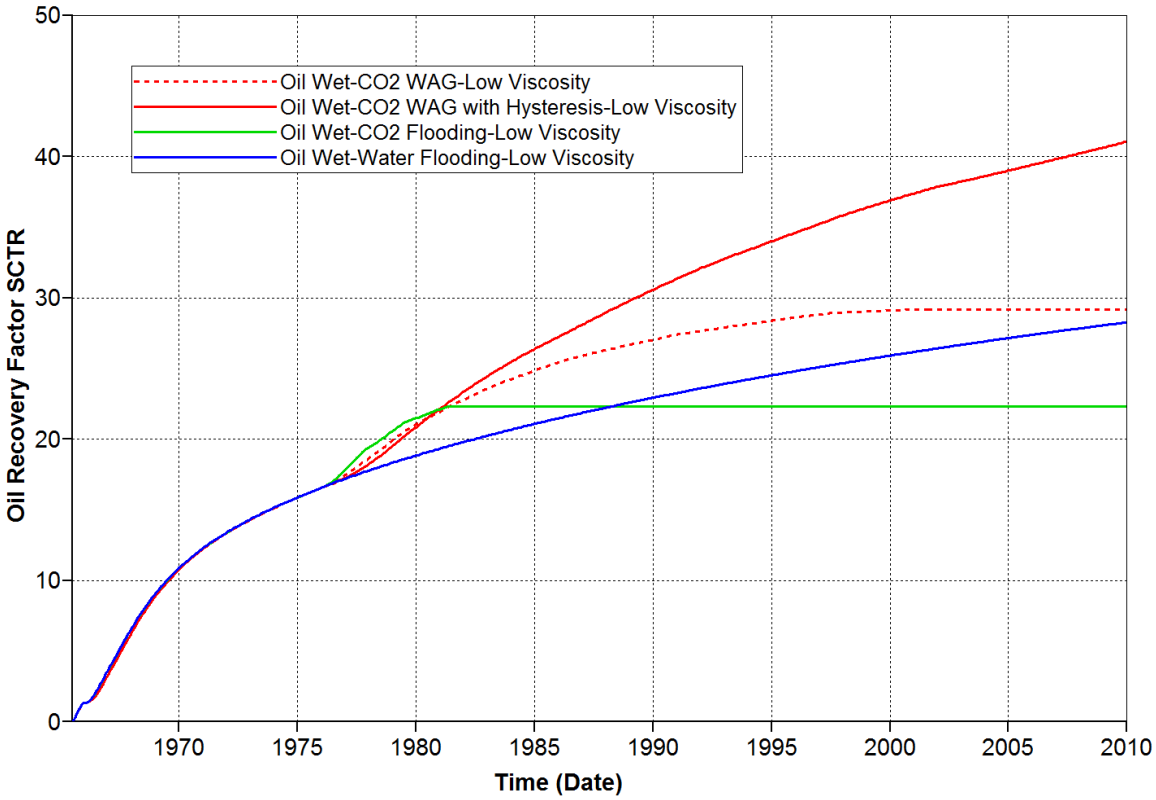

Figure 5.2 Oil Recovery Factor for Oil-Wet Model with Lower Oil Viscosity.

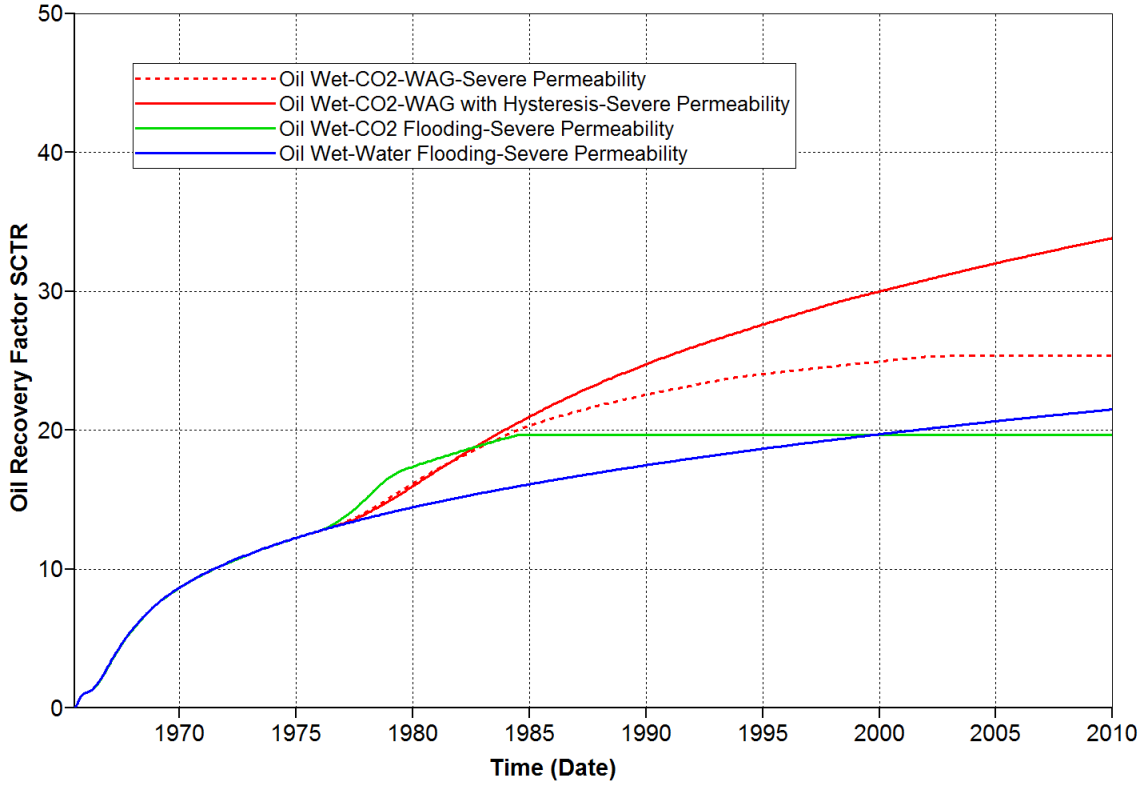

Figure 5.3 Oil Recovery Factor for Oil-Wet Model with High Permeability Contrast.

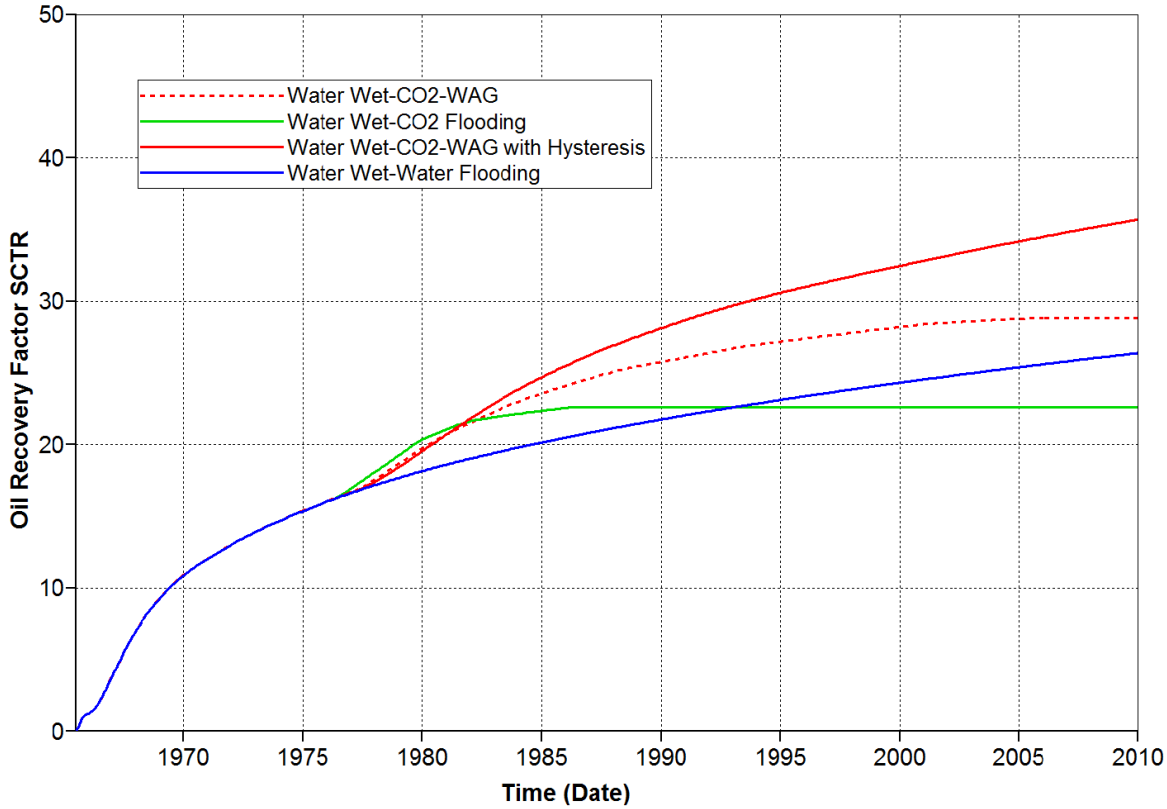

Figure 5.4 Oil Recovery Factor for Water-Wet Model with Higher Oil Viscosity.

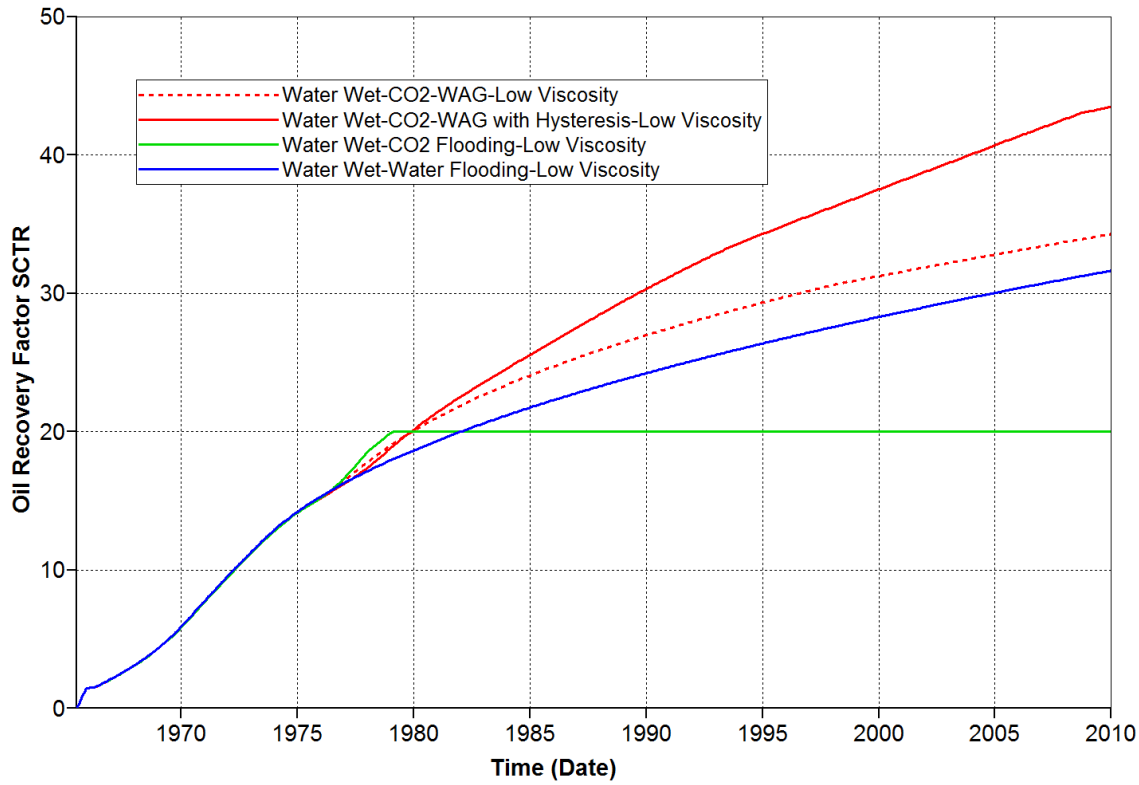

Figure 5.5 Oil Recovery Factor for Water-Wet Model with Lower Oil Viscosity.

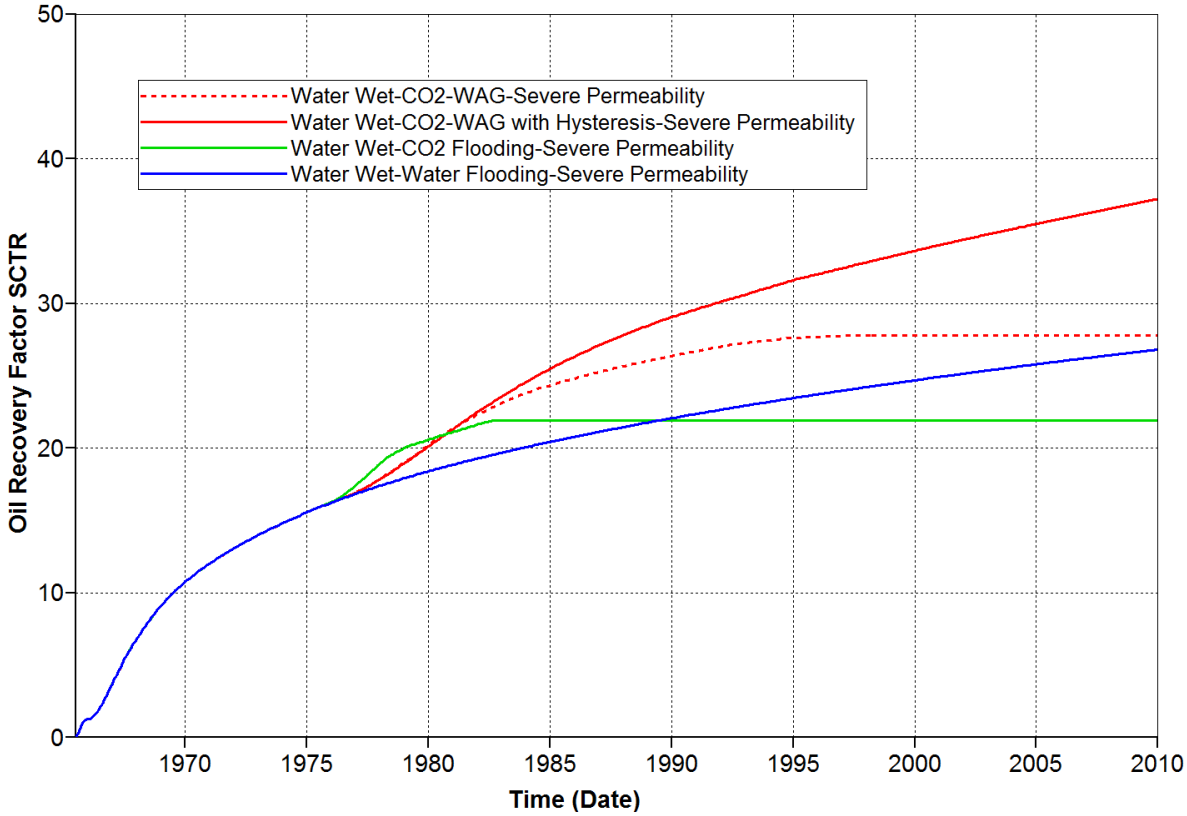

Figure 5.6 Oil Recovery Factor for Water-Wet Model with High Permeability Contrast.

References

Al-Futaisi, A., Patzek, T.W., 2003. Impact of wettability on two-phase flow characteristics of sedimentary rock: a quasi-static description. Water Resour. Res. 39, 1042.

Al-Mamari, F., Al-Shuraiqi, H., Al-Wahaibi, Y. M. 2007, January. Numerical simulation and experimental studies of oil recovery via first-contact miscible water alternating gas injection within shaley porous media. In SPE/EAGE Reservoir Characterization and Simulation Conference. Society of Petroleum Engineers.

Aziz, K., Settari, A., 1979. Petroleum Reservoir Simulation. Elsevier, London.

Baker, L.E., 1988. Three-Phase Relative Permeability Correlations, Paper SPE/DOE 17369 presented at the SPE/DOE Enhanced Oil Recovery Symposium, Tulsa, Oklahoma, April 17–20.

Blunt, M.J., 2000. An empirical model for three-phase relative permeability. SPEJ 5, 435– 445 (December).

Bradley, H. B. 1987. Petroleum engineering handbook.

Carlson, F.M., 1981. Simulation of Relative Permeability Hysteresis to the Nonwetting Phase, Paper SPE 10157 presented at the SPE Annual Technical Conference and Exhibition, San Antonio, Texas, October 5–7.

Christensen, J. R., Stenby, E. H., Skauge, A. 1998, January. Review of WAG field experience. In International Petroleum Conference and Exhibition of Mexico. Society of Petroleum Engineers.

Christensen, J. R.; Stenby, E. H., Skauge, A. 2001, Review of WAG field experience. SPE Reservoir Evaluation & Engineering.

Delshad, M., Pope, G.A., 1989. Comparison of three-phase oil relative permeability models. Transp. Porous Media 4, 59– 83.

Dixit, A.B., McDougall, S.R., Sorbie, K.S., Buckley, J.S., 1999. Porescale modeling of wettability effects and their influence on oil recovery. SPEREE 2, 25– 36 (February).

Egermann, P., Vizika, O., Kallet, L., Requin, C., Sonier, F., 2000. Hysteresis in Three-Phase Flow: Experiments, Modelling and Reservoir Simulations, Paper presented at the IEA Workshop and Symposium on Enhanced Oil Recovery, Edinburgh, Scotland, September 20–22.

Green, D. W., Willhite, G. P. 1998. Enhanced oil recovery. Richardson, Tex.: Henry L. Doherty Memorial Fund of AIME, Society of Petroleum Engineers.

Guzman, R.E., Giordano, D., Fayers, F.J., Aziz, K., Godi, A., 1994. Three-Phase Flow in Field-Scale Simulation of Gas and WAG Injections, Paper SPE 28897 presented at the European Petroleum Conference, London, UK, October 25–27.

Hicks Jr., P.J., Grader, A.S., 1996. Simulation of three-phase displacement experiments. Transp. Porous Media 24, 221– 245.

Jadhunandan, P.P., Morrow, N.R., 1995. Effect of wettability on water-flood recovery for crude-oil/brine/rock systems. SPERE 10, 40– 46. (February).

Jerauld, G.R., 1997. General three-phase relative permeability model for Prudhoe Bay. SPERE 12, 255– 263 (November).

Killough, J.E., 1976. Reservoir simulation with history-dependent saturation functions. SPEJ, Trans., AIME 261, 37– 48 (February).

Kjosavik, A., Ringen, J.K., Skjaeveland, S.M., 2002. Relative permeability correlation for mixed-wet reservoirs. SPEJ 7, 49– 58 (March).

Lake, L.W., 1989. Enhanced Oil Recovery. Prentice Hall, Upper Saddle River, NJ.

Land, C.S., 1968. Calculation of imbibition relative permeability for two- and three-phase flow from rock properties. SPEJ, Trans., AIME 243, 149– 156 (June).

Larsen, J.A., Skauge, A., 1998. Methodology for numerical simulation with cycle-dependent relative permeabilities. SPEJ 3, 163– 173. (June).

Lenhard, R.J., Oostrom, M., 1998. A parametric model for predicting relative permeability–saturation–capillary pressure relationships of oil–water systems in porous media with mixed wettability. Transp. Porous Media 31, 109– 131.

Lenhard, R.J., Parker, J.C., 1987. A model for hysteretic constitutive relations governing multiphase flow: 2. Permeability–saturation relations. Water Resour. Res. 23 (12), 2197– 2206.

Oak, M.J., 1990. Three-Phase Relative Permeability of Water-Wet Berea, Paper SPE/DOE 20183 presented at the SPE/DOE Symposium on Enhance Oil Recovery, Tulsa, Oklahoma, April 22–25.

Oak, M.J., Baker, L.E., Thomas, D.C., 1990. Three-phase relative permeability of Berea sandstone. JPT, Trans., AIME 289, 1054– 1061 (August).

Oliveira, L.I., Demond, A.H., 2003. Estimation of primary drainage three-phase relative permeability for organic liquid transport in the vadose zone. J. Contam. Hydrol. 66, 261– 285.

Øren, P.E., Bakke, S., 2003. Reconstruction of Berea sandstone and pore-scale modelling of wettability effects. J. Pet. Sci. Eng. 39, 231– 246.

Piri, M., Blunt, M.J., 2005. Three-dimensional mixed-wet random pore-scale network modeling of two- and three-phase flow in porous media: I. Model description. Phys. Rev., E 71, 026301.

Sato, K., Aziz, K., 1987. Sensitivity of Steam Displacement Predictions to Three-Phase Relative Permeability Models, Paper SPE 16733 presented at the SPE Annual Technical Conference and Exhibition, Dallas, Texas, September 27–30.

Shahrokhi, O., Fatemi, M., Sohrabi, M., Ireland, S., & Ahmed, K. 2014, April. Assessment of three phase relative permeability and hysteresis models for simulation of water-alternating-gas (WAG) injection in water-wet and mixed-wet systems. In SPE Improved Oil Recovery Symposium. Society of Petroleum Engineers.

Skauge, A., Dale, E. I. 2007, January. Progress in immiscible WAG modelling. In SPE/EAGE Reservoir Characterization and Simulation Conference. Society of Petroleum Engineers.

S.M. Farouq Ali and S. Thomas, "A realistic Look at Enhanced Oil Recovery", Canada, 1994).

Spiteri, E.J., Juanes, R., Blunt, M.J., Orr Jr., F.M., 2005. Relative Permeability Hysteresis: Trapping Models and Application to Geological CO_2 Sequestration, Paper SPE 96448 presented at the SPE Annual Technical Conference and Exhibition, Dallas, Texas, October 9–12.

Spiteri, E. J., & Juanes, R. 2006. Impact of relative permeability hysteresis on the numerical simulation of WAG injection. Journal of Petroleum Science and Engineering, 50(2), 115-139.

Spiteri, E. J., Juanes, R., Blunt, M. J., & Orr, F. M. 2008. A new model of trapping and relative permeability hysteresis for all wettability characteristics. SPE Journal, 13(03), 277-288.

Stone, H.L., 1970. Probability model for estimating three-phase relative permeability. JPT, Trans., AIME 249, 214– 218 (February).

Stone, H.L., 1973. Estimation of three-phase relative permeability and residual oil data. J. Can. Pet. Technol. 12 (4), 53– 61.

Valvatne, P.H., Blunt, M.J., 2004. Predictive pore-scale modeling of two-phase flow in mixed-wet media. Water Resour. Res. 40, W07406.

Whitson, C. H., & Brulé, M. R. (2000). *Phase behavior*. Richardson, TX: Henry L. Doherty Memorial Fund of AIME, Society of Petroleum Engineers.

Wu, X., Ogbe, D. O., Zhu, T., Khataniar, S. 2004, January. Critical Design Factors and Evaluation of Recovery Performance of Miscible Displacement and WAG Process. In Canadian International Petroleum Conference. Petroleum Society of Canada.

Appendix A: Copyright Permission

Chapter 2: Literature Review

License Number	4143680367806
License date	Jul 07, 2017
Licensed Content Publisher	Elsevier
Licensed Content Publication	Journal of Petroleum Science and Engineering
Licensed Content Title	Impact of relative permeability hysteresis on the numerical simulation of WAG injection
Licensed Content Author	Elizabeth J. Spiteri,Ruben Juanes
Licensed Content Date	Feb 16, 2006
Licensed Content Volume	50
Licensed Content Issue	2
Licensed Content Pages	25
Start Page	115
End Page	139
Type of Use	reuse in a thesis/dissertation
Portion	figures/tables/illustrations
Number of figures/tables/illustrations	11
Format	both print and electronic
Are you the author of this Elsevier article?	No
Will you be translating?	No
Order reference number	
Original figure numbers	Figures: 12, 13, 15, 16, 17, 18, 21, 22, 23. Tables: 2, 3.
Title of your thesis/dissertation	Relative Permeability Hysteresis Effects on Water Alternating CO2 Flooding
Expected completion date	Sep 2017
Estimated size (number of pages)	100
Elsevier VAT number	GB 494 6272 12
Requestor Location	Seyedeh Razieh Hosseini 607, 17 Ave., NW Unit 304 Calgary, AB T2M0N6 Canada Attn: Raz Hosseini
Billing Type	Invoice
Billing Address	Raz Hosseini 607, 17 Ave., NW Unit 304 Calgary, AB T2M0N6 Canada Attn: Raz Hosseini
Total	**0.00 CAD**
Terms and Conditions	